64

NASA CONTRACTOR REPORT

NASA CR-124

NASA CR-124

HEAT TRANSFER STUDIES OF VAPOR CONDENSING AT HIGH VELOCITIES IN SMALL STRAIGHT TUBES

by Winthrop E. Hilding and Charles H. Coogan, Jr.

Prepared under Contract No. NsG-204-62 *by*
UNIVERSITY OF CONNECTICUT
Storrs, Conn.
for

NATIONAL AERONAUTICS AND SPACE ADMINISTRATION • WASHINGTON, D. C. • OCTOBER 1964

HEAT TRANSFER STUDIES OF VAPOR CONDENSING AT HIGH VELOCITIES IN SMALL STRAIGHT TUBES

By Winthrop E. Hilding and Charles H. Coogan, Jr.

Prepared under Contract No. NsG-204-62 by
UNIVERSITY OF CONNECTICUT
Storrs, Conn.

for

NATIONAL AERONAUTICS AND SPACE ADMINISTRATION

For sale by the Office of Technical Services, Department of Commerce,
Washington, D.C. 20230 -- Price $2.75

CONTENTS

NOMENCLATURE

Dimensional Variables

a = exponent in pressure function for saturated liquid enthalpy

b = exponent in pressure function for saturated vapor enthalpy

c = exponent in pressure function for latent heat

j = exponent in pressure function for saturated vapor density

A = cross sectional area of tube

A_L = cross sectional area of liquid in tube

A_v = cross sectional area of vapor in tube

C = sound speed in saturated vapor

D = tube diameter

D_v = local diameter of vapor cone

E = total energy of the two phase stream

g = gravitational acceleration at sea level (32.174 ft/sec^2)

g_c = proportionality factor (32.174 $\frac{lb_m\ ft}{lb_f\ sec^2}$)

h_L = specific enthalpy of saturated liquid

h_v = specific enthalpy of saturated vapor

$(h_v - h_L) = h_{fg}$ = latent heat enthalpy change

h_c = surface convection coefficient

H_o = total energy removed per foot of tube

k_L = thermal conductivity of liquid

k = isentropic exponent for vapor

k_v = thermal conductivity of vapor

L = tube length

P = absolute stream pressure (STATIC)

p_e = absolute stream pressure at entrance to tube

p_o = absolute stagnation pressure

t = exponent in empirical expression for sound speed in saturated vapor

μ_L = dynamic viscosity of saturated liquid

μ_v = dynamic viscosity saturated vapor

ρ_L = density of liquid (either mass density or weight density as required)

ρ_v = density of saturated vapor (either mass density or weight density as required)

δ = thickness of annular liquid layer

τ_L = unit shear stress between liquid and tube wall

τ_v = unit shear stress between vapor and liquid at liquid vapor interface

V_L = local mean velocity of liquid along tube

V_{iL} = local interfacial liquid velocity

V_v = local mean velocity of vapor along tube

V_{iv} = local interfacial vapor velocity

V_{v_e} = mean vapor velocity at entrance to tube

W = combined weight rate of flow of vapor plus liquid

W_L = weight rate of flow of liquid

W_v = weight rate of flow of vapor

Non Dimensional Variables

$f_w' \equiv \dfrac{\tau_L}{\rho_v V_v^2/2g_c}$ = superficial friction factor (called superficial because the unit tube wall shear stress τ_L is related to the vapor kinetic energy instead of the liquid kinetic energy)

$f_v \equiv \dfrac{\tau_v}{\rho_v V_v^2/2g_c}$ = interfacial vapor friction factor in annular two phase flow

$\alpha = V_L/V_{v_e}$ = non-dimensional local liquid velocity.

$\beta = V_v/V_{v_e}$ = non-dimensional local vapor velocity.

$\theta = w_{v/w}$ = non-dimensional local vapor flow rate

$1 - \theta = w_{L/w}$ = non-dimensional local liquid flow rate

$\phi = p/p_e$ = non-dimensional local stream pressure

$\chi = L/D$ = non-dimensional tube length

$\lambda_e = \dfrac{g_c h_{fg_e}}{V_{v_e}^2}$ = non-dimensional latent heat at entrance

$\lambda = \lambda_e/\phi c$ = local non-dimensional latent heat

$\epsilon = \dfrac{h_{v_e}}{V_{v_e}^2/g_c}$ = non-dimensional constant

$\eta = \dfrac{h_{L_e}}{V_{v_e}^2/g_c}$ = non-dimensional constant

$\sigma = \rho_{v_e}/\rho_{L_e}$ = non-dimensional constant

$H = \left[\dfrac{g_c D H_o}{W V_{v_e}^2}\right]$ = non-dimensional heat transfer rate

$M = V_v / C$ = local Mach number of the vapor

$N = \left[\dfrac{4gP_e}{\rho_{v_e} V_{v_e}^2}\right]$ = non-dimensional constant

$S = \dfrac{k\left[1 + \frac{k-1}{2} M^2\right]^{1/k-1}}{\left[\left(1 + \frac{k-1}{2} M^2\right)^{k/k-1} - 1\right]}$ dimensionless variable

$\xi = \tau_v/p_e$ = non-dimensional vapor shear stress parameter

$\psi = \tau_L/p_e$ = non-dimensional liquid shear stress at the tube wall

HEAT TRANSFER STUDIES OF VAPOR CONDENSING AT HIGH VELOCITIES IN SMALL STRAIGHT TUBES

by W. E. Hilding and C. H. Coogan, Jr.

Department of Mechanical Engineering, University of Connecticut

SUMMARY

In this report, a set of simultaneous differential equations of change is derived for the concurrent, annular, two-phase, one-dimensional, steady flow of a pure condensing vapor and its liquid in a straight, cylindrical tube with heat transfer through the tube wall. Equations of momentum, continuity, and energy, are combined with empirical relations for the physical properties of the liquid and vapor and with equations for interface velocity pressure and liquid layer thickness; thus, reducing the system to a set of simultaneous, non-linear, first order, differential equations involving only four derivatives.

Starting with the known entrance flow conditions, the equations were solved numerically using variable incremental steps over the required condensing length. Flow properties for several cases were determined at each incremental point along the tube and were compared with experimental data for steam condensing in long, small diameter tubes. The data include local values of velocity, pressure and total quality at each incremental step in the condensing process.

INTRODUCTION

For the effective design of high performance condensing tube type heat exchangers for Rankine power cycle systems, a thorough knowledge of the

mechanics of heat transfer and fluid flow of vapor and liquid during condensation in small tubes is desirable. During the past two decades, an increasing volume of analytical and experimental research on the mechanics of two-phase flow systems has been reported in the technical literature. Investigation of two-phase flow systems has taken several different directions. The accompanying chart (Fig. 1) is an attempt to classify some of the areas in which research in two-phase flow mechanics has or might be done. Introduction of the chart is intended only to show the relationship of the work presented in this paper to the whole spectrum of two-phase flow research. No claim of completeness or originality of the chart is implied. Obviously work done in any one area may be quite similar to research done in another.

Pioneering experimental work in two-component, two-phase flow systems was done by Lockhart and Martinelli (9)[1] in developing empirical correlations for pressure losses in isothermal, two-phase, two-component flow in pipes. Additional experimental work has been done by a number of investigators working with steam-water, air-water, and/or air-oil mixtures.

References covering some of this work include Carpenter (1), Bergelin Gazley (25), Martinelli and Nelson (26), and Boelter and Kepner (27).

Perhaps the chief contributions to the theoretical analysis of two-phase flow systems have been made by Levy (10), (11), and (12). The most recent paper by Levy (10) is an analytical treatment of the two-phase system as a continuous medium with the liquid component thoroughly dispersed as small droplets or mist throughout the vapor component. In an earlier paper (12) Levy assumed an annular model similar to Fig. 2, where the liquid occupies the outer ring and the vapor flows in the cylindrical core. Other investigators,

---

[1] Numbers in parentheses designate references listed in the Bibliography.

including Carpenter (1) and Fauske (15), have assumed the annular flow model in their analysis of two-phase flow mechanics.

The experimental investigations of Fauske (15) included measurements of adiabatic critical mass flow rates of steam and water from small diameter tubes at various supply or header pressures and including total vapor qualities from 1 to 96%. Fauske (15) derives analytical expressions for predicting the critical total mass flow based on the annular flow model similar to Fig. 2, but assuming frictionless flow. In a graphical presentation, Fauske compares the analytically predicted values for critical total flow with experimental measurements of his own and those of several other investigators. In addition, he has analytically calculated the critical total flow assuming a homogeneous mist flow system. The agreement between the analytical values and experimental data for the annular flow model is excellent for all qualities from 1 to 96%. Contrariwise, critical mass flow rates calculated assuming the homogeneous model predict total mass flow rates as small as one quarter of the experimentally measured rate at a total quality of 1%.

The experimental and basic theoretical researches upon which is based the analysis of this paper, were carried out, beginning in 1952 under a subcontract with the United States Air Force supervised by the CANEL Project of the Pratt & Whitney Aircraft Division of United Aircraft Corporation. The results of these investigations are summarized in References 5 and 6. Based on these results and those mentioned previously, the annular flow model was chosen for the analytical work of this paper because it appears to conform more closely to the actual physical conditions in condensation of pure vapors at high velocities in small tubes. It is recognized that, even with an essentially annular flow system, a portion of the liquid present may be dispersed as fine droplets or mist in the vapor cone.

In this paper, the annular flow model has been used to develop a system of differential equations which may be solved numerically in incremental steps over the condensing length in small tubes. The vapor and liquid velccities, stream static pressure, vapor density and total quality are thereby determined at each axial location along the length of the condensing tube.

METHOD OF ANALYSIS

The experimental evidence gathered in earlier investigations, e.g., (5) (6), both qualitative and quantitative including visual observations, indicate that the major fraction of the liquid phase in condensing flow usually flows as an annular ring of pure liquid along the tube wall particularly if the vapor velocities are in excess of one or two hundred feet per second. Depending on the flow conditions, a smaller fraction of the liquid may be dispersed as mist or droplets in the vapor core. The so-called annular flow model (Fig. 2) used by Levy (12), Fauske (15), Carpenter (1), and other investigators in analyzing the mechanics of two-phase flow systems appears to correspond most closely to the experimental evidence encountered in the present work.

In the analysis presented herein, the annular flow model has been used to develop a system of differential equations which may be solved numerically in incremental steps over the condensing length in small tubes. The vapor and liquid velocities, stream static pressure, vapor density and total quality are thereby determined at each axial location along the length of the condensing tube. Following is a summary of the steps taken in developing the system of differential equations.

Differential control volumes were drawn for the annular liquid layer and for the vapor cone at a cross section of the condenser tube (see Figs. 3, 4,

and 5). Differential equations for momentum, energy, and flow continuity were written for the vapor cone and for the annular liquid layer (Appendixes B, C, and D). In addition, empirical equations were established for: (a) the density of saturated vapor, (b) the enthalpy of saturated vapor, (c) the enthalpy of saturated liquid, and (d) the latent heat of condensation. The empirical relations referred to are simple power functions of the saturated stream pressure P of the condensing vapor. That is, $h_v = C_1 P^a$ where C_1 and 'a' are particular constants. See Appendix A and Fig. 6 through 13 for the development of the empirical equations referred to above for saturated steam and for saturated potassium vapor. Satisfactory accuracy of representation of these properties (within about ± 1 per cent of the tabulated values) may be obtained by using appropriate values of the exponents given in Figs. 6 through 13 for the range of pressures to be encountered in a particular condenser tube.

Experimental investigation (6) of the variation in both stagnation and stream static pressure across the tube diameter (Fig. 14) showed that in the direction normal to the flow axis no discontinuity in velocity pressure occurs at the essentially cylindric, wavy interface between the annular liquid layer and the vapor cone. It is possible, therefore, to write an expression equating the velocity pressure of the liquid to the velocity pressure of the vapor at the annular interface between the control volumes for the liquid and vapor. The development of the differential form of the equation of equal velocity pressures is given in Appendix E. The differential equation of equal interfacial velocity pressures has been applied to that portion of the condenser tube where both the vapor cone and the annular liquid layer are in fully developed turbulent flow.

For the viscous, annular liquid flow near the tube mouth at the beginning of vapor condensation, it was necessary to write an equation relating the viscous

shearing forces acting between the developing annular liquid layer and the high velocity central vapor cone. The development of this equation and resulting differential form of the equation is presented in Appendix F.

The several differential equations which have been derived in this analysis are summarized in non-dimensional form in Table I.

A precise mathematical model of the condensing two-phase flow system would require that the presence of the liquid droplets in the vapor core be considered in the analytical treatment. The aforementioned paper by Levy (10) using a so-called mixing length model gives such an analytical treatment.

In the Levy analysis, however, the whole liquid phase is assumed to be continuously distributed throughout the vapor phase with liquid concentration being greatest at the tube wall or solid boundary. No finite annular liquid layer is presumed to be present in this mixing length treatment. It is felt that this model describes the physical conditions of two-phase boiling flow in tubes more accurately than condensing flow since in boiling flow the vapor continuously originating at the tube wall would tend to prevent the formation of an annular liquid layer on the wall thus forcing the distribution of the liquid throughout the tube cross section. However, there does not seem to be any reason why the annular flow model cannot be combined with the Levy mixing length model to mathematically describe a system which conforms closer to the actual physical system existing in two-phase condensing flow. A combination of the mixing length treatment with that of the annular flow model has not been attempted in this paper. The task of solving the simultaneous system of differential equations of change for the separate phases of the annular model was considered a sufficient undertaking. However, the problem of solving a system of equations incorporating features of both the annular and mixing length models, offers an interesting challenge.

Solution of the System of Equations

By combining equations and by substituting the empirical property functions given in Appendix A, it is possible to reduce the system of equations to a set of simultaneous first-order, non-linear differential equations involving only four derivatives. The four fundamental, dimensional, dependent variables are then: 1) the local stream static pressure P; 2) the local mass average vapor velocity V_v; 3) the local mass average liquid velocity V_L; 4) the local total vapor quality Θ. The single independent variable is the axial distance along the tube in diameters,

An analytical solution giving local values of the four dependent variables requires a system of four independent differential equations which satisfactorily represent the physical flow system at that location. At the entrance to a condenser tube the flow regime may begin with laminar vapor flow accompanied by a developing annular laminar liquid layer. For the region of interest of this investigation, the vapor flow either begins or changes to a fully developed turbulent flow system in a very short axial distance. With dry saturated vapor at the entrance to the condenser tube, an annular liquid layer begins to develop in laminar flow near the tube mouth. The development of the annular liquid layer continues until the liquid thickness is such that the outer surface becomes unstable and a cylindrical wavy interface between the liquid and vapor begins to firm. The flow regime downstream of this point consists of a turbulent vapor core surrounded by a turbulent annular liquid layer. Normally the laminar liquid layer will exist for only a very short distance (1 to 5 diameters or less) near the mouth of the tube. The distance depends primarily on the heat transfer rate per unit length (see Equation 25F , Appendix F). The non-dimensional boundary layer thickness parameter $Y^+ = \frac{y}{\nu}\sqrt{\frac{\tau g_c}{\rho}}$ has been used to determine the

point of transition from laminar to turbulent flow in the liquid layer. A value $5 \leq Y^{+} \leq 11$ appears to give a satisfactory indication of this transition point.

Near the tube mouth, the four differential equations of 1) combined continuity, 2) vapor momentum, 3) energy change, and 4) viscous boundary layer have been solved to determine the flow properties. After the point of transition to turbulent flow of the liquid, the equation of equal interfacial velocity pressures replaces the boundary layer equation in the stepwise integration process discussed below.

Mathematical solution of the set of non-linear equations appears to be possible or practical only by numerical or analogical methods. For the purposes of numerical solution it is useful to normalize the fundamental variables and to express the variable coefficients in non-dimensional form (see Nomenclature and/or Table II). By introducing the particular conditions in the tube mouth as a reference state, the fundamental variables were converted to the non-dimensional form, with the axial tube length represented in terms of tube diameters, i.e., axial distance $X = \frac{L}{D}$ (diameters).

Starting with the particular values of the four normalized fundamental variables in the tube mouth, the set of differential equations was solved to determine the local values of the four derivatives at that point in X. The derivatives so determined were then applied over a small increment in X (ΔX diameters) to determine new values of the four dependent variables at the end of the increment. Proceeding forward in the X direction the above process was continued until the total quality (Θ) became zero, i.e., the vapor is completely condensed.

Because of the tremendous amount of labor involved in an incremental integration of this kind with inherent possibilities of error accumulation, the

stepwise integration process was programmed for machine computation on an I.B.M. 1620 digital computer. All the analytical data presented has been compiled by this system of machine computation. The Fortran program for the computer solution to this system of equations can be made available to other investigators.

Successful analytical integration over the length of a proposed condenser tube requires considerable auxiliary information. First, the entering stream pressure, vapor velocity and vapor quality must be known. Secondly, the local heat transfer rate must be known or determined at each point. Fortunately, the steam side heat transfer surface coefficients for condensing steam are so high that external heat transfer resistances will control the heat transfer rate in most cases. Therefore, the variation of the vapor side surface coefficient of heat transfer plays a minor role in the determination of the flow characteristics of the condensing system. The third important factor is the determination of the location of the point of transition from the laminar or viscous annular liquid layer to the turbulent flow of the same layer. As indicated previously, this point of transition seems best to be determined at the point where the non-dimensional liquid layer thickness $5 \leq Y^{+} \leq 11$. The vapor-liquid velocity slip ratio (K) is another parameter which appears to be a useful indicator of the location of the transition point. (See Appendix F for details on the location of the point of transition from the laminar to turbulent liquid layers.)

The input data which seems to be most critical in the analytical integration process is the value of the local interfacial vapor friction factor. Slight deviations of input data on vapor friction factors from observed values have a strong cumulative effect on the calculated downstream flow characteristics

as can be observed in Figs. 15 through 18, which show analytical solutions for identical input data except for values of the interfacial vapor friction factor.

The difficulty encountered in carrying the analytical integration from subsonic to supersonic vapor velocities through Mach 1 is an extreme example of the effect of small variations in the input value of the interfacial friction factor. For Test No. 71052, it was necessary to express the interfacial vapor friction factor (f_v) to an accuracy of three significant figures in order to integrate successfully up through and down through the Mach one ($M = 1$) point on the vapor velocity curve (Fig. 19). Any friction factor greater or less than the precise figure required, resulted in extremely large derivatives which could not be successfully integrated by the computer. The large values of the vapor velocity derivatives and pressure derivatives at Mach one are to be expected. However, it is interesting to note that the particular values of the interfacial vapor friction factors necessary to analytically integrate through Mach one were in very close agreement with the values of the same quantity calculated from the experimental data (Fig. 21).

No completely satisfactory correlations for the local interfacial vapor friction factor were found for the experimental data recorded during this investigation for condensing steam vapor. A discussion of the problem of the determination and correlation of interfacial vapor friction factors as well as tube wall friction factors for condensing high velocity vapors is presented in Appendix I and in a separate note in Part II. It has been demonstrated, however, (see Figs. 19 through 23) that the solution of the system of differential equations described above will give close agreement with experimental data if the precise interfacial vapor friction factor for the existing local flow conditions is fed into the stepwise integration process.

APPENDIX A

Empirical Expressions for the Physical Properties of Saturated Vapor and of Saturated Liquid

For the two-phase system with condensing pure vapors, it was assumed that the two phases present are continuously in equilibrium at the saturation state of the respective phase. For a rapidly expanding vapor in the entrance of a tube this assumption might not be true. It is well known that a dry saturated vapor may expand well into the saturated region before condensation begins at the so-called Wilson "line." In the normal condenser tube this condition may or may not exist near the entrance to the tube. In any case, the region of such supersaturation would constitute a negligibly short section of the condenser tube and examination of this very local phenomena was not considered necessary in this investigation. After condensation has begun, the presence of liquid droplets as fog or mist in the vapor insures a continuous near equilibrium state for the saturated vapor and for any small liquid particles suspended therein. For the liquid layer on the inside tube surface there is a necessary temperature gradient in the direction normal to the tube surface. The degree of subcooling in the liquid layer will depend on the thickness of the layer, the rate of heat transfer, and the degree of turbulence in the layer. Since the physical properties of the liquid are not sharply affected by small variations in pressure or temperature, the effect of subcooling on the physical properties in the liquid layer has been neglected.

Simple empirical functions may be used to represent the physical and thermodynamic properties of the pure saturated vapor and liquid over moderate pressure ranges. The various properties have been expressed as simple power

functions of the saturation pressure in each case. The value of the saturated pressure exponent for a particular property is not necessarily constant over a large range of pressures. Examination of such exponents plotted in Figs. 6 through 8 for H_2O and Figs. 9 through 13 for potassium indicate that the range of values encountered in any normal condenser tube is small enough so that no significant error will be encountered by use of a mean value of the empirical exponent for the particular range of pressures involved. The necessary property functions are listed below.

(1) Specific Enthalpy of Saturated Liquid

Assuming the empirical function

$$h_L = C_1 P^a \qquad 1A$$

therefore,

$$h_L / h_{Le} = P/P_e{}^a = \phi^a \qquad 2A$$

or

$$h_L = h_{Le} \phi^a \qquad 3A$$

introducing the non-dimensional constant

$$\eta = \frac{h_{Le}}{V_{ve}^2 / g} \qquad 4A$$

then

$$\frac{h_L}{V_{ve}^2 / g} = \eta \, \phi^a \qquad 5A$$

(2) Specific Enthalpy of Saturated Vapor

Assuming the empirical function

$$h_v = C_2 P^b \qquad 6A$$

therefore,

$$h_v / h_{ve} = P/P_e{}^b = \phi^b \qquad 7A$$

or

$$h_v = h_{ve}\phi^b \qquad 8A$$

introducing the non-dimensional constant

$$\epsilon = \frac{h_{ve}}{V_{ve}^2 / g_c} \qquad 9A$$

then

$$\frac{h_v}{V_{ve}^2 / g_c} = \epsilon\ \phi^b \qquad 10A$$

(3) Latent Heat of Evaporation of Saturated Liquid

Assuming the empirical function

$$h_v - h_L = h_{fg} = C_3 / P^c \qquad 11A$$

therefore,

$$h_{fg} / h_{fge} = \left(P/P_e\right)^{-c} \qquad 12A$$

or

$$h_{fg} = \frac{h_{fge}}{\phi^c} \qquad 13A$$

introducing the non-dimensional constant

$$\lambda = \frac{h_{fge}}{V_{ve}^2 / g_c} \qquad 14A$$

then

$$\frac{h_v - h_L}{V_{ve}^2 / g_c} = \frac{h_{fg}}{V_{ve}^2 / g_c} = \lambda / \phi^c \qquad 15A$$

(4) Density of Saturated Vapor

Assuming the empirical function

$$\rho_v = C_4 P^j \qquad 16A$$

therefore,

$$\rho_v / \rho_{ve} = P/P_e{}^j = \phi^j \qquad 17A$$

or

$$\rho_v = \rho_{ve} \phi^j \qquad 18A$$

introducing the non-dimensional constant

$$\sigma = \rho_{ve} / \rho_L \qquad 19A$$

Where ρ_L the density of liquid is very nearly constant in the range of temperatures normally encountered in a condenser tube, therefore

$$\rho_v / \rho_L = \frac{\rho_{ve}}{\rho_L} \phi^j = \sigma \phi^j \qquad 20A$$

(5) Viscosity of Saturated Vapor

Assuming the empirical function

$$\mu_v = C_5 P^n \qquad 21A$$

therefore,

$$\frac{\mu_v}{\mu_{ve}} = P/P_e{}^n = \phi^n \qquad 22A$$

or

$$\mu_v = \mu_{ve}\phi^n \qquad 23A$$

(6) Viscosity of Saturated Liquid

Assuming the empirical function

$$\mu_L = C_6 P^m \qquad 24A$$

therefore,

$$\frac{\mu_L}{\mu_{Le}} = P/P_e{}^m = \phi^m \qquad 25A$$

or

$$\mu_L = \mu_{Le}\phi^m \qquad 26A$$

APPENDIX B

The Differential Equations for Continuity of Two-Phase Steady Flow In a Straight Tube

Assumptions: (See Fig. 3.)

(a) Flow is steady and one-dimensional in each phase.

(b) Pressure is constant across the tube at any point, i.e., at any radius.

Applying the continuity equation first to the liquid phase and then to the vapor phase at any point leads to

$$\text{(liquid)} \quad W_L = A_L V_L \rho_L \tag{1B}$$

$$\text{(vapor)} \quad W_v = A_v V_v \rho_v \tag{2B}$$

Differentiating 1B and 2B logarithmically, dividing by the differential length dL and assuming the liquid density constant, the equations become:

$$\frac{1}{W_L}\frac{dW_L}{dL} = \frac{1}{A_L}\frac{dA_L}{dL} + \frac{1}{V_L}\frac{dV_L}{dL} \tag{3B}$$

and

$$\frac{1}{W_v}\frac{dW_v}{dL} = \frac{1}{A_v}\frac{dA_v}{dL} + \frac{1}{V_v}\frac{dV_v}{dL} + \frac{1}{\rho_v}\frac{d\rho_v}{dL} \tag{4B}$$

The continuity equation applied to the length dL, requires that

$$W = W_L + W_v = W_L + dW_L + W_v + dW_v \tag{5B}$$

therefore

$$dW_L = -dW_v \tag{6B}$$

and similarly for the tube of constant cross-sectional area

$$A = A_L + A_v = A_L + dA_L + A_v + dA_v \qquad 7B$$

therefore,

$$dA_L = - dA_v \qquad 8B$$

combining Equations 6B , 7B and 8B into 3B , we obtain

$$\frac{A_L/A_v}{V_L}\frac{dV_L}{dL} + \frac{A_L/A_v}{W_L}\frac{dW_v}{dL} - \frac{dA_v}{A_v dL} = 0 \qquad 9B$$

Rearrangement of 4B results in the form

$$\frac{1}{\rho_v}\frac{d\rho_v}{dL} + \frac{1}{V_v}\frac{dV_v}{dL} - \frac{1}{W_v}\frac{dW_v}{dL} + \frac{1}{A_v}\frac{dA_v}{dL} = 0 \qquad 10B$$

Adding Equations 9B and 10B leads to the continuity equation in differential form for combined liquid and vapor flow

$$\frac{A_L/A_v}{V_L}\frac{dV_L}{dL} + \frac{1}{V_v}\frac{dV_v}{dL} + \left[\frac{A_L/A_v}{W_L} - \frac{1}{W_v}\right]\frac{dW_v}{dL} + \frac{1}{\rho_v}\frac{d\rho_v}{dL} = 0 \qquad 11B$$

In order to write the combined continuity equation in non-dimensional form, the following substitutions are now made in Equation 11B

$$X = L/D \quad \text{(Local tube length to diameter ratio)} \qquad 12B$$

therefore,

$$dL = DdX \qquad 13B$$

But, from Appendix A

$$\rho_v/\rho_L = \frac{\rho_{ve}}{\rho_L}\phi^j = \sigma\phi^j \qquad 14B$$

differentiating 14B logarithmically leads to

$$d\rho_v/\rho_v = j\frac{d\phi}{\phi} \qquad 15B$$

Introducing a non-dimensional variable for the average velocity in the annular liquid layer

$$\alpha = V_L / V_{ve} \qquad 16B$$

therefore,

$$dV_L / V_L = d\alpha / \alpha \qquad 17B$$

Introducing a non-dimensional variable for the average vapor velocity in the vapor cone

$$\beta = V_v / V_{ve} \qquad 18B$$

therefore,

$$\frac{dV_v}{V_v} = \frac{d\beta}{\beta} \qquad 19B$$

Introducing the expression for the local total vapor quality

$$\theta = W_v / W \qquad 20B$$

therefore,

$$\frac{dW_v}{W_v} = \frac{d\theta}{\theta} \qquad 21B$$

From Equations 1B and 2B

$$A_L / A_v = \frac{W_L \rho_v V_v}{W_v \rho_L V_L} = \frac{(W - W_v) \rho_v V_v}{W_v \rho_L V_L} \qquad 22B$$

Now substituting the non-dimensional Equations 17A , 19A , 16B , 18B and 20B leads to the ratio

$$A_L / A_v = \frac{1-\theta}{\theta} \frac{\sigma \beta \phi^j}{\alpha} \qquad 23B$$

also

$$\frac{A_L / A_v}{W_L} = \frac{\rho_v V_v}{W_v \rho_L V_L} \qquad 24B$$

and therefore,

$$\frac{A_L/A_v}{W_L} - \frac{1}{W_v} = \frac{1}{W_v}\left[\frac{\sigma\beta\phi^j}{\alpha} - 1\right] \qquad 25B$$

Equation 11B can then be written in non-dimensional form as a function of the four dependent variables α, β, θ, and ϕ as follows:

$$\frac{1-\theta}{\theta}\frac{\sigma\beta\phi^j}{\alpha^2}\frac{d\alpha}{dX} + \frac{1}{\beta}\frac{d\beta}{dX} + \frac{1}{\theta}\left[\frac{\sigma\beta\phi^j}{\alpha} - 1\right]\frac{d\theta}{dX} + \frac{j}{\phi}\frac{d\phi}{dX} = 0 \qquad 26B$$

Equation 26B is then the normalized general form for the combined continuity equation in annular two-phase flow with mass interchange between phases.

APPENDIX C

The Differential Equations of Momentum for Two-Phase Steady Flow In a Straight Tube Without Gravity Forces

Vapor Phase Analysis

Summation of forces acting in the axial flow direction for the vapor cone: (Gravity forces neglected, other assumptions same as in Appendix B, see Fig. 4.)

Positive Forces	Negative Forces	
1. PA_v	1. $(P + dP)(A_v - dA_v)$	1C
2. $\frac{W_v V_v}{g}$	2. $\frac{W_v + dW_v}{g}(V_v + dV_v)$	
	3. $V_i \frac{dW_L}{g}$	
	4. $\left(P + \frac{dP}{2}\right)(dA_v)$	
	5. $\tau_v \pi \left(D_v - \frac{dD_v}{2}\right) dL$	

Now summing up the positive and negative forces, eliminating differentials of higher order and dividing throughout by dL leads to the differential equation for vapor momentum:

$$\frac{V_i}{g}\frac{dW_L}{dL} + \frac{V_v}{g}\frac{dW_v}{dL} + \frac{W_v}{g}\frac{dV_v}{dL} + A_v\frac{dP}{dL} = -\tau_v \pi D_v \qquad 2C$$

Liquid Phase Analysis

Summation of forces acting in the axial flow direction for the annular liquid layer: (See Fig. 5.)

Positive Forces	Negative Forces
1. PA_L	1. $(P + dP)(A_L + dA_L)$

2. $\frac{W_L V_L}{g}$ 2. $\frac{W_L + dW_L}{g} (V_L + dV_L)$

3. $(V_i)(dW_L/g)$ 3. $\tau_L \pi DdL$ 3C

4. $\left(P + \frac{dP}{2}\right) dA_L$

5. $\tau_v \pi \left(D_v - \frac{dD_v}{2}\right) dL$

Again summing up the positive and negative forces, eliminating differentials of higher order and dividing throughout by dL results in the following expression:

$$\frac{W_L}{g} \frac{dV_L}{dL} + A_L \frac{dP}{dL} + \frac{V_L}{g} \frac{dW_L}{dL} - \frac{V_i dW_L}{gdL} = (\tau_v \pi D_v - \tau_L \pi D) \qquad 4C$$

In the above equation V_i is the time average axial component of the velocity at which the condensing liquid particles or diffusional vapor molecules leave the vapor core and enter the liquid layer. This velocity could be anywhere between the vapor velocity in the core center and the interfacial liquid velocity. In this analysis it has been assumed that this interfacial velocity has a value of the order of magnitude of the time average interfacial axial liquid velocity. The chief support for this assumption is based on the fact that the diffusional molecules leaving the vapcr core and entering the liquid layer could only travel a distance of one mean free path since their last molecular impact in the vapor. For saturated steam vapor at 212°F, the mean free path of the vapor molecules is about 2×10^{-6} inches. The experimental evidence shown in Fig. 14B indicates that liquid layer wave amplitudes are of the order of 0.020 inches at vapor velocity of several hundred feet per second. Comparing the liquid wave height to the mean free path of the vapor molecule,

we find that the vapor molecule would suffer at least 10,000 molecular impacts in traveling through this interfacial region of wave activity before entering the liquid layer. Considering these facts, it seems reasonable to conclude that the diffusional vapor molecule entering the liquid layer does so at an axial velocity of the same order of magnitude as the interfacial liquid wave velocity.

For want of more exact knowledge of the interfacial wave velocity, the following relation has been used:

$$V_i = 2\,V_L \qquad 5C$$

where V_L is, of course, the time and area average liquid layer velocity. A more accurate value of the interfacial velocity V_i remains to be determined. Since the time average vapor velocity is of the order of one hundred times greater than the similar liquid velocity the exact value of V_i may not be of critical importance in Equation 4C . Now defining an interfacial vapor friction factor

$$f_v = \frac{\tau_v}{\rho_v V_v^2/2g} \qquad 6C$$

making use of the relations

$$dW_L = -\,dW_v \qquad 6B$$

$$A_v = W_v / \rho_v V_v \qquad 7C$$

and

$$\pi D^2 = 4A = 4W/\rho_{ve} V_{ve} \qquad 8C$$

also introducing the non-dimensional constant

$$N = gP_e / \rho_{ve} V_{ve}^2 \qquad 9C$$

again introducing the necessary non-dimensional terms of Appendix A, it is possible to write Equation 2C for vapor momentum in the form

$$\theta \frac{d\beta}{dX} + (\beta - 2\alpha) \frac{d\theta}{dX} + \frac{\theta N}{\beta \phi^j} \frac{d\phi}{dX} = -2f_v \beta^{3/2} \sqrt{\theta \phi^j} \qquad 10C$$

where all terms are non-dimensional and are as previously defined.

Adding Equations 2C and 4C leads to

$$\frac{W_L}{g} \frac{dV_L}{dL} + \frac{W_v}{g} \frac{dV_v}{dL} + \frac{(V_v - V_L)}{g} \frac{dW_v}{dL} + A \frac{dP}{dL} = -\tau_w \pi D \qquad 11C$$

which can then be expressed in the non-dimensional form

$$(1 - \theta) \frac{d\alpha}{dX} + \theta \frac{d\beta}{dX} + (\beta - \alpha) \frac{d\theta}{dX} + N \frac{d\phi}{dX} = -4N\Psi \qquad 12C$$

This is the combined differential equation for momentum change in non-dimensional form where $\Psi = \tau_w / P_e$ and Ψ is a non-dimensional wall shear stress. The other non-dimensional terms are as previously defined.

If a superficial wall friction factor is defined by

$$f_w' = \tau_w / KE_v = 2g\tau_w / \rho_v V_v^2 \qquad 13C$$

then Equation 12C can be written in the form

$$(1 - \theta) \frac{d\alpha}{dX} + \theta \frac{d\beta}{dX} + (\beta - \alpha) \frac{d\theta}{dX} + N \frac{d\phi}{dX} = -2f_w' \beta^2 \phi^j \qquad 14C$$

Equation 14C is the same as 12C except that the non-dimensional wall shear stress Ψ has been replaced by the more common superficial wall friction factor f_w'.

Either the vapor momentum equation 10C or the combined momentum equation may be used as an equation in the system of four fundamental equations necessary to find a solution to the values of the flow properties over the

condensing length. The choice of equations will depend on the available empirical data for the local friction factors f_v or f_w'. To date, no fully satisfactory correlations have been found for either friction factor for condensing two-phase flow.

APPENDIX D

The Differential Equation of Energy Transfer for Steady High Speed Annular Two-Phase Flow in a Straight Tube

The total flow rate of energy E of the two-phase stream at any position L in the flow direction may be written (BTU per second).

$$E = \frac{W_L V_L^2}{2g} + \frac{W_v V_v^2}{2g} + W_L h_L + W_v h_v \qquad 1D$$

This equation can be rewritten in non-dimensional form by dividing through by

$$WV_{ve}^2/g$$

thus

$$\frac{E}{WV_{ve}^2/g} = \frac{1-\theta}{2}\alpha^2 + \frac{\theta\beta^2}{2} + (1-\theta)\frac{h_L}{V_{ve}^2/g} + \theta\frac{h_v}{V_{ve}^2/g} \qquad 2D$$

Differentiating with respect to the tube length L and introducing

$$dE/dL = -H_o$$

where H_o is the energy abstracted per unit length of tube at L, we then have the non-dimensional differential equation for energy transfer

$$-gDH_o/WV_{ve}^2 = \alpha(1-\theta)\frac{d\alpha}{dX} + \beta\theta\frac{d\beta}{dX} + \left[\frac{\beta^2-\alpha^2}{2} + \frac{h_v - h_L}{V_{ve}^2/g}\right]\frac{d\theta}{dX} + \frac{1-\theta}{V_{ve}^2/g}\frac{dh_L}{dX} + \frac{\theta}{V_{ve}^2/g}\frac{dh_v}{dX} \qquad 3D$$

But from Appendix A

$$\frac{h_L}{V_{ve}^2/g} = \eta\,\phi^a \qquad 5A$$

therefore,

$$\frac{1}{V_{ve}^2/g}\ \frac{dh_L}{dX} = a\eta\,\phi^{a-1}\ \frac{d\phi}{dX} \qquad 4D$$

Also from Appendix A,

$$\frac{h_v}{V_{ve}^2/g} = \epsilon\ \phi^b \qquad 12A$$

therefore,

$$\frac{1}{V_{ve}^2/g}\ \frac{dh_v}{dX} = b\epsilon\ \phi^{b-1}\ \frac{d\phi}{dX} \qquad 5D$$

and also

$$\frac{h_v - h_L}{V_{ve}^2/g} = \frac{h_{fg}}{V_{ve}^2/g} = \lambda/\phi^c \qquad 15A$$

By introducing a non-dimensional expression for the rate of heat transfer through the tube wall

$$\mathbf{H} = g\ DH_o\ /W\ V_{ve}^2 \qquad 6D$$

and substituting these terms in Equation 3D , we can write

$$(1-\theta)\boldsymbol{\alpha}\frac{d\boldsymbol{\alpha}}{dX} + \theta\boldsymbol{\beta}\frac{d\boldsymbol{\beta}}{dX} + \left[\frac{\lambda}{\phi^c} + \tfrac{1}{2}\left(\boldsymbol{\beta}^2 - \boldsymbol{\alpha}^2\right)\right]\frac{d\theta}{dX}$$

$$+\left[\frac{b\epsilon\,\theta}{\phi^{(1-b)}} + \frac{a\eta\,(1-\theta)}{\phi^{(1-a)}}\right]\frac{d\phi}{dX} = -\mathbf{H} \qquad 7D$$

This then is the normalized differential equation for energy change with axial distance in the total two-phase flow. Note that the term $\mathbf{H}$ is usually variable. If such is the case, an expression $\mathbf{H} = \mathbf{H}(X)$ must be introduced to make possible a solution to the equation set.

APPENDIX E

The Differential Equation of Equal Velocity Pressures at the Interface of the Liquid and Vapor Flow Regimes

Experimental investigation of the variation in both stagnation and stream pressure at the interface between the liquid and vapor phases indicates that in the radial direction normal to the streamline no discontinuity in either pressure occurs as the pressure probe passes from the vapor core into the annular liquid layer. Fig. 14 shows a plot of the radial variation in stream and stagnation pressure across the diameter of a 0.550 I.D. condenser tube measured by a hypodermic pressure probe. Evidently an equality of velocity pressures for the liquid and for the vapor exists at the annular interface between the vapor and liquid layers.

For a pitot pressure probe in a stream up to moderate vapor velocities of several hundred feet per second, a form of the Bernoulli equation can be used to represent the relation between the stagnation pressure (P_o) and stream pressure (P) as follows:

$$\frac{V^2}{2g} + \frac{P}{\rho} = \frac{P_o}{\rho} \qquad 1E$$

which may be written

$$P_o - P = \rho V^2/2g \qquad 2E$$

Equation 2E is, therefore, an expression for the velocity pressure for incompressible flow. For incompressible flow, the ratio

$$\frac{P_o - P}{\rho V^2/2g} = 1 \qquad 3E$$

will be exact. Up to a vapor velocity of about M = 0.3 (Mach number) the velocity pressure of the liquid and of the vapor at the annular interface may be related with sufficient accuracy by the expression

$$\rho_L V_{iL}^2 = \rho_v V_{iv}^2 \qquad 4E$$

where V_{iL} and V_{iv} are the time average interfacial liquid and vapor velocities respectively.

Introducing the constants

$$C_L = V_{iL}/V_L \quad \text{and} \quad C_v = V_{iv}/V_v \qquad 5E$$

where C_L and C_v are assumed to vary insignificantly relative to changes in the average axial velocities V_L and V_v. Now substituting in 4E gives

$$\rho_L (C_L V_L)^2 = \rho_v (C_v V_v)^2 \qquad 6E$$

Assuming the liquid density to be nearly constant and differentiating 6E logarithmically leads to the expression

$$\frac{2dV_L}{V_L} = \frac{d\rho_v}{\rho_v} + \frac{2dV_v}{V_v} \qquad 7E$$

Again, introducing the non-dimensional expressions of Appendix A for the above variables, leads to the form

$$\frac{1}{\alpha}\frac{d\alpha}{dX} - \frac{1}{\beta}\frac{d\beta}{dX} - \frac{j}{2\phi}\frac{d\phi}{dX} = 0 \qquad 8E$$

Equation 8E is the normalized differential equation relating vapor and liquid velocity pressure at the interface between the two-flow regimes for low subsonic vapor velocities ($M \leq 0.3$).

Equation 8E and its compressible form 28E have been applies in the analysis of the flow characteristics in the region of fully developed vapor

and liquid turbulence. For the region of the developing laminar, annular liquid layer at the beginning of vapor condensation a different analytical approach has been followed. For the analysis of the developing laminar annular liquid layer, see Appendix F.

For compressible fluids, the ratio $\frac{P_o - P}{\rho V^2/2g}$ will increase steadily from unity as a function of the Mach number. The ratio has been plotted in Fig. 26 as a function of the Mach number for saturated steam vapor. The values of Fig. 26 were calculated from data taken from the tables of "Thermodynamic Properties of Steam," by Keenan and Keyes. Isentropic compression from saturated vapor at the stream pressure P to the stagnation pressure P_o is assumed in this calculation.

In order to relate the velocity pressures of a liquid and a compressible vapor, it was expected that it would be necessary to represent the curve of Fig. 26 by an empirical polynomial function of the vapor Mach number and then to incorporate this function into the differential equation derived from the expression for equal velocity pressures. It was discovered, however, that an expression derived from perfect gas relations would accurately describe the actual ratio for saturated steam vapor up to quite high pressures or densities (see Fig. 26). Starting from the well-known relation for isentropic flow of a perfect gas, a functional relation has been derived for a compressible vapor. For isentropic flow of a perfect gas

$$P_o/P = \left(1 + \frac{k-1}{2} M^2\right)^{k/k-1} \qquad 9E$$

or

$$P_o = P\left(1 + \frac{k-1}{2} M^2\right)^{k/k-1} \qquad 10E$$

Where k is the isentropic exponent and is not necessarily constant for all pressure ranges of the pure vapor. Subtracting P from both sides and also dividing by P results in the equation

$$(P_o - P)/P = \left[\left(1 + \frac{k-1}{2} M^2\right)^{k/k-1} - 1\right] \qquad 11E$$

For a perfect gas $M = \frac{V}{C}$, where the sonic velocity $C = \sqrt{kgRT}$, therefore, $M^2 = V^2/kgRT$. Now dividing both sides of Equation 11E by M^2 and also substituting the perfect gas equation $P = \rho RT$ leads to the equation

$$\frac{P_o - P}{\rho_v V_v^2/2g} = \left\{\frac{2}{kM^2}\left[\left(1 + \frac{k-1}{2} M^2\right)^{k/k-1} - 1\right]\right\} \qquad 12E$$

By use of l'Hospital's rule, it is easily shown that when $M \rightarrow 0$ Equation 12E reduces to

$$\frac{P_o - P}{\rho_v V_v^2/2g} = 1 \qquad 3E$$

which is identical to Equation 3E as is required. Values of the ratio $\frac{P_o - P}{\rho_v V_v^2/2g}$ have been calculated by Equation 12E for saturated steam vapor up to M = 2 at a pressure P = 10 psia and also P = 100 psia (see Fig. 26). The agreement is surprisingly close between the values calculated from steam table data and by use of the perfect gas based Equation 12E . Evidently Equation 12E gives a satisfactory expression for the velocity pressure of pure saturated steam vapor up to a Mach number of 2 and a vapor pressure of at least 100 psia.

Again making use of the experimentally observed phenomena of the equality of velocity pressures across the liquid-vapor interface in annular two-phase

flow (see Fig. 14), we may write

$$(P_o - P)\ (\text{liquid phase}) = (P_o - P)\ (\text{vapor phase}) \qquad 13E$$

Using

$$P_o - P\ (\text{liquid}) = \rho_L C_L^2 V_L^2$$

and substituting Equation 12E in 13E, we obtain the expression

$$\rho_L C_L^2 V_L^2 = \rho_v C_v^2 V_v^2 \left\{ \frac{2}{kM^2} \left[\left(1 + \frac{k-1}{2} M^2\right)^{k/k-1} - 1 \right] \right\} \qquad 14E$$

where the constants C_L and C_v are defined the same as before and are assumed to vary insignificantly relative to the time average velocities V_L and V_v over the condensing length.

Considering the terms g, C_L, C_v, ρ_L and k as constant and differentiating 14E logarithmically, we obtain

$$2\frac{dV_L}{V_L} = \frac{d\rho_v}{\rho_v} + 2\frac{dV_v}{V_v} - \frac{2dM}{M} + \frac{k\left(1 + \frac{k-1}{2} M^2\right)^{\left(\frac{k}{k-1} - 1\right)} MdM}{\left(1 + \frac{k-1}{2} M^2\right)^{k/k-1} - 1} \qquad 15E$$

The Mach number M is defined as

$$M = \frac{V_v}{C} \qquad 16E$$

where C is the sound speed in the vapor. Differentiating 16E logarithmically gives

$$\frac{dM}{M} = \frac{dV_v}{V_v} - \frac{dC}{C} \qquad 17E$$

which may also be written

$$MdM = \frac{V_v dV_v}{C^2} - \frac{V_v^2 dC}{C^3} \qquad 18E$$

Substituting 18E in 15E leads to

$$\frac{2dV_L}{V_L} = \frac{d\rho_v}{\rho_v} + \frac{2dC}{C} + \frac{k(1 + \frac{k-1}{2} M^2)^{1/k-1}}{(1 + \frac{k-1}{2} M^2)^{k/k-1} - 1}\left[\frac{V_v dV_v}{C^2} - \frac{V_v^2 dC}{C^3}\right] \qquad 19E$$

Fig. 25 shows the variation of sound speed versus pressure in dry saturated steam. This curve can be approximated by the function

$$C = 1432\ P^{0.030} \qquad 20E$$

where C is the sound speed in feet per second and P the saturation pressure in psia. From a pressure of 1 psia to a pressure of 100 psia this expression 20E has a maximum error of about ± 4 feet per second or ± 0.25%. In general, therefore,

$$C = BP^t \qquad 21E$$

where B and t are constants.

Differentiating Equation 21E logarithmically gives

$$dC/C = t\,\frac{dP}{P} = t\,\frac{d\phi}{\phi} \qquad 22E$$

where ϕ is the normalized pressure as defined in Appendix A.

Making use of the definition $M = \frac{V_v}{C}$, we may write the equality

$$V_v dV_v / C^2 = M^2\,\frac{d\beta}{\beta} \qquad 23E$$

where $\beta = V_v / V_{ve}$ and is the normalized vapor velocity.

From 22E , we may also write the equality

$$V_v^2 dC/C^3 = tM^2\,\frac{d\phi}{\phi} \qquad 24E$$

Again drawing on the empirical property functions of Appendix A, we have

$$\rho_v = \rho_{ve} \phi^j \qquad 17A$$

where ρ_{ve} is the particular inlet vapor density. Differentiating 17A logarithmically yeilds

$$d\rho_v / \rho_v = j \frac{d\phi}{\phi} \qquad 25E$$

For purposes of simplification, it is useful to define a secondary variable

$$S = \frac{k\left(1 + \frac{k-1}{2} M^2\right)^{\frac{1}{k-1}}}{\left[\left(1 + \frac{k-1}{2} M^2\right)^{k/k-1} - 1\right]} \qquad 26E$$

Now substituting Equations 23E , 24E , 25E , and 26E into Equation 19E we obtain the normalized form

$$\frac{2d\alpha}{\alpha} = j \frac{d\phi}{\phi} + 2t \frac{d\phi}{\phi} + SM^2 \left[\frac{d\beta}{\beta} - t \frac{d\phi}{\phi}\right] \qquad 27E$$

Rearranging 27E and dividing through by dX where $X = \frac{L}{D}$, the local length to diameter ratio for the tube we obtain finally

$$\frac{2}{\alpha} \frac{d\alpha}{dX} - \frac{SM^2}{\beta} \frac{d\beta}{dX} + \left\{\frac{SM^2 t - 2t - j}{\phi}\right\} \frac{d\phi}{dX} = 0 \qquad 28E$$

The quantity SM^2 is a secondary dependent variable which is a function of the local vapor velocity and the particular isentropic exponent of the vapor. For saturated pure vapor, the isentropic exponent may be taken at an average value over the range of pressures encountered in a particular condenser tube. By use of l'Hospital's rule, it can be shown that at low velocities ($M \rightarrow 0$) the variable SM^2 reduces to $SM^2 = 2$. The differential Equation 28E then

reduces to

$$\frac{1}{\alpha}\frac{d\alpha}{dX} - \frac{1}{\beta}\frac{d\beta}{dX} - \frac{j}{2}\frac{d\phi}{dX} = 0 \qquad 8E$$

This is identical to Equation 8E derived at the beginning of this Appendix for an incompressible vapor.

Equation 28E must be applied in the analysis of two-phase flow characteristics for fully developed turbulent flow whenever the vapor velocity is such that the ratio $\frac{P_o - P}{\rho_v V^2/2g}$ is significantly greater than unity.

APPENDIX F

Initial Liquid Boundary Layer Equation

Assuming that liquid condensate flows in an annular cross section with an area A_L and a thickness δ, we may write

$$A_L = \frac{\pi D^2 - (D - 2\delta)^2}{4} \qquad 1F$$

which reduces to

$$A_L = \pi(D\delta - \delta^2) = \pi(D - \delta)\delta \qquad 2F$$

The rate of flow of liquid condensate W_L can then be expressed

$$W_L = \pi(D - \delta)\delta \rho_L V_L \qquad 3F$$

Differentiating 3F logarithmically and assuming ρ_L varies insignificantly we obtain

$$\frac{dW_L}{W_L} = \frac{d\delta}{\delta} + \frac{dV_L}{V_L} - \frac{d\delta}{(D - \delta)} \qquad 4F$$

When δ is small relative to D ($\delta << D$) 4F reduces to

$$\frac{dW_L}{W_L} = \frac{d\delta}{\delta} + \frac{dV_L}{V_L} \qquad 5F$$

We then introduce the well-known non-dimensional universal distribution functions

$$Y^+ = Y/\nu \sqrt{\frac{\tau_w g}{\rho}} \qquad 6F$$

and

$$V^+ = V \sqrt{\frac{\rho}{\tau_w g}} \qquad 7F$$

In the present analysis $Y = \delta$, the liquid layer thickness. Up to $Y^+ \cong 5$ von Karman (7) has proposed that $Y^+ = V^+$. For the region where $Y^+ = V^+$, therefore,

$$V_{iL} = Y_L \frac{\tau_w g}{\mu_L} = \delta \frac{\tau_w g}{\mu_L} \qquad 8F$$

where V_{iL} is the time average interfacial liquid velocity. This linear relation 8F requires that the time and area average liquid velocity (V_L) equal one-half the time average interfacial liquid velocity, V_{iL}, thus

$$V_{iL} = 2 V_L \qquad 9F$$

The laminar liquid boundary layer thickness may, therefore, be expressed by

$$\delta = \frac{2\mu_L}{\tau_w} V_L \qquad 10F$$

Differentiating 10F logarithmically gives

$$\frac{d\delta}{\delta} = \frac{dV_L}{V_L} - \frac{d\tau_w}{\tau_w} \qquad 11F$$

Equation 11F may be substituted into 5F to obtain

$$\frac{dW_L}{W_L} = 2 \frac{dV_L}{V_L} - \frac{d\tau_w}{\tau_w} \qquad 12F$$

At the beginning of vapor condensation the total liquid flow W_L is a very small quantity with virtually negligible momentum. In this region, it may therefore be assumed that $\tau_v = \tau_w$. If the vapor flow begins to develop a boundary layer in either laminar or turbulent flow after inlet to a condenser tube, the friction factor may be expressed in the form

$$f_v = C_f / (Re_x)^s \qquad 13F$$

where C_f and s are particular constants and the length Reynolds number is $Re_x = V_v \rho_v L/\mu_v$. We may, therefore, write

$$\tau_w = \tau_v = f_v \rho_v V_v^2/2g = C_f \rho_v V_v^2/(Re_x)^s 2g \qquad 14F$$

Differentiating 14F logarithmically and neglecting the variation in dynamic viscosity leads to the expression

$$\frac{d\tau_w}{\tau_w} = (2 - s)\frac{dV_v}{V_v} + (1 - s)\frac{d\rho_v}{\rho_v} - s\frac{dL}{L} \qquad 15F$$

Now substituting 15F into 12F, we obtain

$$2\frac{dV_L}{V_L} - (2 - s)\frac{d\beta}{\beta} - \frac{dW_L}{W_L} - (1 - s)\frac{d\rho_v}{\rho_v} = -s\frac{dL}{L} \qquad 16F$$

Again normalizing the terms of 16F and dividing by dL, we have the differential equation

$$\frac{2}{\alpha}\frac{d\alpha}{dX} - \frac{(2 - s)}{\beta}\frac{d\beta}{dX} + \frac{1}{1 - \theta}\frac{d\theta}{dX} - \frac{j(1 - s)}{\phi}\frac{d\phi}{dX} = -\frac{s}{X} \qquad 17F$$

In most cases the region of the developing laminar annular liquid layer is so short--i.e., several diameters or less--that the variation in vapor velocity and density over this length may be neglected. Equation 17F may then be simplified to the form

$$\frac{2}{\alpha}\frac{d\alpha}{dX} + \frac{1}{1 - \theta}\frac{d\theta}{dX} = -\frac{s}{X} \qquad 18F$$

If the initial vapor boundary layer develops in laminar flow from the tube entrance, the constant s has the value $s = 1/2$. If the vapor layer develops in turbulent flow, $s = 1/5$.

If the vapor flow enters the condensing region in fully developed laminar or turbulent flow, the initial boundary layer equation will take still another form. Burbank and Hilding (28) have derived an expression for the liquid boundary layer equation for fully developed laminar or turbulent vapor flow. For the turbulent flow of steam in smooth pipes at moderate pressures, the equation given is

$$\frac{2}{\alpha}\frac{d\alpha}{dX} - \frac{1.75}{\beta}\frac{d\beta}{dX} + \frac{1}{1-\theta}\frac{d\theta}{dX} - \frac{(0.732)}{\phi}\frac{d\phi}{dX} = 0 \qquad 19F$$

For fully developed laminar vapor flow at the beginning of condensation, the liquid boundary layer equation simplifies to

$$\frac{2}{\alpha}\frac{d\alpha}{dX} - \frac{1}{\beta}\frac{d\beta}{dX} + \frac{1}{1-\theta}\frac{d\theta}{dX} = 0 \qquad 20F$$

If the variation in stream pressure and vapor velocity are neglected over the short length of the developing liquid boundary layer the equation simplifies to the form

$$2(1-\theta)\frac{d\alpha}{dX} + \alpha\frac{d\theta}{dX} = 0 \qquad 21F$$

Except for the right-hand term of 18F , Equations 18F and 21F are identical. The term $\frac{s}{X}$ plays a strong role in Equation 18F , since the term is infinite at the tube entrance where $X = \frac{L}{D} = 0$.

For the integrated solutions presented in this paper, Equation 17F , with $\frac{d\beta}{dX} \rightarrow 0$, has been used for the region up to $Y^+ = 5$. The value $s = \frac{1}{2}$ has been assumed for a laminar development of the vapor layer starting at zero tube length.

Either form of the initial liquid boundary layer equation must be limited in application to the region of developing laminar liquid flow, i.e.,

$Y^+ \simeq 5 \rightarrow 11$. In the numerical solution of the system of equations, it is necessary, therefore, to determine the axial position at which the liquid interface will begin to become turbulent. From this point, the equation of equal interfacial velocity pressures may be employed (see Appendix E).

Rearranging Equation 6F and, since $\delta = Y$, we obtain

$$\delta^2 = Y^{+2} \mu_L^2 g_c / \rho_L \tau_w \qquad 22F$$

At the start of condensation, we have assumed a linear development of the velocity distribution in the very thin liquid layer, thus Equation 9F gives $V_{iL} = 2 V_L$ and Equation 10F relates the liquid layer thickness with the average liquid layer velocity, thus

$$\delta = 2 \mu_L V_L / \tau_w \qquad 10F$$

In addition, the continuity equation for the thin annular liquid layer 3F may be simplified to

$$W_L \cong \pi D \delta \rho_L V_L \qquad 23F$$

Combining Equations 10F , 22F , and 23F , the local liquid flow rate can be expressed as a function of the dimensionless liquid layer thickness Y^+, thus

$$W_L = \pi D \mu_L g (Y^+)^2 / 2 \qquad 24F$$

An expression for the local liquid flow rate as a function of the axial tube length after start of condensation is given in Appendix G, as follows:

$$\Delta W_L = \frac{H_o \Delta L}{h_{fg} + \frac{V_{ve}^2}{2g\ 778}} \qquad 2G$$

Assuming this equation holds with sufficient accuracy over the first few diameters of the condensing length, i.e., $W_L = \Delta W_L$ in this region and equating 24F and 2G leads to the equation

$$X = L/D = 778\pi g\, h_{fg}\, (Y^+)^2\, \mu_L\, /2H_o \qquad 25F$$

Equation 25F may be solved for the initial distance X in diameters over which the developing liquid layer remains in a laminar flow. The value $Y^+ = 5$ has been used in the solutions presented in this paper.

APPENDIX C

Calculation of Initial Conditions Necessary for Digital Computer Solution of the Differential Equations of Change

It is not possible to perform a direct integration of the system of non-linear differential equations of change developed in this paper and summarized in Table I. However, it is possible to find approximate solutions of sufficient accuracy by employing numerical methods of solution. Beginning with dry saturated vapor at the mouth of a condenser tube, the system of equations of Table I may be solved numerically by use of a digital computer. The following information must be specified to permit programming a solution for a proposed condenser tube:

1. Tube I.D.
2. Local heat transfer rate per unit length or surface area
3. Inlet static pressure of saturated steam
4. Inlet average steam velocity or total mass flow rate
5. Local interfacial vapor friction factor or local wall friction factor.
6. Empirical data on the thermo-physical properties of the particular saturated vapor and its saturated liquid.

Examination of the equations of Table I reveals that singularities in the values of several of the coefficients will exist at the beginning of condensation when the total quality is unity ($\theta = 1$) and the liquid velocity is zero. This situation presents no difficulty for a direct integration process, but cannot be handled with a numerical solution on a digital computer. It is possible to avoid the problem of coefficient singularities by establishing finite values of

these coefficients at a very short length increment after the beginning of condensation by the method outlined below. It should be pointed out that it is not possible to begin the numerical solution in the middle of a condenser tube since the values of the normalized dependent variables are always related to the conditions at a total quality of unity at the onset of condensation. A condenser tube which is expected to receive wet vapor may, of course, be designed from the point at which the expected total inlet quality corresponds to the quality of the analytical solution.

In order to establish finite coefficients at the start of the numerical solution process, the equation of energy conservation is applied to the process of condensation of a small fraction of saturated inlet vapor, thus

$$H_o \Delta L = \Delta W_L \left[(h_{ve} - h_L) + \frac{V_{ve}^2 - V_L^2}{2g778} \right] \qquad 1G$$

where H_o is the heat transfer rate per unit axial tube length and ΔL is a small but finite increment of length usually a tenth of a diameter or less. Solving for the condensed liquid fraction, we find

$$\Delta W_L \approx \frac{H_o \Delta L}{h_{fge} + \frac{V_{ve}^2}{2g778}} \qquad 2G$$

where h_{fge} is the latent heat of condensation taken at the inlet saturation pressure. The local quality (θ) at ΔL will, therefore, be

$$\theta = \frac{W_v}{W_{total}} = \frac{W_{total} - \Delta W_L}{W_{total}} = 1 - \frac{H_o \Delta L}{W_{tot}\left(h_{fge} + \frac{V_{ve}^2}{2g778}\right)} \qquad 3G$$

From the equation of continuity,

$$\rho_L V_L A_L = W_L \qquad 4G$$

the annular liquid layer cross section is

$$A_L \cong \pi D \delta \qquad 5G$$

For the developing laminar liquid layer, we have

$$\tau_w = \mu_L \, dV_L / dy \qquad 6G$$

Assuming a linear development of the velocity in the very thin liquid layer at the beginning of condensation with respect to the liquid layer thickness δ , we may write

$$V_{mean} = V_L = V_{iL} / 2 \qquad 7G$$

where V_{iL} is the time average interfacial liquid velocity and, therefore,

$$\tau_w = \mu_L \, 2V_L / \delta \qquad 8G$$

If it is assumed that a laminar vapor layer begins to develop from the leading edge of the tube mouth, the local interfacial vapor shear stress can be expressed as

$$\tau_v = 0.332 \frac{V_{ve} \mu_{ve}}{\Delta L} \sqrt{\frac{V_{ve} \rho_{ve} \Delta L}{\mu_{ve}}} \qquad 9G$$

At the start of condensation the small amount of low velocity liquid has virtually negligible momentum and, therefore, we may write

$$\tau_w \cong \tau_v = 0.332 \frac{V_{ve} \mu_{ve}}{\Delta L} \sqrt{\frac{V_{ve} \rho_{ve} \Delta L}{\mu_{ve}}} \qquad 10G$$

Combining Equations 10G and 8G , we may solve for V_L, and also the normalized liquid velocity α , thus

$$\alpha = \frac{V_L}{V_{ve}} = 0.166 \frac{\delta \mu_{ve}}{\Delta L \mu_L} \sqrt{\frac{V_{ve} \rho_{ve} \Delta L}{\mu_{ve}}} \qquad 11G$$

From continuity, we also have

$$\rho_v A_v V_v = W_v = W_T - W_L \qquad 12G$$

The vapor core cross section is

$$A_v = A - A_L \qquad 13G$$

It is, therefore, possible to find an expression for the local vapor velocity and its normalized form, thus

$$\beta = \frac{V_v}{V_{ve}} = \frac{W - W_L}{\rho_v A_v V_{ve}} = \frac{W - W_L}{\rho_v V_{ve} (A - A_L)} \qquad 14G$$

Actually the vapor velocity changes very little over a short increment near the tube mouth, i.e., $\beta \cong 1$.

For a developing laminar vapor layer near the tube entrance, it may be shown by simple integration, that the average shear stress over an interval beginning at zero length is twice the local value, thus

$$\bar{\tau}_v = 2\tau_v = 0.664 \frac{V_v \mu_v}{\Delta L} \sqrt{\frac{V_v \rho_v L}{\mu_v}} \qquad 15G$$

Writing the momentum equation over the short increment ΔL, we have

$$(P_e - P_L) A - \bar{\tau}_v \pi D \Delta L \cong \frac{W_L (V_L - V_{ve})}{g} \qquad 16G$$

This expression neglects any small changes in the vapor momentum per unit vapor mass over the small increment ΔL.

Solving for the normalized pressure (ϕ), we obtain

$$\phi = \frac{P_L}{P_e} = 1 - \frac{4\pi D \tilde{\tau}_v \Delta L}{P_e A} + \frac{W_L (V_{ve} - V_L)}{P_e Ag} \qquad 17G$$

It is necessary to evaluate $\tilde{\tau}_v$ from Equation 15G above, to find a numerical value for Equation 17G .

For a very short, finite, initial increment ΔL, we may thereby find finite values for the normalized dependent variables α , β , θ, and ϕ. The coefficients of each term of the several differential equations of change will now have finite values and the numerical solution may be begun on a digital computer.

If the vapor is in fully developed laminar or turbulent flow at the start of condensation, a similar analysis can be made using the proper expression for the interfacial vapor shear stress at the beginning of condensation.

APPENDIX H

Analysis of Experimental Data for University of Connecticut Tests

Beginning in June 1952, experimental research on steam condensation in long small tubes was conducted by the Mechanical Engineering Department at The University of Connecticut. This research was done under a sub-contract with the United States Air Force and under the supervision of the CANEL Project of the Pratt and Whitney Division of the United Aircraft Corporation. The results of this research on steam condensation were reported in fifteen [15] monthly 'Progress Reports' and two [2] 'Final Summary Reports' submitted to Pratt and Whitney Aircraft, East Hartford, Connecticut. The dates and titles of the two [2] final summary reports are as follows:

1. 'Final Summary Report' on "Steam Condensation in Small Tubes," dated October 15, 1952.
2. 'Final Summary Report' on "Steam Condensation in Small Tubes," dated November 30, 1953.

The experimental data and experience with steam condensation gained during the period of this earlier work has been of invaluable assistance in the development of the analytical studies which have been made during the period of the present NASA sponsored research program.

Some of the more useful experimental data gathered during the earlier research program has been tabulated in Tables 1-H through 8-H and is reported at the end of this Appendix. In each case, the original experimental data on local pressure and temperature measurement over the length of the condenser tube are reported. In addition, computed data on local vapor and liquid velocities, liquid layer thickness, local steam side heat transfer coefficients,

local tube wall friction factors, and local interfacial vapor friction factors are reported. The major portion of the necessary computations have been made during the period of the present research program.

Recorded and Computed Data

For the experimental tests conducted on condensing steam, the following data was recorded in most tests:

1. axial distance along tube from onset of condensation (L)
2. local static pressure (P)
3. local stagnation pressure (P_o)
4. local vapor temperature (T_v)
5. local cooling water temperature (T_c)
6. total flow rate of condensate at exit (W_T)
7. total flow rate of cooling water (W_c)

From the above data the following information was computed for most tests cases:

1. local heat transfer rate (H_o)
2. local liquid flow rate (W_L)
3. local vapor flow rate (W_v)
4. local vapor velocity (V_v)
5. local average liquid velocity (V_L)
6. local vapor cone cross section (A_v)
7. local liquid layer thickness (δ)
8. local interfacial vapor friction factor (f_v)
9. local superficial wall friction factor (f_w')
10. local vapor Reynolds number (Re_v)
11. local superficial vapor Reynolds number (Re_v')
12. local surface coefficient of heat transfer of the condensing vapor (h_v)

Method of Computation

1. Local Vapor Velocity -

For the local saturation pressure P the local saturated vapor enthalpy (H_v) is determined from the steam tables of Ref. 19. Assuming isentropic compression of the saturated vapor in the mouth of the stagnation pressure probe from the static pressure P to the stagnation pressure P_o, the stagnation enthalpy H_{vo} is determined at P_o. From the energy equation, we obtain

$$V_v = \sqrt{2gJ\ (H_{vo} - H_v)} \qquad 1H$$

which is the local vapor velocity indicated by pressure probe measurements.

2. Local Vapor Fraction -

From energy conservation, we have

$$E_T = W_T\, H_{voe} = W_L\, H_L + W_v \left[H_v + \frac{V_v^2}{2gJ}\right] + Q_R \qquad 2H$$

where E_T is the total energy rate entering the condenser tube, H_{voe} is the stagnation enthalpy of the supply steam and Q_R is the total rate of heat removed up to $R = L$ feet. From the principle of conservation of mass

$$W_T = W_L + W_v \qquad 3H$$

and since W_T is a measured quantity, we solve for W_v and obtain

$$W_v = \frac{W_T\,(H_{voe} - H_L) - Q_R}{H_v + \frac{V_v^2}{2gJ} - H_L} \qquad 4H$$

which may be reduced to

$$W_v = \frac{W_T\,(H_{voe} - H_L) - Q_R}{H_{vo} - H_L} \qquad 5H$$

This equation gives the local flow rate of the remaining vapor.

3. Local Liquid Fraction -

From Equation 3H

$$W_L = W_T - W_v \qquad 3H$$

4. Local Vapor Cone Cross Section -

From the equation of continuity, we have

$$W_v = \rho_v A_v V_v \qquad 6H$$

solving for the vapor area A_v, we obtain

$$A_v = W_v \rho_v / V_v \qquad 7H$$

5. Local Annular Liquid Cross Section and Thickness -

$$A_L = A - A_v \qquad 8H$$

The vapor cone diameter is

$$D_v = 2\sqrt{A_v/\pi} \qquad 9H$$

from which we obtain an expression for the thickness of the annular liquid layer thus

$$\delta = \frac{D - D_v}{2} = \frac{D}{2} - \sqrt{\frac{A_v}{\pi}} \qquad 10H$$

6. Local Interfacial Vapor Friction Factor -

The vapor friction factor is defined in Appendix C by the expression

$$f_v = \frac{\tau_v}{\rho_v V_v^2/2g} \qquad 6C$$

Solving the vapor momentum Equation 2C explicitly for the vapor friction factor (f_v) results in the expression

$$f_v = \frac{-1}{V_v} \left(\frac{W_v}{\pi \rho_v V_v}\right)^{\frac{1}{2}} \left[\left(\frac{V_v - V_i}{W_v}\right)\frac{dW_v}{dL} + \frac{dV_v}{dL} + \frac{g_c}{\rho_v V_v}\frac{dP}{dL}\right] \qquad 11H$$

In order to compute local values of the interfacial vapor friction factor f_v from experimental data, it is necessary to determine each of the terms in the above equation from the experimental data. The method of evaluating local flow properties has been outlined in this Appendix. The local derivatives of the same properties must be found by graphical means from suitable plots of the several properties.

7. Local Superficial Wall Friction Factor -

The superficial wall friction factor is defined in Appendix C by the expression

$$f_w' = \frac{\tau_w}{\rho_v V_v^2/2g} \qquad 13C$$

Solving the combined momentum Equation 11C explicitly for the superficial wall friction factor (f_w') leads to the expression

$$f_w' = \frac{-2}{\pi D \rho_v V_v^2}\left[W_L \frac{dV_L}{dL} + W_v \frac{dV_v}{dL} + (V_v - V_L)\frac{dW_v}{dL} + g_c A \frac{dP}{dL}\right] \qquad 12H$$

Computation of (f_w') from experimental data must be done by the same methods as used in computing the vapor friction factor.

8. Local Vapor Reynolds Number -

The local vapor Reynolds number is defined by the expression

$$Re_v = V_v D_v \rho_v / \mu_v \qquad 13H$$

The quantities on the right-hand side of this equation are taken from the computed local flow properties and from tables of the physical properties of saturated vapor taken at the local static pressure.

9. Local Superficial Reynolds Number -

The local superficial vapor Reynolds number is defined by the expression

$$Re_v' = V_v D \rho_v / \mu_v \qquad 14H$$

This definition is identical to the definition of the ordinary vapor Reynolds number except that the inside tube diameter has replaced the vapor cone diameter. The definition used by many earlier investigators assumes the vapor fraction flows in the condenser tube without the liquid being present, thus

$$Re_v' = G_v D/\mu_v \qquad 15H$$

In this definition the quantity G_v is the local vapor mass flow rate based on the tube cross section. In most experimental work conducted by other investigators no attempt was made to determine the actual vapor velocity and so no alternative to the above Reynolds number definition was possible.

10. The Local Heat Transfer Coefficient of the Condensing Vapor -

Two methods were used for computing the local coefficient of heat transfer (h_v) for the condensing vapor. The first method which will be called the direct method, requires measurement of the outside surface temperature of the inner or condenser pipe. Only heat exchanger No. 2 was instrumented so as to measure this temperature directly. The local rate of heat flow in the radial direction at any point along the pipe was determined by taking the product of

the cooling water flow rate in the annulus and the local axial gradient of the cooling water temperature. The axial gradient was determined graphically from the slope of the temperature curve for the cooling water. Using the well-known equation for radial heat flow through a cylindric wall, the temperature drop (Δ_{Tcu}) across the wall was calculated. Adding the drop in temperature across the wall to the measured outside wall temperature gives the inner surface temperature of the condenser pipe.

Using the local heat transfer rate per foot of tube (H_o) as determined above, the local surface coefficient of heat transfer was then derived from Newton's cooling law as follows:

$$H_o = h_v \pi D_i (T_v - T_w) \qquad 16H$$

Solving for h_v, we obtain

$$h_v = \frac{H_o}{\pi D_i (T_v - T_w)} \qquad 17H$$

Note that H_o is the local radial heat transfer flux in BTU per hour foot. D_i is the inner diameter of the condenser tube, T_v is the local saturation temperature of the condensing vapor, and T_w is the local inside wall temperature determined by the method outlined above.

The second method which will be called the <u>indirect</u> method, requires the calculation of the temperature drop across the cooling water film on the outside of the condenser tube. The local temperature drop across the cooling water film was determined by dividing the local rate of radial heat flow per foot of tube by the local outside cooling water surface coefficient of heat transfer (h_c). (See succeeding paragraphs for the method of determining h_c.) Having indirectly determined the outer surface temperature of the condenser tube the

procedure is then identical with that of the direct method of calculation described above.

For the two condenser heat exchangers (Nos. 1 and 3) not instrumented with condenser tube surface thermocouples, it was necessary to experimentally determine a correlation for the outside surface coefficient (h_c). For these two heat exchangers, tests were conducted using hot water in the condenser tube cooled by cold water in the annulus between the inner and outer tubes. It was assumed that the dimensionless correlation for a hot liquid flowing inside the circular condenser tube was known with good accuracy. For example, in turbulent flow in a tube the correlation

$$Nu = 0.027\ (Re)^{0.80}\ (P_r)^{0.33}(\mu/\mu_v)^{0.14} \qquad 18H$$

is well documented for the conditions encountered in this test. The local rate of radial heat flow can be determined from either the heated or cooled stream, since the flow rate of both and the local axial temperature distribution of both was recorded. Employing the well-known expression for fluid to fluid heat transfer through a circular wall, the local coolant surface coefficient was calculated. The equation is as follows:

$$H_o = \frac{\pi (T_v - T_w)}{\frac{1}{D_o h_c} + \frac{\ln (D_o/D_i)}{2 k_w} + \frac{1}{D_i h_v}} \qquad 19H$$

Solving for the outside cooling surface coefficient (h_c) results in the expression

$$h_c = \frac{1}{D_o \left[\frac{\pi (T_v - T_w)}{H_o} - \frac{\ln (D_o/D_i)}{2 k_w} - \frac{1}{D_i h_v} \right]} \qquad 20H$$

For the correlation of the annulus cooling surface coefficient, the so-called j factor or Colburn number was used, thus

$$Co = j = \frac{h_c}{G\,C_p}\,(Pr)^{2/3}\left(\frac{\mu_v}{\mu}\right)^{0.14} = f\,\frac{D_e G}{\mu} \qquad 21H$$

where μ_v is taken at the outside wall surface temperature and the equivalent diameter $D_e = (D_2 - D_1)$ and D_2 is the inside diameter of the outer tube of the annulus and $D_1 = D_o$ is the outer diameter of the condenser tube.

TABLE H-1

UConn Test 7-10-52

Experimental Data					Data From Steam Table		
Tube Length	P	P_o	T_v	T_c	H_{vc}	H_v	H_L
0	36.4	44.9	283	105.1	1177.15	1160.72	229.67
0.25	34.9	44.8	261	103.0		1163.20	227.73
0.50	34.9		263		1167.01	1167.01	227.73
0.75	34.0				1187.75	1166.50	226.18
1.00	33.1	43.9	255	97.3	1187.42	1166.05	224.59
1.50	31.3					1164.95	221.38
2.00	29.5	39.9	243	91.0	1187.57	1163.75	217.84
2.50	27.6					1162.42	213.30
3.00	25.5	36.2	234	85.0	1187.89	1160.95	209.52
3.50	23.5					1159.40	204.96
4.00	21.5	32.4	226	79.0	1189.92	1157.65	197.48
4.50	19.6					1155.95	195.20
5.00	17.9	28.8	216	73.0	1190.61	1154.09	190.26
5.50	16.3					1152.28	185.21
6.00	14.7	25.7	207	66.5	1194.41	1150.28	179.71
6.25	13.4					1148.59	175.21
6.50	12.1					1146.75	170.36
6.75	11.1					1145.16	165.95
7.00	10.4	22.8	193	61.0	1205.24	1143.98	162.99
7.25	9.8					1142.90	160.20
7.50	9.4	21.2	186	58.7	1205.82	1142.12	158.24
7.75	9.1					1141.60	156.73
8.00	8.9	19.8	178	56.4	1203.42	1141.20	155.69
8.25	9.0	19.3		55.5	1201.08	1141.40	156.22
8.50	10.6	18.6	182	54.3	1187.38	1143.32	163.91
8.75	11.4					1145.64	167.43
9.00	12.0	17.5	201	52.7	1175.05	1146.60	169.96
9.50	12.8	16.2	205	51.4	1165.43	1147.80	173.12
10.00	13.3	15.3	207	50.8	1158.73	1148.59	175.21
10.50	14.0					1149.43	177.43
11.00	14.5			50.7	1150.15	1150.15	179.36

Test Conditions

A) Counter flow

B) Condenser tube I.D. = 0.550 in.

C) Cooling water rate = 131 lbm/min

TABLE H-1 (cont.)

Computed Data												
Tube Length	Q_R	V_v	V_L	W_v	W_L	A_v	δ	f_v	f'_w	R_{ev}	R'_{ev}	h_v
	10^{-3}					10^{-3}	10^{-2}	10^{-3}	10^{-3}	10^5	10^5	
0	0	946	0	474.0	0	1.648	0	6.643				
0.25	14.40	993	0.66	456.0	18.0	1.522	0.11	1.672		4.177	4.351	
0.50	31.40	1011	0.86	436.0	38.0	1.430	0.19	6.536	6.677	4.121	4.430	
0.75	49.50	1025	1.03		60.0							
1.00	67.50	1040	1.15		76.0	1.335	0.28					
1.50	97.50	1071	1.30	368.0	106.5	1.260	0.35					
2.00	125.00	1107	1.41	340.0	134.0	1.191	0.41	5.614	6.042	3.582	4.219	8130
2.50	150.00	1147	1.50	315.0	160.0	1.134	0.47	5.638	6.123	3.421	4.124	
3.00	174.40	1187	1.58	290.0	184.0	1.087	0.52	5.837	6.448	3.248	4.008	
3.50	197.20	1223	1.63	268.0	206.0	1.051	0.56	5.927	6.579	3.076	3.859	
4.00	221.50	1266	1.67	245.0	229.0	1.055	0.55	5.691	6.253	2.897	3.711	7700
4.50	246.00	1314	1.70	221.0	254.0	0.953	0.66	5.492	6.000	2.715	3.582	
5.00	268.50	1370	1.72		275.0				6.023			12200
5.50	294.00	1438	1.73	175.0	299.0	0.824	0.81	5.476		2.359	3.349	
6.00	320.00	1515	1.72	150.0	324.0	0.744	0.90	6.006	6.785	2.153	3.220	
6.25	333.00	1560	1.71		332.0	0.741	0.91					
6.50	343.00	1630	1.70	130.0	344.0	0.715	0.94	5.720	6.913	1.964	3.046	
6.75	353.70	1710	1.69		353.0	0.686	0.98					13400
7.00	367.00	1776	1.67	109.0	365.0	0.632	1.05	6.154	5.695	1.756	2.849	
7.25	377.00	1792	1.65		374.0	0.609	1.08					
7.50	388.60	1797	1.63	90.0	384.0	0.567	1.14	6.610	5.083	1.547	2.651	
7.75	399.20	1792	1.60		393.5	0.527	1.20					
8.00	407.60	1773	1.57	73.0	401.0	0.491	1.25	6.796	3.968	1.356	2.499	18300
8.25	416.80	1700	1.55	64.4	410.0	0.446	1.32	8.201				
8.50	424.20	1546	1.53	54.6	419.5	0.358	1.47	6.684	-2.488	1.167	2.519	
8.75	431.50	1387	1.51		428.0	0.316	1.55					
9.00	439.20	1230	1.49	38.0	436.0	0.278	1.62	9.232	2.489	0.909	2.222	4080
9.50	448.60	927	1.45	27.5	446.5	0.219	1.75	11.408	0.191	0.687	1.767	
10.00	460.50	621	1.41	15.0	459.0	0.193	1.81	15.233	-2.319	0.417	1.222	2040
10.30				5.0				22.089	-22.271	0.175	0.631	
10.50	469.00	313	1.37	5.0	469.0	0.125	1.99					
11.00	474.00	0	1.33	0	474.0	0	2.75					

Computer Conditions

A) Condensing length = 11.0 ft.
B) Total steam condensed = 474 lbm/hr (probe in)
C) Average heat transfer rate = 11.96 BTU/ft sec
D) Average heat gained by cooling water = 8160 BTU/min
E) Average heat lost by condensing vapor = 7900 BTU/min
F) Heat balance error = 3.2%

TABLE H-2

UConn Test 7-17-52

Experimental Data					Data From Steam Table		
Tube Length	P	P_o	T_v	T_c	H_{vo}	H_v	H_L
0	33.4	34.7	277.8	93.2	1177.21	1174.16	225.12
0.1	26.8	34.7			1177.21	1157.41	212.31
0.3	26.7	34.6			1182.11	1161.83	212.22
0.5	26.2	34.6	251.5	84.4	1183.24	1161.44	211.05
1.0	25.0	34.1	245.0	82.0	1184.80	1160.60	208.42
2.0	21.8	31.5	227.4	78.0	1185.15	1157.92	200.83
3.0	18.5	27.6	218.6	72.7	1186.62	1154.75	191.99
4.0	15.3	24.0	209.8	69.2	1186.65	1151.16	182.10
4.5	13.6	22.4			1186.79	1148.94	176.13
5.0	12.1	21.0	203.3	65.0	1189.34	1146.75	170.36
5.5	12.2	19.9	200.0	63.3	1184.40	1146.90	170.75
6.0	12.4	18.9	199.0	61.5	1179.30	1147.20	171.54
7.0	12.5	16.7	203.0	55.7	1169.11	1147.35	171.93
8.0	13.3	14.9	207.0	52.7	1156.98	1148.52	175.02
9.0	14.0	14.5	188.0	51.3	1152.03	1149.50	177.61
10.0	14.4	14.5	162.5	50.7	1150.04	1150.04	179.01
10.3	14.4		153.0	50.7	1150.04	1150.04	179.19

Test Conditions

A) Counter Flow

B) Condenser tube I.D. = 0.550 in.

C) Cooling water rate = 142 lbm/min

TABLE H-2 (cont.)

Computed Data												
Tube Length	Q_R	V_v	V_L	W_v	W_L	A_v	ε	f_v	f'_w	$R_{\epsilon v}$	$R'_{\epsilon v}$	h_v
	10^3					10^{-3}	10^{-1}	10^{-3}	10	10^5	10^5	
0	0	392	0	363.0	0	1.550	0					
0.1	17.90	950	0.796	345.4	17.7	1.543	0.09					
0.3	48.55	1027	0.686	311.3	51.9	1.291	0.32					
0.5	65.56	1050	0.765	293.9	69.5	1.220	0.39	6.867	6.994	2.779	3.236	
1.0	91.90	1100	0.829	267.2	96.7	1.100	0.50	6.267	6.657	2.664	3.256	7900
2.0	131.20	1182	0.979	228.6	136.1	0.996	0.61	5.312	5.933	2.425	3.110	5270
3.0	170.50	1268	1.097	190.9	174.7	0.905	0.71	5.497	6.163	2.156	2.897	4930
4.0	208.80	1344	1.199	155.3	211.1	0.829	0.80	6.269	6.908	1.863	2.608	5550
4.5	220.70	1394	1.264	145.2	221.7	0.835	0.79	6.219	6.967	1.754	2.444	
5.0	248.00	1470	1.245	119.8	247.6	0.728	0.92	5.307	4.289	1.565	2.331	6120
5.5	266.00	1390	1.237	102.9	264.9	0.657	1.01	6.652	4.027	1.415	2.220	
6.0	283.00	1290	1.229	86.8	281.4	0.588	1.11	6.748	3.675	1.260	2.089	4540
7.0	314.00	995	1.258	57.6	311.5	0.502	1.23					3050
8.0	340.0	690	1.231	31.6	338.4	0.374	1.44		1.467	0.570	1.187	2200
9.0	357.00	396	1.210	14.3	356.5	0.281	1.62		-1.615	0.297	0.712	760
10.0	360.50	100	2.081	11.1	360.6				-1.606	0.133	0.184	450
10.3	363.00	0	2.250	0	372.0	0	2.75					203

Computed Conditions

A) Condensing length = 10.3 ft

B) Total steam condensed = 372 lbm/hr

C) Average heat transfer rate = 9.8 BTU/ft sec

D) Average heat gain of cooling water = 6570 BTU/min

E) Average heat loss of condensing vapor = 6180 BTU/min

F) Heat balance error = 5.9%

TABLE H-3

UConn Test 7-18-52

Experimental Data					Data From Steam Table		
Tube Length	P	P_o	T_v	T_c	H_{vo}	H_v	H_L
0	23.4	24.6	266.0	92.2	1172.0	1168.03	202.35
0.1	18.5	24.6			1176.24	1154.74	192.34
0.3	18.5	24.6			1176.49	1154.65	191.99
0.5	18.3	24.5	238.5	77.5	1176.95	1154.47	191.42
0.7	18.1	24.4			1177.26	1154.29	190.85
1.0	17.6	24.1	228.3	75.4	1177.96	1153.76	189.36
1.5	16.7	23.3	217.5	72.7	1178.36	1152.77	186.62
2.0	15.6	22.2	210.8	70.8	1178.45	1151.52	183.09
2.5	14.8	20.8			1176.34	1150.54	180.41
3.0	14.0	19.5	206.7	67.4	1174.08	1149.63	177.96
4.0	13.4	17.3	205.6	63.5	1167.83	1148.66	175.39
5.0	13.5	16.0	207.7	59.0	1161.48	1148.80	175.76
5.5	13.7	15.5			1158.34	1149.08	177.50
6.0	14.0	15.1	209.5	55.0	1155.07	1149.50	177.61
7.0	14.3	14.3	191.0	52.7	1150.02	1150.02	159.01

Test Conditions

A) Counter flow

B) Condenser tube I.D. = 0.550 in.

C) Cooling water rate = 140 lbm/min

TABLE H-3 (cont.)

Computed Data												
Tube Length	Q_R	V_v	V_L	W_v	W_L	A_v		f_v	f'_w	R_{ev}	R'_{ev}	h_v
	10^{+3}					10^{-3}	10^{-1}	10^{-3}	10^{-3}	10^5	10^5	
0	0	447	0	273.0	0	1.650	0					
0.1	16.8	1020	0.465	255.3	17.9							
0.3	42.0	1050	0.616	230.2	43.6	1.317	0.29					
0.5	63.0	1068	0.672	209.4	65.0			8.258	7.582	2.128	2.505	14400
0.7	81.5	1082	0.702	191.1	83.8			7.610	7.023	2.038	2.514	
1.0	101.0	1106	0.725	172.2	103.5	0.982	0.63	7.827	7.393	1.935	2.509	13500
1.5	126.0	1140	0.764	148.6	128.5	0.865	0.76	7.285	7.063	1.789	2.472	
2.0	147.0	1161	0.749	129.3	149.2	0.721	0.93	7.422	7.121	1.641	2.374	6080
2.5	165.0	1148	0.848	113.2	166.6			6.671	6.424	1.497	2.244	
3.0	182.0	1110	0.878	95.2	186.0	0.664	1.01	6.897	5.406	1.321	2.068	4200
4.0	218.0	994	0.915	65.7	218.1	0.543	1.17	6.425	3.750	1.022	1.784	4300
5.0	252.0	803	0.899	34.3	252.2	0.347	1.49	10.633	3.359	0.665	1.450	3260
5.5	265.0	681	0.888	24.4	265.5	0.262	1.65	9.500				
6.0	277.0	528	0.870	11.3	278.0	0.166	1.88	13.398	0.151	0.314	0.984	2080
7.0	294.0	0	0.850	0	291.0	0						1070

Computed Conditions

A) Condensing length = 7.0 ft.

B) Total steam condensed = 273 lbm/hr (probe in) 291 lbm/hr (probe out)

C) Average heat transfer rate = 11.7 BTU/sec ft.

D) Average heat gained by cooling water = 5530 BTU/min

E) Average heat loss of condensing vapor = 4920 BTU/min

F) Heat balance error = 11.0%

TABLE H-4

UConn Test 8-6-52

Experimental Data						Data From Steam Table		
Tube Length	P	P_o	T_v	T_{wall}	T_c	H_{vo}	H_v	H_L
0	24.9	24.9						
0.5	20.7	24.7	230.0	210.3	118.7	1170.20	1156.93	198.00
1.0	20.0	24.6	228.0	208.4	115.5	1172.23	1156.30	196.16
1.5	19.3	24.1	226.5	206.6	112.3	1172.75	1155.55	194.10
2.0	18.5	23.5	224.0	204.8	108.5	1172.50	1151.75	191.98
2.5	17.8	22.6	222.0	202.7	104.5	1172.40	1153.98	189.96
3.0	17.1	21.7	219.6	200.5	101.0	1171.52	1153.21	187.86
3.5	16.4	20.8	217.0	198.3	97.7	1169.88	1152.44	185.67
4.0	15.7	20.0	215.0	196.3	94.6	1170.17	1151.64	183.41
4.5	15.1	19.2	213.0	194.0	91.5	1168.97	1150.92	181.44
5.0	14.6	18.4	211.2	191.8	87.8	1167.58	1150.28	180.31
5.5	14.2	17.8	210.0	188.9	83.6	1166.45	1149.76	178.51
6.0	13.9	17.1	209.0	185.8	79.5	1164.83	1149.36	177.24
6.5	13.7	16.4	208.5	182.3	75.8	1162.81	1149.08	176.50
7.0	13.6	15.9	208.0	178.1	72.7	1161.09	1148.94	176.13
7.5	13.6	15.5	208.0	173.9	70.1	1158.65	1148.94	176.13
8.0	13.6	15.2	208.0	169.8	67.5	1157.32	1148.94	176.13
8.5	13.6	14.9	207.3	165.7	65.1	1155.75	1148.94	176.13
9.0	13.6	14.7	203.0	160.6	62.6	1155.79	1148.94	176.13
9.5	13.8	14.4	195.0	156.5	60.4	1154.51	1149.22	176.79
10.0	13.9	14.2	185.5	151.5	58.3	1151.12	1149.29	177.04
10.3		14.1	176.4	148.4	57.0	1150.40	1149.36	177.24

Test Conditions

A) Counter Flow

B) Condenser Tube I.D. = 0.550

C) Cooling water rate = 64.5 lbm/min

TABLE H-4 (cont.)

Computed Data												
Tube Length	Q_R	V_v	V_L	W_v	W_L	A_v	δ	f_v	f'_w	R_{ev}	R'_{ev}	h_v
	10^3					10^{-3}	10^{-1}	10^{-3}	10^{-3}	10^5	10^5	
0	0				0		0					
0.5	12.0				12.5	1.530	0.10					8850
1.0	24.0	894	0.384	219.0	24.8	1.370	0.24	4.083	4.395	2.490	2.269	9040
1.5	38.7	928	0.479	205.3	39.2	1.280	0.33	5.253	5.458	2.206	2.501	9350
2.0	54.6	942	0.577	190.2	55.3	1.210	0.39	5.670	5.838	2.107	2.459	10900
2.5	69.4	959	0.637	176.3	69.9	1.140	0.46	5.997	6.141	2.107	2.416	10600
3.0	83.4	959	0.702	163.4	83.5	1.100	0.50	5.934	6.105	1.912	2.334	9700
3.5	96.5	949	0.776	151.5	97.3	1.070	0.54	5.998	6.165	1.802	2.226	9320
4.0	108.5	963	0.779	140.6	108.0	1.02	0.59	5.592	5.795	1.721	2.178	9190
4.5	120.5	951	0.832	129.8	120.8	0.982	0.63	5.939	5.965	1.619	2.080	9620
5.0	135.0	932	0.852	116.4	135.0	0.937	0.68	6.875	6.511	1.499	1.980	10750
5.5	149.0	914	0.882	103.7	149.0	0.872	0.75	7.588	6.737	1.386	1.896	10300
6.0	164.0	880	0.889	89.8	164.0	0.801	0.83	8.720	7.024	1.256	1.793	9120
6.5	177.5	830	0.899	77.5	177.0	0.743	0.90	7.367	5.746	1.126	1.670	6670
7.0	188.5	783	0.904	67.5	188.4	0.692	0.97	7.170	4.955	1.018	1.565	5200
7.5	200.0	700	0.923	57.0	198.7	0.653	1.02	7.313	4.775	0.885	1.399	4170
8.0	208.5	646	0.926	49.5	208.0	0.614	1.07	7.162	4.391	0.792	1.291	3510
8.5	219.0	585	0.914	39.8	218.4	0.546	1.17	7.169	3.544	0.676	1.169	3040
9.0	227.0	565	0.883	32.7	227.0	0.464	1.29	2.864	1.713	0.602	1.129	2850
9.5	229.0	520	0.903	31.6	228.6	0.480	1.27	6.880	1.652	0.570	1.053	2990
10.0	242.5	304	0.963	18.8	232.4	0.487	1.26	19.070				3230
10.3	248.0	225		14.0	240.0	0.481	1.27					3850

Computed Conditions

A) Condensing length = 10.3 ft.
B) Total steam condensed = 260 lbm/hr.
C) Average heat transfer rate = 6.7 BTU/ft sec.
D) Average heat gained by cooling water = 3980 BTU/min.
E) Average heat lost by condensing vapor = 4300 BTU/min.
F) Heat balance error = 7.0%

TABLE H-5

UConn Test 8-13-52

Experimental Data				Data From Steam Table		
Tube Length	P	P_o	T_c	H_{vo}	H_v	H_L
0	38.7	45.5	56.8	1181.86	1169.05	
0.25	38.2	44.7	66.6	1181.31	1168.80	233.21
0.50	36.9	43.7	71.4	1181.53	1168.14	231.09
1.0	34.4	40.7	87.5	1179.92	1166.74	226.88
1.5	31.6	36.9	118.6	1176.99	1165.12	221.85
2.0	28.7	34.0	127.4	1176.34	1163.19	216.26
2.5	26.9	31.4	145.0	1173.86	1161.93	212.51
3.0	24.1	29.0	157.2	1173.34	1159.88	206.37
3.5	22.3	27.0	164.2	1173.03	1158.37	202.04
4.0	20.5	25.0	168.8	1172.00	1156.75	196.97
5.0	18.3	22.5	173.8	1170.25	1154.47	191.99
6.0	16.7	20.2	181.2	1167.13	1152.77	186.62
6.5	16.1	18.1		1160.78	1152.11	184.64
7.0	15.6	17.1	185.2	1158.29	1151.52	183.10
8.0	15.2	15.8	188.8	1153.86	1150.92	181.77
9.0	14.8	14.9	190.6	1151.04	1150.54	180.41
10.0	14.5	14.6	193.5	1150.68	1150.15	179.36
11.0	14.4	14.4	194.5	1150.02	1150.02	179.19

Test Conditions

A) Parallel flow

B) Condenser tube I.D. = 0.190 in.

C) Cooling water rate = 5.76 lbm/min.

TABLE H-5 (cont.)

Computed Data											
Tube Length	Q_R	V_v	V_L	W_v	W_L	A_v	δ	f_v	f'_w	R_{ev}	R'_{ev}
	10^3					10^{-4}	10^{-2}	10^{-3}	10^{-3}	10^5	10^4
0		802		44.70	0	1.960	0				
0.25	2.40	792	0.358	42.34	2.51	1.628	0.86	3.260	2.706	1.079	11.853
0.50	4.44	817	0.540	40.39	4.61	1.555	1.06	4.511	3.134	1.056	11.878
1.0	9.54	813	0.943	35.38	9.92	1.462	1.31	5.920	3.923	0.962	11.147
1.5	16.30	761	1.360	28.78	16.82	1.376	1.56	7.076	4.846	0.813	9.719
2.0	23.00	811	1.284	22.21	23.69	1.090	2.43	7.131	4.672	0.712	9.557
2.5	28.90	806	1.278	16.50	29.70	0.866	3.20	5.251	3.808	0.597	8.997
3.0	33.00	821	1.287	12.78	33.72	0.730	3.72	3.738	3.690	0.509	8.360
3.5	36.00	857	1.259	10.15	36.65	0.596	4.27	2.552	3.092	0.451	8.178
4.0	37.70	875	1.271	8.91	38.18	0.556	4.45	2.378	2.832	0.414	7.783
5.0	39.70	890	1.300	7.68	40.02	0.524	4.60	1.804	1.828	0.371	7.199
6.0	41.70	848	1.338	6.50	41.80	0.506	4.68	1.654	1.585	0.323	6.355
6.5		657	1.492	6.11	42.49	0.636	4.10	3.465	2.109	0.272	4.775
7.0	43.10	582	1.602	5.89	43.01	0.713	3.78	2.746	1.661	0.248	4.120
8.0	44.40	383	2.117	5.25	44.25	0.990	2.76	3.698	1.451	0.188	2.653
9.0	45.40	158		4.92	45.18						
10.0	46.20	163		4.76	45.94						
11.0		0		0	50.40						

Computed Conditions

A) Condensing length = 11.0 ft.

B) Total steam condensed = 50.4 lbm/hr (probe out) 44.7 lbm/hr (probe in)

C) Average heat transfer rate = 11.7 BTU/ft sec.

D) Average heat gained by cooling water = 792 BTU/min

E) Average heat lost by condensing vapor = 791 BTU/min

F) Heat balance error = 0.1%

TABLE H-6

UConn Test 8-14-52

Experimental Data					Data From Steam Table		
Tube Length	P	P_o	T_v	T_c	H_{vo}	H_v	H_L
0	29.2	34.4	250	54.1	1168.72	1155.25	217.25
0.25	29.2	34.0			1175.30	1163.54	217.25
0.50	28.1	33.3	247	60.0	1175.92	1162.77	215.03
0.75	26.8	31.8			1175.13	1161.86	212.33
1.00	25.5	30.5	241	66.2	1174.71	1160.95	209.52
1.50	22.8	27.7	235	71.9	1173.69	1158.82	203.29
2.00	20.2	24.7	228	77.7	1171.86	1156.48	196.69
2.50	18.2	22.0	223	83.3	1168.85	1154.42	191.13
3.00	16.6	19.9	218	88.8	1166.36	1152.66	189.31
3.50	15.5	18.1	215	93.8	1162.93	1151.40	182.77
4.00	14.7	16.5	212	98.9	1158.93	1150.41	180.06
5.00	14.5	14.5	211	107.5	1150.15	1150.15	179.36

Test Conditions

A) Parallel flow

B) Condenser tube I.D. = 0.190 in.

C) Cooling water rate = 12.67 lbm/min.

TABLE H-6 (cont.)

Computed Data												
Tube Length	Q_R	V_v	V_L	W_v	W_L	A_v	δ	f_v	f'_w	R_{ev}	R'_{ev}	h_v
	10^3					10^{-4}	10^{-2}	10^{-3}	10^{-3}	10^4	10^4	
0	0	826	0	40.8	0	1.96	0					20600
0.25	2.280	770	6.040	38.1	2.7	1.94	0.07	3.57				
0.50	4.480	797	1.740	35.9	4.9	1.83	0.34	5.27	5.39	8.648	8.953	13900
0.75	6.910	820	1.500	33.4	7.4	1.73	0.60	5.37	5.57	8.307	8.843	
1.00	9.200	839	1.422	31.0	9.8	1.64	0.83	5.40	5.65	7.950	8.669	10600
1.50	13.520	867	1.480	26.7	14.1	1.52	1.15	5.93	6.22	7.182	8.137	10250
2.00	17.100	874	1.560	23.1	17.7	1.46	1.32	6.11	6.31	6.355	7.391	11400
2.50	22.250	860	1.560	18.6	22.2	1.28	1.84	6.28	6.32	5.485	6.649	12600
3.00	26.360	830	1.475	14.5	26.3	1.12	2.34	6.78	6.57	4.594	5.929	14200
3.50	30.240	775	1.391	10.2	30.6	0.93	2.97	7.53	6.67	3.627	5.219	18200
4.00	34.150	657	1.298	6.3	34.5	0.72	3.76	11.58	8.30	2.577	4.227	17900
5.00	40.500	0	1.12	0	40.8	0	8.50					1510

Computed Conditions

A) Condensing length = 5.0 ft.

B) Total steam condensed = 37.4 lbm/hr (probe in) 43.2 lbm/hr (probe out)

C) Average heat transfer rate = 2.25 BTU/ft sec.

D) Average heat gained by cooling water = 676 BTU/min.

E) Average heat lost by condensing vapor = 673 BTU/min.

F) Heat balance error = 0.4%

TABLE H-7

UConn Test 8-28-52

Experimental Data					Data From Steam Table		
Tube Length	P	P_o	T_v	T_c	H_{vo}	H_v	H_L
0	87.0	99.5	294.8	53.5	1187.43	1176.53	288.08
0.25	85.0	99.0		61.4	1196.85	1184.20	286.39
0.50	82.0	96.0		67.9	1197.42	1183.50	283.79
0.75	78.5	92.0		73.5	1195.88	1182.70	280.66
1.00	75.0	88.0	293.0	79.3	1195.01	1181.90	277.43
1.50	68.0	81.5		90.0	1194.82	1180.00	270.60
2.00	61.5	74.5	295.5	99.3	1193.65	1178.05	263.75
2.50	55.5	69.0		108.0	1193.72	1176.10	256.90
3.00	50.0	64.0	255.6	115.5	1194.10	1174.10	250.90
3.50	45.0	60.0	242.6	122.6	1195.35	1172.00	243.36
4.00	40.5	56.8	237.0	128.5	1196.53	1169.95	236.79
4.50	36.5	53.6	225.8	133.5	1199.13	1167.90	230.48
5.00	32.8	50.7	218.3	138.2	1201.12	1165.88	224.05
5.50	29.6	48.5	210.2	142.2	1203.76	1163.82	218.03
6.00	26.7	46.3	205.6	146.0	1206.39	1161.79	212.07
6.50	23.8	44.0	201.0	149.2	1209.37	1159.64	205.67
7.00	21.5	41.5	196.0	152.3	1210.91	1157.65	200.06
7.25	20.5	40.4		153.9	1211.71	1156.75	197.48
7.50	19.5	39.0	194.0	155.2	1211.90	1155.80	194.79
7.75	18.6	37.0		156.8	1210.25	1154.86	192.28
8.00	18.0	35.0	192.0	158.1	1207.54	1154.20	190.56
8.50	16.8	30.5	190.4	160.2	1200.11	1152.88	186.93
9.00	15.7	26.4	189.5	162.0	1192.08	1151.64	183.43
9.50	15.0	22.5	184.0	163.8	1181.82	1150.80	181.11
10.00	14.2	19.0	188.1	165.3	1171.72	1149.76	178.31
10.50	13.8	16.4	187.6	166.8	1162.06	1149.22	176.85
11.00	13.5	14.7	186.9	168.1	1156.21	1148.80	175.86
11.50	13.5	13.5	186.7	169.5	1148.8	1148.8	175.86

Test Conditions

A) Parallel flow

B) Condenser tube I.D. = 0.190 in.

C) Cooling water rate = 159 lbm/min.

TABLE H-7 (cont.)

Computed Data												
Tube Length	Q_R	V_v	V_L	W_v	W_L	A_v	δ	f_v	f'_w	R_{ev}	R'_{ev}	h_v
	10^3					10^{-4}	10^{-2}	10^{-3}	10^{-3}	10^5	10^5	
0	0			94.20	0	1.96	0					
0.25	7.55	792	1.067	85.20	9.29	1.54	1.10	4.714	4.885	2.179	2.475	
0.50	13.38	811	1.469	79.20	15.65	1.45	1.35	4.839	5.142	2.097	2.457	
0.75	19.10	824	1.793	73.40	21.81	1.38	1.55	4.966				
1.00	24.65	837	2.038	67.80	27.75	1.31	1.75	5.369	6.021	1.905	2.348	
1.50	34.85	872	2.336	57.60	38.53	1.17	2.18	5.219	6.030	1.727	2.249	
2.00	43.75	911	2.502	49.00	47.78	1.05	2.56	4.566	5.417	1.567	2.155	17900
2.50	52.10	957	2.585	41.10	56.33	0.92	3.01	4.161	5.100	1.415	2.073	
3.00	59.20	1012	2.620	34.90				3.622	4.549	1.289	2.004	10600
3.50	66.00	1080	2.622	28.60	70.18	0.69	3.88	3.192	4.027	1.158	1.953	8540
4.00	71.60	1160	2.613	23.80	75.59	0.59	4.30	2.536	3.380	1.052	1.916	7180
4.50	76.40	1260	2.593	19.90	80.13	0.50	4.71	2.195	2.870	0.963	1.903	5860
5.00	80.90	1349	2.588	16.50	84.26	0.43	5.06	1.840	2.470	0.872	1.858	4840
5.50	84.70	1443	2.582	13.70	87.66	0.37	5.38	1.691	2.213	0.790	1.820	4060
6.00	88.30	1515	2.583	11.20	90.80	0.32	5.67	1.721	2.074	0.70	1.749	3660
6.50	91.40	1578	2.593	9.34	93.34	0.28	5.92	1.645	1.926	0.628	1.650	3260
7.00	94.40	1632	2.593	7.51	95.82	0.24	6.18	1.558	1.769	0.551	1.564	2900
7.25	95.90	1660	2.589	6.59	97.07	0.22	6.32	1.504				
7.50	97.10	1685	2.582	5.98	98.01	0.20	6.47	1.561	1.649	0.481	1.484	2750
7.75	98.80	1674	2.583	4.88	99.43	0.17	6.71	1.788				
8.00	99.80	1642	2.589	4.40	100.24	0.17	6.71	1.908	1.689	0.395	1.350	2690
8.50	101.00	1560	2.625	4.25	101.04	0.18	6.63	1.900	1.761	0.369	1.209	2690
9.00	103.70	1270	2.608	1.83	103.34	0.13	7.06	2.549	2.028	0.209	0.893	2700
9.50	105.40				104.76	0.11	7.25					2640
10.00	106.80	1030	2.632	1.40	105.85	0.10	7.36	3.016	2.439	0.161	0.691	2440
10.50	108.20	700	2.644	0.82	107.08	0.09	7.47	4.632	3.796	0.101	0.458	
11.00	109.50	350	2.633	0.28	108.27	0.06	7.84	6.013				2540
11.50	110.80	0		0	109.2	0	8.50					2490

Computed Conditions

A) Condensing length = 11.5 ft.

B) Total steam condensed = 94.2 lbm/hr (probe in) 10.92 lbm/hr (probe out)

C) Average heat transfer rate = 2080 ft lbf/ft sec.

D) Average heat gained by cooling water = 1840 BTU/min

E) Average heat lost by condensing vapor = 1840 BTU/min

F) Heat balance error = 0.0%

TABLE H-8

UConn Test 8-29-52

Experimental Data					Data From Steam Table		
Tube Length	P	P_o	T_v	T_c	H_{vo}	H_v	H_L
0	99.3	111.8	336.0	57.6	1189.81	1180.78	297.87
0.5	93.0	108.3	317.1	59.8	1199.03	1185.90	292.98
1.0	85.0	100.5	311.6	66.8	1198.53	1184.20	286.39
1.5	76.6	92.8	305.7	71.3	1198.15	1182.28	278.93
2.0	69.0	86.0	299.3	74.6	1198.39	1180.30	271.61
2.5	62.0	80.0	293.5	79.5	1199.20	1178.20	264.30
3.0	55.5	73.5	287.3	83.6	1199.98	1176.10	256.90
3.5	49.5	68.5	280.7	88.3	1196.17	1173.90	249.44
4.0	44.0	63.3	273.7	99.7	1198.12	1171.60	241.95
4.5	39.2	61.4	267.5	105.8	1206.12	1169.30	235.72
5.0	34.8	58.4	260.3	111.4	1209.40	1166.98	226.53
5.5	30.4	53.0	252.8	119.4	1209.76	1164.34	219.97
6.0	26.9	51.5	246.2	130.3	1215.22	1161.93	210.83
6.5	24.0	50.0	240.2	134.2	1220.16	1159.80	206.14
7.0	21.4	49.0	233.8	138.3	1226.09	1157.56	199.81
7.5	18.8	47.8	222.3	148.2	1242.42	1155.08	192.85
8.0	16.3	47.0	220.7	150.8	1240.85	1152.33	185.46
8.5	14.6	46.5	214.2	157.5	1247.51	1150.27	179.71
9.0	13.7	46.1	210.3	160.0	1251.36	1149.08	180.06
9.5	13.2	46.0	207.5	162.2	1253.85	1148.38	174.65
10.0	13.0	46.0	207.1	166.2	1254.93	1148.10	173.91
10.5	12.6	45.5	204.2	166.7	1256.18	1147.15	172.33
11.0	12.1	30.0	199.8	166.7	1219.90	1146.75	170.34

Test Conditions

A) Parallel flow

B) Condenser tube I.D. = 0.190 in.

C) Cooling water rate = 18.2 lbm/min.

TABLE H-8 (cont.)

Computed Data											
Tube Length	Q_R	V_v	V_L	W_v	W_L	A_v	δ	f_v	f'_w	R_{ev}	R'_{ev}
	10^3					10^{-4}	10^{-2}	10^{-3}	10^{-3}	10^5	10^5
0	0	673	0	101.00	0	1.960	0				
0.5	10.38	810	1.212	89.36	12.49	1.455	1.334	3.822	3.987	2.423	2.819
1.0	21.50	846	1.892	78.16	24.55	1.326	1.704	4.170	4.243	2.240	2.731
1.5	31.65	891	2.302	68.19	35.37	1.212	2.047	4.985	4.837	1.996	2.423
2.0	41.50	924	2.608	58.74	45.68	1.111	2.364	3.975	3.975	1.880	2.505
2.5	50.20	1022	2.632	50.50	54.75	0.955	2.884	3.179	3.249	1.762	2.534
3.0	58.40	1091	2.732	43.06	63.06	0.847	3.269	2.750	2.901	1.614	2.466
3.5	66.10	1055	2.977	36.45	70.54	0.825	3.351	2.904	3.113	1.400	2.170
4.0	73.10	1150	2.947	30.45	77.38	0.706	3.811	2.627	2.661	1.279	2.141
4.5	79.60	1348	2.825	24.85	83.84	0.548	4.488	2.167	2.051	1.199	2.278
5.0	85.20	1452	2.834	20.69	88.86	0.474	4.839	1.796	1.768	1.087	2.221
5.5	89.50	1503	2.889	17.76	92.64	0.446	4.979	1.853	1.697	0.975	2.054
6.0	92.50	1662	2.894	16.32	94.94	0.415	5.139	1.832	1.413	0.940	2.050
6.5	96.10	1703	2.928	14.02	98.09	0.390	5.272	1.147	1.433	0.845	1.910
7.0	100.20	1825	2.911	11.36	101.61	0.326	5.634	0.885	1.140	0.755	1.859
7.5	103.00	1945	2.929	10.10	103.73	0.307	5.749	0.717	0.927	0.701	1.778
8.0	105.80	2095	2.957	8.89	105.79	0.297	5.810	0.534	0.710	0.647	1.700
8.5	108.00	2270	2.947	8.11	107.43	0.268	5.995	0.469	0.479	0.618	1.680
9.0	109.20	2450	2.934	6.37	110.02	0.203	6.450	0.390	0.317	0.554	1.709
9.5	111.10	2590									
10.0	112.20	2850	2.927		111.26						
10.5	113.30	2640	2.977		112.01						
11.0	114.50	2070	3.157		112.61						

Computed Conditions

A) Condensing length = 11.0 ft.
B) Total steam condensed = 121 lbm/hr (probe out) 101 lbm/hr (probe in)
C) Average heat transfer rate = 2250 ft lbm/ft sec.
D) Average heat gained by cooling water = 1985 BTU/min.
E) Average heat lost by condensing vapor = 1888 BTU/min.
F) Heat balance error = 4.9%

APPENDIX I

Correlation of Friction Factors

An accurate solution of the system of non-linear differential equations of change developed during this research program requires input data of considerable precision. In particular, it is necessary to introduce the values of either the local interfacial vapor friction factor (f_v) or the superficial wall friction factor (f_w') within several percent of the true value. Because of the nature of the physical system, a small deviation in the input friction data seems to have a snowballing effect on the subsequent variation in stream pressure and vapor velocity. Figs. 15 through 18 have been computed specifically to demonstrate the very marked effect which a small variation in either friction factor has on the analytical solution of the system of equations. Note that the vapor friction factor must be used with the vapor momentum equation in the numerical solution of the system of equations. The superficial wall friction factor must be used in the combined momentum equation in the numerical solution of the system of equations. Both equations have been used in the numerical solution, but not both at the same time. Figs. 19, 20, and 21 have been plotted to demonstrate that an analytical solution of the system of equations will agree almost identically with the experimental data if the input friction factor data corresponds closely with experimentally determined friction factor. For the solution plotted in Figs. 19, 20, and 21, the input friction factor was carefully chosen so as to cause the vapor velocity to agree with the experimental data. It is gratifying to note that this arbitrary input friction factor agrees almost precisely with the friction factor computed from the experimental data. In addition, the other flow properties such as stream

pressure and liquid velocity (Figs. 19 and 20) also show good agreement between the experimental and analytical values. The agreement obtained between analytical and experimental data demonstrated in Figs. 19, 20, and 21, also Figs. 22, 23, and 24, demonstrates the general validity of the mathematical model used in the development of the system of equations of this paper. This is not to imply that a more precise model and accompanying analysis cannot be found. Indeed, work is being done at the present time to improve our understanding of the true physical model and to develop an analytical treatment of such a model.

Considerable effort has been expended in attempts to find satisfactory empirical correlations of the two local friction factors in terms of the experimentally determined flow properties. No really satisfactory empirical correlation of either friction factor has been found. The most promising attack on this important problem involves the division of the respective friction factors into their component parts. Examination of the form of the vapor momentum follows thus

$$f_v = \frac{-1}{V_v}\left(\frac{W_v}{\pi \rho_v V_v}\right)^{\frac{1}{2}}\left[\left(\frac{V_v - V_i}{W_v}\right)\frac{dW_v}{dL} + \frac{dV_v}{dL} + \frac{g_c}{\rho_v V_v}\frac{dP}{dL}\right] \qquad 11H$$

It is observed that the derivative (dW_v/dL) is primarily a function of the local radial heat transfer rate H_o. Since the heat transfer rate is, in large part, controlled by external factors such as temperature of the cooling fluid and external heat transfer resistances, it is seen that the derivative (dW_v/dL) remains essentially an arbitrary function which is independent of the internal local flow properties. For this reason, no empirical correlation can hope to accurately predict the vapor friction factor (f_v) unless it includes

these external factors in the correlation. Since it was the intent to confine the present analysis to an attack on the internal flow mechanics of the condenser tube, it was decided to split the vapor friction factor into component parts as follows:

$$f_v = f_{v\theta} + f_{v\beta} + f_{v\phi} \qquad 1I$$

where the three subscripts relate to the three derivatives of Equation 11H . Taking the sum of the second two terms, we have then a reduced form

$$f_{v\beta\phi} = -\frac{1}{V_v}\left(\frac{W_w}{\pi \rho_v V_v}\right)^{\frac{1}{2}}\left[\frac{dV_v}{dL} + \frac{g_c}{\rho_v V_v}\frac{dP}{dL}\right] \qquad 2I$$

This fraction of the interfacial vapor friction factor has been plotted in Figs. 32, 33, and 34. These figures indicate that there is more promise of correlating this fraction of the vapor friction factor as a function of the internal flow mechanics of the two-phase system.

A similar treatment of the superficial wall friction factor leads to the reduced form

$$f'_{w\beta\phi} = \frac{-2}{\pi D \rho_v V_v^2}\left[W_L \frac{dV_L}{dL} + W_v \frac{dV_v}{dL} + g_c A \frac{dP}{dL}\right] \qquad 3I$$

Values of this term have been plotted in Figs. 35, 36, and 37. Here again, there appears to be more promise of correlating the above fraction of the wall friction factor.

It should be noted that four fundamental differential equations are required in order to find a numerical solution which will determine local values of the four normalized fundamental flow properties α , β , θ, and ϕ. If a

satisfactory correlation of the partial vapor friction factor ($f_{v\beta\phi}$) as a function of the local flow properties is available, the differential Equation 2I may serve as one of the required differential equations, replacing the vapor momentum equation in the programmed system of equations.

Work has been done by a number of investigators (1), (9), (17), (24) on the problem of flow friction and pressure loss in two-phase flow. Most of the experimental data reported is for two-phase, two-component mixtures of air and water or other fluids. Usually the two-component data is for adiabatic flow with no interphase mass transfer. Correlation parameters commonly used are liquid and vapor Reynolds numbers based on mass flow rates using the total tube cross section for both the liquid and the vapor rate calculated independently. Mass flow rates calculated in this fashion are obviously fictitious, consequently Reynolds numbers calculated on this basis are commonly referred to as fictitious or superficial.

As indicated previously, attempts were made to correlate the friction data accumulated for two-phase condensing flow by these conventional methods. The results obtained were essentially negative and it was not considered worthwhile to present them in this report. However, some of the important differences between the adiabatic two-phase, two-component system and the single component condensing system will be noted:

1. The momentum change of the condensing vapor fraction plays a significant role in the vapor momentum equation and enters into the determination of the interfacial friction factor. Obviously this factor is not present in adiabatic, two-phase, two-component flow.
2. In condensing flow, the vapor velocity and static pressure may both rise and fall at some point over the condensing length. The local

derivatives of these flow properties may therefore, be both positive and negative at different axial locations. It is obvious that considerable variation of the local vapor friction factor may occur over the length of a single condenser tube. For this reason, the use of average flow properties and the overall pressure drop in calculating an overall or average friction factor in condensing two-phase flow leads to inconclusive results by any method of correlation.

3. In condensing two-phase flow, it has been observed that under certain conditions it is possible to have a local upstream or reverse flow of the liquid at the tube wall. This condition will exist when the vapor is deceleration results in a local pressure rise or momentum regain in the axial flow direction. Since no significant pressure gradient exists in the radial direction, there must be a corresponding pressure rise in the liquid layer at the same axial location. The rate of liquid velocity deceleration necessary to support the same pressure rise as occurs in the vapor cone results in a reverse flow in the liquid layer close to the tube wall. The net or average liquid velocity remains positive since the liquid carried forward by the interfacial liquid waves and any entrained liquid fraction in the vapor dominates the total liquid flow. A local reverse liquid flow at the tube wall results in a reverse wall shear stress and a corresponding negative wall friction factor at that location. Such a condition is never encountered in adiabatic two-phase, two-component flow. It is obvious that the empirical correlation of negative local wall friction factors would be a difficult feat by any method of correlation. The possibility of negative wall friction factors in two-phase condensing flow is the most important reason for choosing the vapor momentum equation as

the preferable fourth equation in the analytical solution of the system of differential equations developed in this paper. The analytical solutions obtained by the methods developed in this paper require quite precise input information on local friction factors. The problem of satisfactory correlation of either interfacial or wall friction factors for two-phase condensing flow certainly is the chief hurdle to be overcome in achieving satisfactorily accurate analytical solutions to the flow characteristics of the condensing two-phase fluid system.

APPENDIX J

Empirical Correlation of Local Heat Transfer Surface Coefficients In Two-Phase Condensing High Velocity Flow

Depending on the external resistance to heat transfer from the condenser tube, the internal or condensing layer resistance plays a lesser or greater role in determining the flow characteristics in the tube during condensation. For the case of low external resistance to heat transfer, it is necessary to determine the internal local surface coefficient accurately.

Very little experimental data on local heat transfer coefficients for high velocity condensing flow have been found in the literature. Several investigators have proposed methods for correlating surface heat transfer coefficients in two-phase high velocity condensing flow.

Powell, (17) proposed a method to predict average coefficients of heat transfer in low-speed, two-phase flow with condensation on the basis of a weighting or equivalent flow procedure.

Carpenter, (1) suggested a method whereby the Nusselt number is given as a function of the liquid Prandtl number and the so-called "friction Reynolds number." Carpenter's correlation, when applied to the conditions of high velocity tests conducted at the University of Connecticut, predicted surface coefficients about 70 per cent lower than the experimentally determined values.

A paper by S. S. Kutateladze, (16) suggests the following empirical correlation for the local heat transfer surface coefficients of a condensing vapor:

$$\frac{hD}{k_L} = C \left[\left(\frac{\nu_L}{a_L} \right)^a \left(\frac{gD^3}{V_L^2} \right)^b \left(\frac{\lambda c}{C_{pL} \Delta t} \right)^c \left(\frac{f_v V_v^2 \rho_v}{gD\rho_L} \right)^d \right] \qquad 1J$$

where the nomenclature is as follows:

h	local surface coefficient of heat transfer
D	tube diameter
C	constant
k_L	thermal conductivity of the liquid
ν_L	kinematic viscosity of the liquid
α_L	thermal diffusivity of the liquid
g	acceleration due to gravity
ρ_v	weight density of vapor
ρ_L	weight density of liquid
C_{pL}	specific heat capacity of the liquid
λc	latent heat of vaporization of the fluid
Δt	difference between the phase temperature and its equilibrium temperature
f_v	vapor friction factor
V_v	average vapor velocity

When the methods of the several references given above were applied to the conditions for which test data on condensing steam were recorded at the University of Connecticut, no successful correlation could be obtained. Consequently, it was necessary to make a fresh attack on the problem by the well-known methods of dimensional analysis. Various dimensionless groupings involving the Nusselt number and the so-called 'j' factor or Colburn number were tried with little success.

It was theorized that the local heat transfer coefficient could be affected by the following fundamental local variables: h_c, Δt, ρ_v, V_v, δ, D, ρ_L, V_L, μ_L, and μ_v. Where Δt is the difference between the local steam saturation

temperature and the inside tube wall temperature. The other variables have been defined in the Nomenclature.

It is seen that with the above choice of variables, the combination $h\Delta t$ occurs necessarily to satisfy non-dimensionality. It appears, therefore, that what is really being correlated is the heat transfer rate per unit area as expressed by $(h\Delta t)$ rather than the surface coefficient itself. This is a common occurrence in boiling and condensing heat transfer.

Grouping the above variables in a non-dimensional manner led to the following arrangement that appears to give a useful correlation of the experimental data recorded at the University of Connecticut for condensing steam vapor.

$$\frac{h\Delta t}{\rho_v V_v \delta g} = 1.186 \times 10^7 \left[\left(\frac{\mu_v}{\rho_v V_v D} \right)^{0.887} \left(\frac{\rho_L V_L \delta}{\mu_L} \right)^{0.374} \left(\frac{V_v}{V_L} \right)^{0.167} \left(\frac{D}{\delta} \right)^{1.446} \right] \qquad 2J$$

Equation 2J may be written in the functional form

$$\frac{h\Delta t}{\rho_v V_v \delta g} = f \left[(Re_v)^{-8/9} (Re_L)^{3/8} \left(\frac{V_v}{V_L} \right)^{1/6} \left(\frac{D}{\delta} \right)^{13/9} \right] \qquad 3J$$

Fig. 42 shows the experimental data for condensing steam vapor plotted using the left- and right-hand sides of Equation 3J as ordinate and abscissa respectively on log-log paper. If the correlation is written in the functional form

$$h\Delta t = f \left[D^a, \delta^b, \rho_v^c, \rho_L^d, V_v^e, V_L^f, \mu_v^g, \mu_L^h \right] \qquad 4J$$

we find that

$$h\Delta t = f \left[D^{5/9} \delta^{-1/14} \rho_v^{1/9} \rho_L^{3/8} V_v^{5/18} V_L^{5/24} \mu_v^{8/9} \mu_L^{-3/8} \right] \qquad 5J$$

Surprisingly this correlation indicates that the tube diameter and vapor velocities play a stronger role in determining the rate of heat transfer than does the mean thickness (δ) of the annular liquid layer.

Obviously this correlation applies specifically to steam vapor and may be unsatisfactory for other vapors. The necessary data on the local flow characteristics of other vapors evidently is not available at the present time.

The details of the method of determining the exponents of the correlation, Equation 2J , will be described briefly. In order to derive the desired exponent values from the available volume of experimental data, the following equation set was established.

$$X_{01} = C\,(X_{11})^{a}\,(X_{21})^{b}\,(X_{31})^{c} \text{ ----- } (X_{n1})^{z}$$

$$X_{02} = C\,(X_{21})^{a}\,(X_{22})^{b}\,(X_{32})^{c} \text{ ----- } (X_{n2})^{z} \qquad 6J$$

$$X_{0n} = C\,(X_{1n})^{a}\,(X_{2n})^{b}\,(X_{3n})^{c} \text{ ----- } (X_{nn})^{z}$$

Where $n = z + 1$ since there are z unknown exponents and also one unknown constant. Eliminating the constant C from the n equations by dividing the first equation by the second, the first by the third, and so on leads to the following set of z equations.

$$\frac{X_{01}}{X_{02}} = \frac{X_{11}}{X_{12}}^{a}\ \frac{X_{21}}{X_{22}}^{b}\ \frac{X_{31}}{X_{32}}^{c} \text{ ----- } \frac{X_{n1}}{X_{n2}}^{z}$$

$$\frac{X_{01}}{X_{0n}} = \frac{X_{11}}{X_{1n}}^{a}\ \frac{X_{21}}{X_{2n}}^{b}\ \frac{X_{31}}{X_{3n}}^{c} \text{ ----- } \frac{X_{n1}}{X_{nn}}^{z} \qquad 7J$$

Taking the natural logarithm of both sides of all equations results in the following equation set:

$$\ln \frac{X_{01}}{X_{0n}} = a \ln \frac{X_{11}}{X_{12}} + b \ln \frac{X_{21}}{X_{22}} + c \ln \frac{X_{31}}{X_{32}} \text{ ----- } + z \ln \frac{X_{n1}}{X_{n2}} \qquad 8J$$

$$\ln \frac{X_{01}}{X_{0n}} = a \ln \frac{X_{11}}{X_{1n}} + b \ln \frac{X_{21}}{X_{2n}} + c \ln \frac{X_{31}}{X_{3n}} \text{ ----- } + z \ln \frac{X_{n1}}{X_{nn}}$$

In this system of equations, X quantities represent the experimental data. We have then a set of simple linear algebraic equations with unknowns a, b, c, d, ----- z and with coefficients determined from experimental data. Using a digital computer program available at the University of Connecticut Computer Center, in conjunction with a sub program written to evaluate the natural logarithms, it was possible to solve for the desired exponents on an I.B.M. 1620 computer.

As indicated previously, the results of this work are shown in Fig. 42. In addition, Figs. 43 and 44 have been plotted to show the wide variation in local surface coefficients which are encountered in high velocity condensation of steam vapor. Since the data plotted in Figs. 43 and 44 were the source information used in obtaining the correlation presented in this Appendix, it is not surprising that values of the local surface coefficient calculated by use of the empirical Equation 2J give close agreement with the experimental data.

It should be noted that the necessary data to obtain a satisfactory correlation for the local surface coefficient for condensing steam includes: 1) the local mean thickness of the liquid layer (δ), 2) the local mean liquid layer velocity (V_L), 3) the local vapor velocity (V_v), and 4) the local

surface to vapor temperature difference (Δt), plus the local physical properties of the liquid and vapor. Experimental data on the value of these local flow properties is difficult to obtain. No other investigators known to the author have made the necessary experimental measurements to permit determination of these local flow properties. However, such data will be necessary in order to successfully correlate local heat transfer surface coefficients for other condensing vapors in high velocity two-phase flow.

TABLE I

A TABLE OF NON-DIMENSIONAL DIFFERENTIAL EQUATIONS OF HIGH SPEED TWO-PHASE FLOW WITH CONDENSATION IN LONG SMALL TUBES

The general differential equation is written in the following non-dimensional form

$$A\frac{d\alpha}{dX} + B\frac{d\beta}{dX} + C\frac{d\theta}{dX} + D\frac{d\phi}{dX} = K$$

The coefficients A, B, C, D and K for the different physical equations are as follows:

	Equation source	A	B	C	D	K
1.	Combined equations of continuity	$\left[\frac{1-\theta}{\theta}\right]\frac{\sigma\beta\phi^j}{\alpha^2}$	$+ 1/\beta$	$+\frac{1}{\theta}\left[\frac{\sigma\beta\phi^j}{\alpha} - 1\right]$	$+ j/\phi$	$= 0$
2.	Equation of motion of vapor	0	$+ \theta$	$+ \left[\beta - 2\alpha\right]$	$+ \frac{\theta N}{\beta\phi^j}$	$= -2f_v\beta^{3/2}\sqrt{\theta\phi^j}$
3.	Combined equations of vapor and liquid motion	$\left[1-\theta\right]$	$+ \theta$	$+ \left[\beta - \alpha\right]$	$+ N$	$= -2f'_w\beta^2\phi^j$
4.	Combined energy equation of vapor and liquid	$\left[1-\theta\right]\alpha$	$+\beta\theta$	$+\left[\frac{\lambda}{\phi^c} + \frac{1}{2}(\beta^2 - \alpha^2)\right]$	$+\left[\frac{b\epsilon\theta}{\phi^{1-b}} + \frac{a\eta(1-\theta)}{\phi^{1-a}}\right]$	$= -\}[$
5.	Velocity pressure at interface for incompressible flow	$\frac{1}{\alpha}$	$-\frac{1}{\beta}$	$+ 0$	$-\frac{j}{2\phi}$	$= 0$
6.	Velocity pressure at interface for compressible flow	$\frac{2}{\alpha}$	$-\frac{SM^2}{\beta}$	$+ 0$	$+\left[\frac{SM^2 t - 2t - j}{\phi}\right]$	$= 0$
7.	Initial liquid boundary layer	$\frac{2}{\cdot}$	$+ 0$	$+\frac{1}{1-\theta}$	$-\frac{j}{2\phi}$	$= -\frac{1}{2X}$

The derivations of the equations summarized in this table are reported in the appendices of the "First Interim Report" of April 1962, in "Project Note 3", and in the "Final Summary Report" for this project.

TABLE II

Dimensionless Constant Coefficients for the Equation Set

$$N \equiv \left[\frac{g_c P_e}{\rho_{v_e} V_{v_e}^2}\right] \qquad \epsilon \equiv \left[\frac{h_{v_e}}{V_{v_e}^2/g_c}\right]$$

$$\sigma \equiv \rho_{v_e}/\rho_L \qquad \eta \equiv \left[\frac{h_{L_e}}{V_{v_e}^2/g_c}\right]$$

$$\lambda \equiv \left[\frac{h_{v_e} - h_{L_e}}{V_{v_e}^2/g_c}\right] = \left[\frac{h_{fg_e}}{V_{v_e}^2/g_c}\right]$$

Dimensionless Variable Coefficients for the Equation Set

$$H \equiv \left[\frac{g_c D H_o}{W V_{v_e}^2}\right]$$

A dimensionless heat transfer number where for example in test Uconn 81452.

$$H_o = (2030 - 1.37X) \quad \left(\frac{\text{ft lb}_f}{\text{sec}}\right)$$

Near the tube mouth from "Appendix F" of the "First Interim Progress Report".

$$\tau_v/p_e \cong \tau L/p_e = 0.332 \left[\frac{V_{v_e}^3}{g_c D}\frac{\mu_{v_e}\rho_{v_e}}{p_e^2}\right]^{1/2} \times \left[\frac{\phi^i}{X}\right]^{1/2}$$

For the developing liquid boundary layer near the tube mouth then

$$\Psi \equiv \tau_L/p_e = \psi \left[\frac{\phi^i}{X}\right]^{1/2} \quad \text{where} \quad \psi = 0.332 \left[\frac{V_{v_e}^3 \mu_v \rho_{v_e}}{g_c D p_e^2}\right]^{1/2}$$

and ψ is a constant for a particular test in the region up to approximately

$Re_{v_x} = 500{,}000$

$$S \equiv \frac{k\left(1 + \frac{k-1}{2} M^2\right)^{1/k-1}}{\left[\left(1 + \frac{k-1}{2} M^2\right)^{k/k-1} - 1\right]}$$

Table III

Major Dimensions of Experimental Condenser Heat Exchangers from Which the Tabulated Data Was Recorded

Test Unit	Condenser Tube I.D. Inches	Condenser Tube O.D. Inches	Outer Tube I.D. Inches	Overall Condenser Tube Length In Feet	Cooling Water Flows	Annulus Thermo-couples	Detailed Diagram In
Heat Exchanger No. 1	0.550	0.625	1.026	10.3	Counter Flow	Traveling probe only	
Heat Exchanger No. 2	0.550	0.625	1.026	10.3	Parallel Flow	Fixed in wall of outer tube and traveling*	Figure 28
Heat Exchanger No. 3	0.190	0.250	0.550	11.7	Parallel Flow	Fixed in wall of outer tube and traveling	Figure 29

*In this heat exchanger thermocouples were also fastened to the outer wall of the inner condensing tube.

List of References

1. F. G. Carpenter, "Heat Transfer and Pressure Drop for Condensing Pure Vapors Inside Vertical Tubes at High Vapor Velocities," Ph.D. Thesis, University of Delaware, 1948.

2. D. A. Charvonia, "An Experimental Investigation of the Mean Liquid Film Thickness and the Characteristics of the Interfacial Surface in Annular, Two-Phase Flow," A.S.M.E. Paper, 61-WA-243.

3. J. C. Y. Koh, "An Integral Treatment of Two-Phase Boundary Layer in Film Condensation," A.S.M.E. Paper, 60-WA-253.

4. C. J. Baroczy and V. D. Sanders, "Pressure Drop for Flowing Vapors Condensing in a Straight Horizontal Tube," A.S.M.E. Paper, 61-WA-257.

5. C. H. Coogan, Jr. and W. E. Hilding, "Final Summary Report on Steam Condensation in Small Tubes," (Summary of Reports 1, 2, and 3) U. S. Air Force Subcontract, University of Connecticut, October 15, 1952.

6. C. H. Coogan, Jr., W. E. Hilding and H. H. Samuelson, "Final Summary Report on Steam Condensation in Small Tubes," (Summary of Reports 4 through 15) U. S. Air Force Sub-contract, University of Connecticut, November 30, 1953.

7. M. Jakob, "Heat Transfer," vol. I, John Wiley and Sons, New York, 1949.

8. P. K. Kegel, "Two-Phase Flow in a Vertical Column," B. Ch.E. Thesis, University of Delaware, 1948.

9. R. W. Lockhart and R. C. Martinelli, "Proposed Correlation of Data for Isothermal Two-Phase, Two-Component Flow in Pipes," Chemical Engineering Progress, vol. 45, no. 1, 1949.

10. S. Levy, "Prediction of Two-Phase Pressure Drop and Density Distribution from Mixing Length Theory," A.S.M.E. Paper No. 62-HT-6.

11. S. Levy, "Steam Slip—Theoretical Prediction from Momentum Model," A.S.M.E. Paper No. 59-HT-15.

12. S. Levy, "Theory of Pressure Drop and Heat Transfer for Annular Steady-State Two-Phase Two-Component Flow in Pipes," Second Midwestern Conference on Fluid Mechanics, Proceedings, 1952.

13. S. F. Chien, and W. Ibele, "Pressure Drop and Liquid Film Thickness of Two-Phase Annular-Mist Flows," A.S.M.E. Paper No. 62-WA-170.

14. P. G. Hill, H. Witting and E. P. Demetri, "Condensation of Metal Vapors During Rapid Expansion," A.S.M.E. Paper No. 62-WA-123.

15. H. Fauske, "Critical Two-Phase Steam Water Flow," Heat Transfer & Fluid Mechanics Institute, 1961.

16. S. S. Kutateladze, "Heat Transfer In Condensation and Boiling," Second Edition, Publication of the State Scientific and Technical Publishers - Moscow-Lenningrad, 1952, AEC-tr-3770.

17. C. K. Powell "Condensation Inside a Horizontal Tube With High Vapor Velocity," Master's Thesis, Purdue University, 1961.

18. A. H. Shapiro, "The Dynamics and Thermodynamics of Compressible Fluid Flow," vol. I, The Ronald Press Co., New York, 1953.

19. Keenan and Keyes, "Thermodynamic Properties of Steam," John Wiley and Sons.

20. Bird, Stewart and Lightfoot, "Transport Phenomena," John Wiley and Sons.

21. W. E. Hilding "First Interim Progress Report" to NASA, April 1962, (Code SC-NsG-204-62) Mechanical Engineering Department, University of Connecticut.

22. W. E. Hilding, "Second Interim Progress Report" to NASA, January 1963, (Code SC-NsG-204-62) Mechanical Engineering Department, University of Connecticut.

23. H. Schlichting, "Boundary Layer Theory," Fourth Edition, McGraw-Hill Book Company, Inc., New York, 1960.

24. D. A. Charvonia, "A Review of the Published Literature Pertaining to the Annular, Two-Phase Flow of Liquid and Gaseous Media In a Pipe," Report No. TM-58-1, Purdue University and Purdue Research Foundation, November 1958.

25. O. P. Bergelin and G. Gazley, Jr., "Co-Current Gas-Liquid Flow-I-Flow In Horizontal Tubes," Heat Transfer and Fluid Mechanics Institute, Berkeley, California, 1949.

26. R. C. Martinelli and D. B. Nelson, "Prediction of Pressure Drop During Forced-Circulation Boiling of Water," Trans. A.S.M.E., vol. 70, 1948.

27. L. M. K. Boelter and R. H. Kepner, "Pressure Drop Accompanying Two-Component Flow Through Pipes," Industrial Engineering Chemistry, No. 31, pp. 426-434, 1939.

28. W. E. Hilding and A. Burbank, Project Note NASA No. 6, April 1963, (Code SC-NsG-204-62) Mechanical Engineering Department, University of Connecticut.

FIG 1 A CLASSIFICATION OF AREAS OF TWO PHASE FLOW RESEARCH

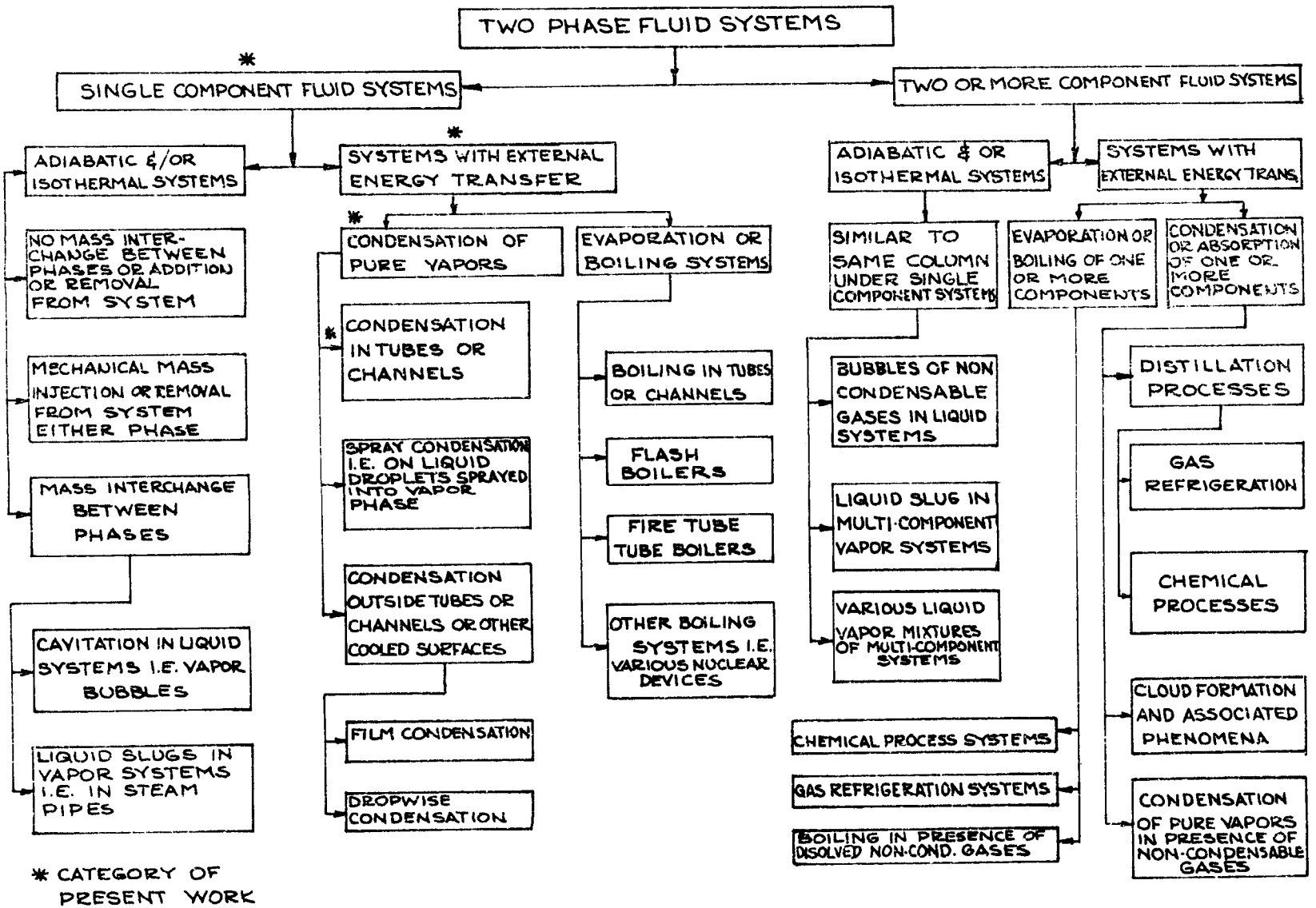

* CATEGORY OF PRESENT WORK

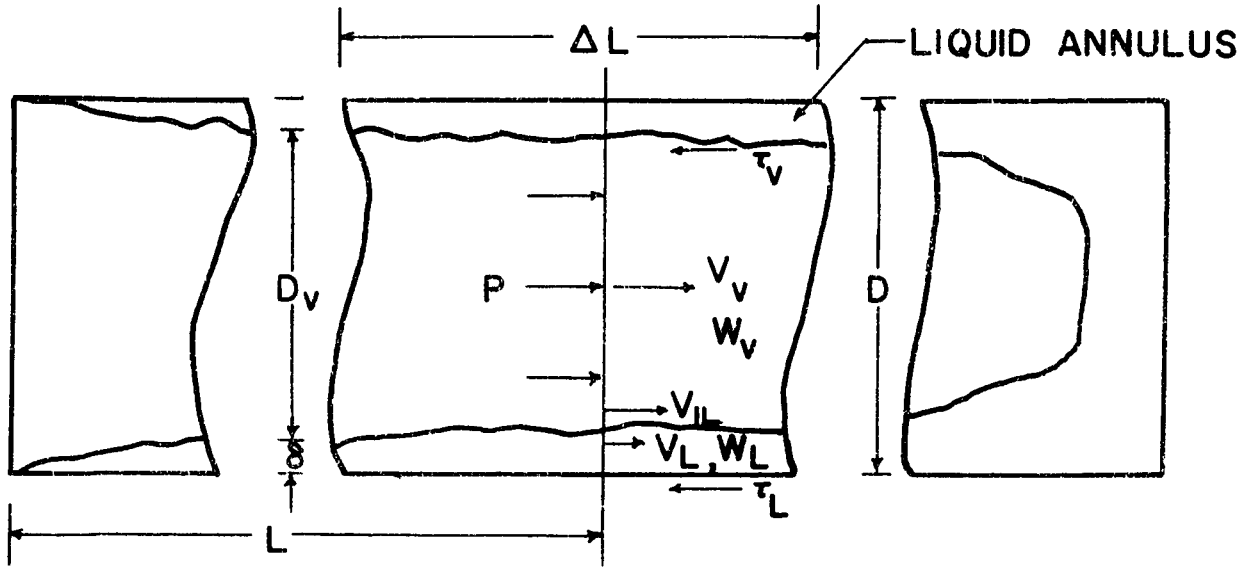

FIG 2 - Annular Two-Phase Flow Model

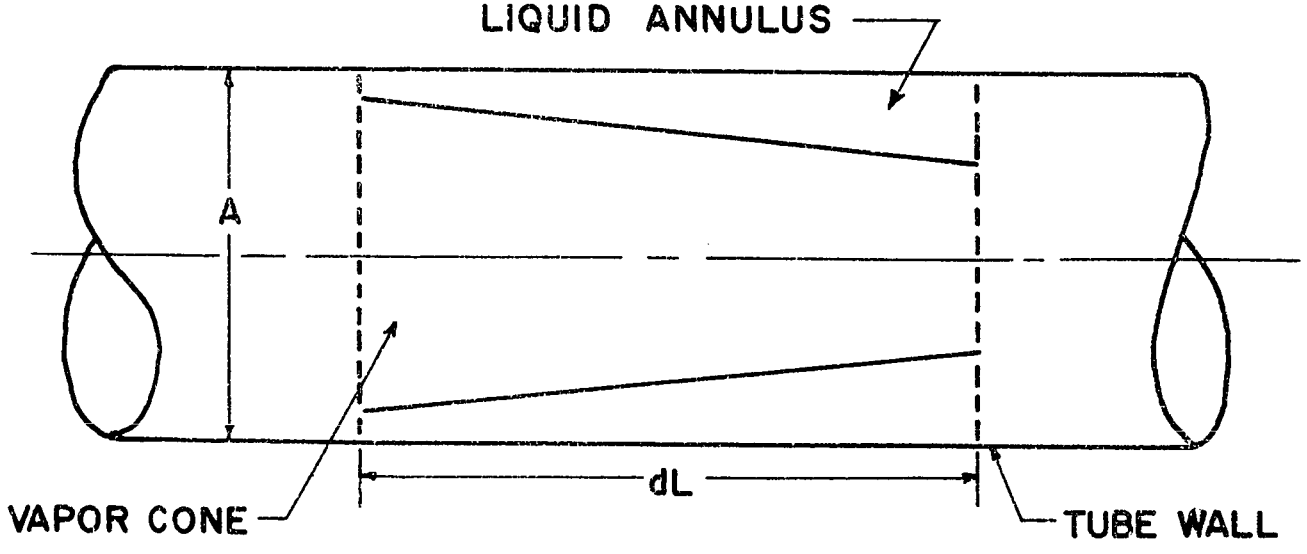

FIG 3 - Differential Tube Length Control Volume

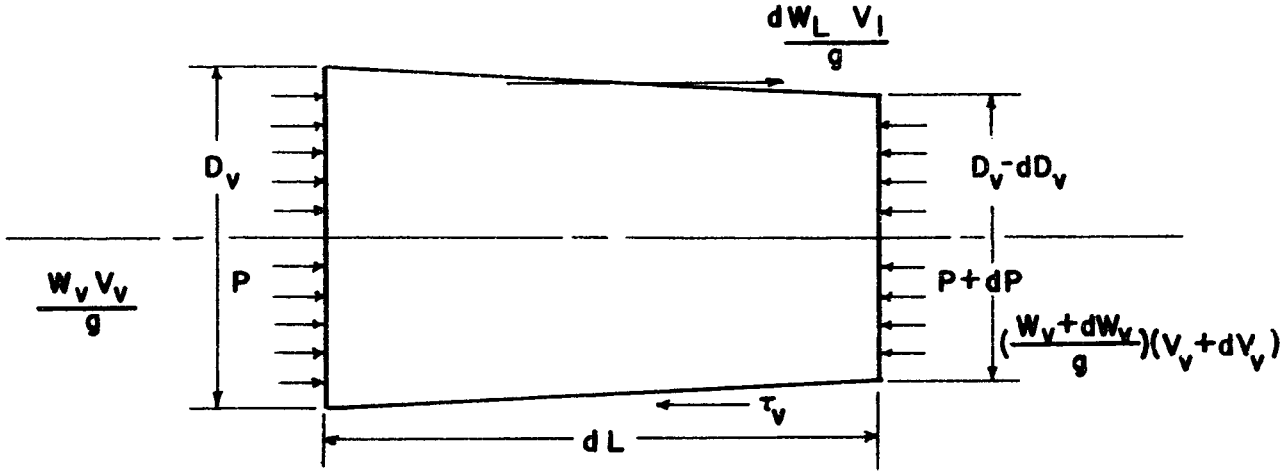

FIG 4 - Control Volume for Vapor Phase

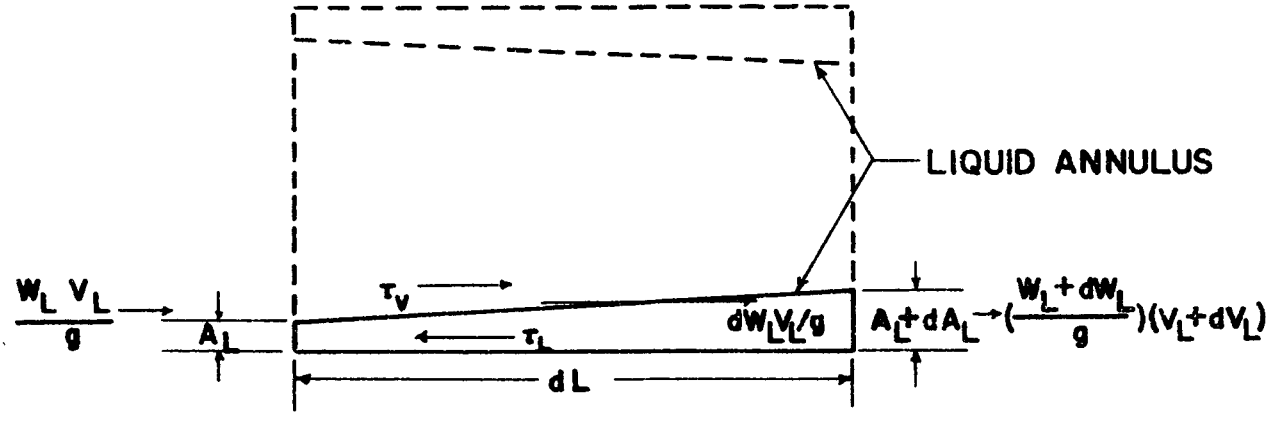

FIG 5 - Control Volume for Liquid Phase

FIG 6

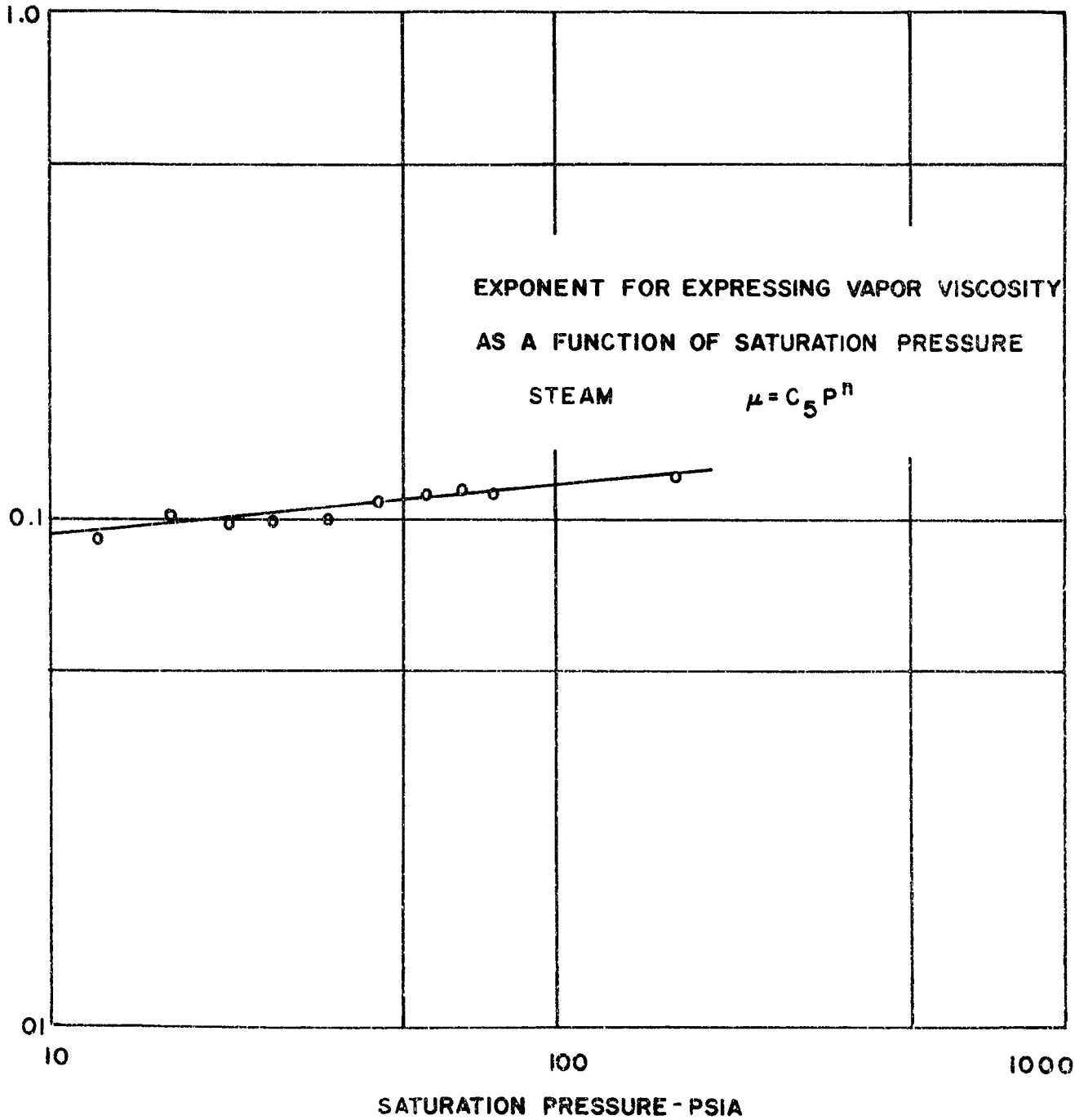
1.0
0.1
01
10
100
1000
EXPONENT FOR EXPRESSING VAPOR VISCOSITY
AS A FUNCTION OF SATURATION PRESSURE
STEAM
$\mu = C_5 P^n$
SATURATION PRESSURE - PSIA

FIG 7

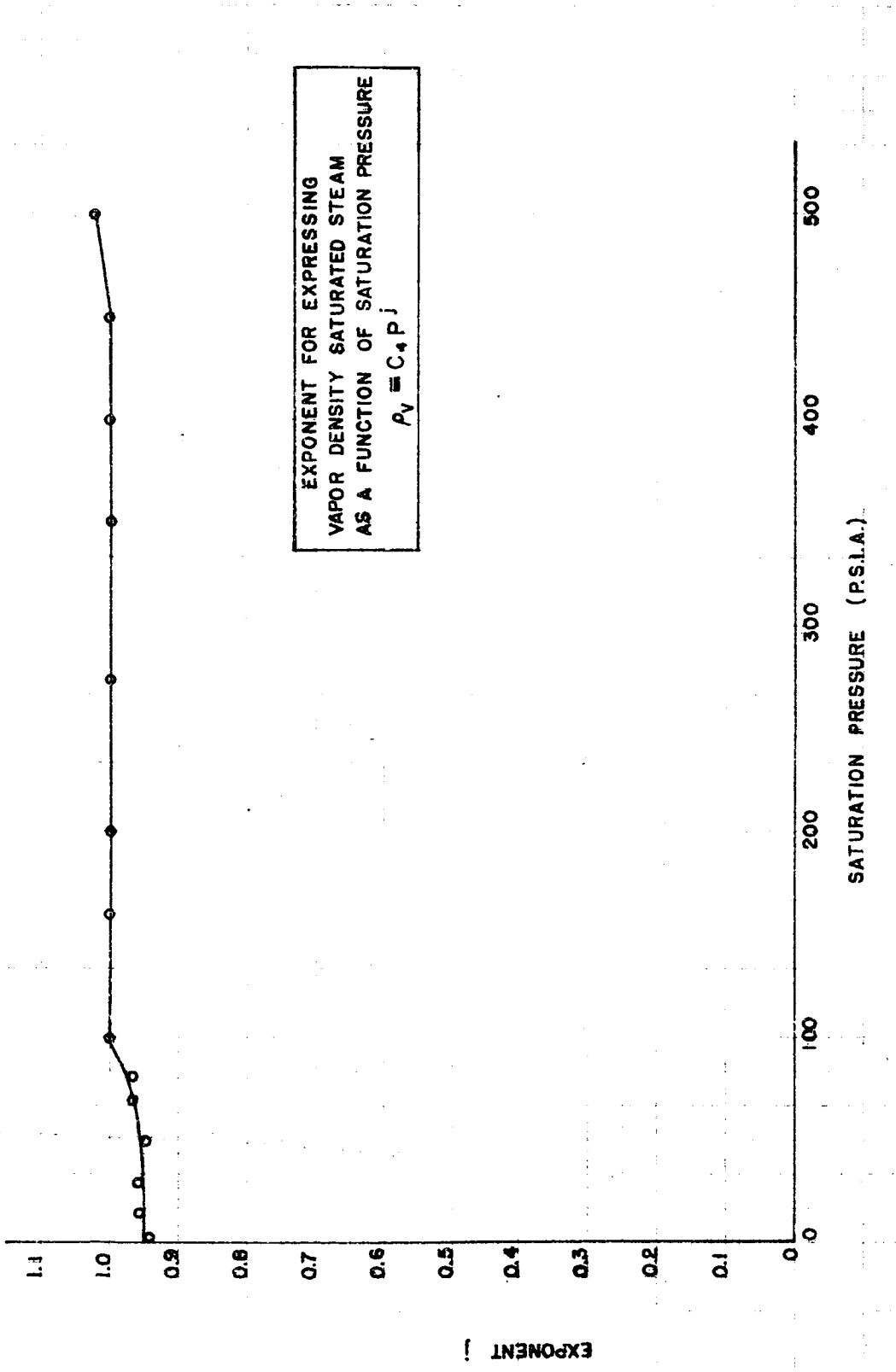
EXPONENT FOR EXPRESSING
VAPOR DENSITY SATURATED STEAM
AS A FUNCTION OF SATURATION PRESSURE
$\rho_v = C_4 P^j$
EXPONENT j
1.1
1.0
0.9
0.8
0.7
0.6
0.5
0.4
0.3
0.2
0.1
0
0
100
200
300
400
500
SATURATION PRESSURE (P.S.I.A.)

FIG 8

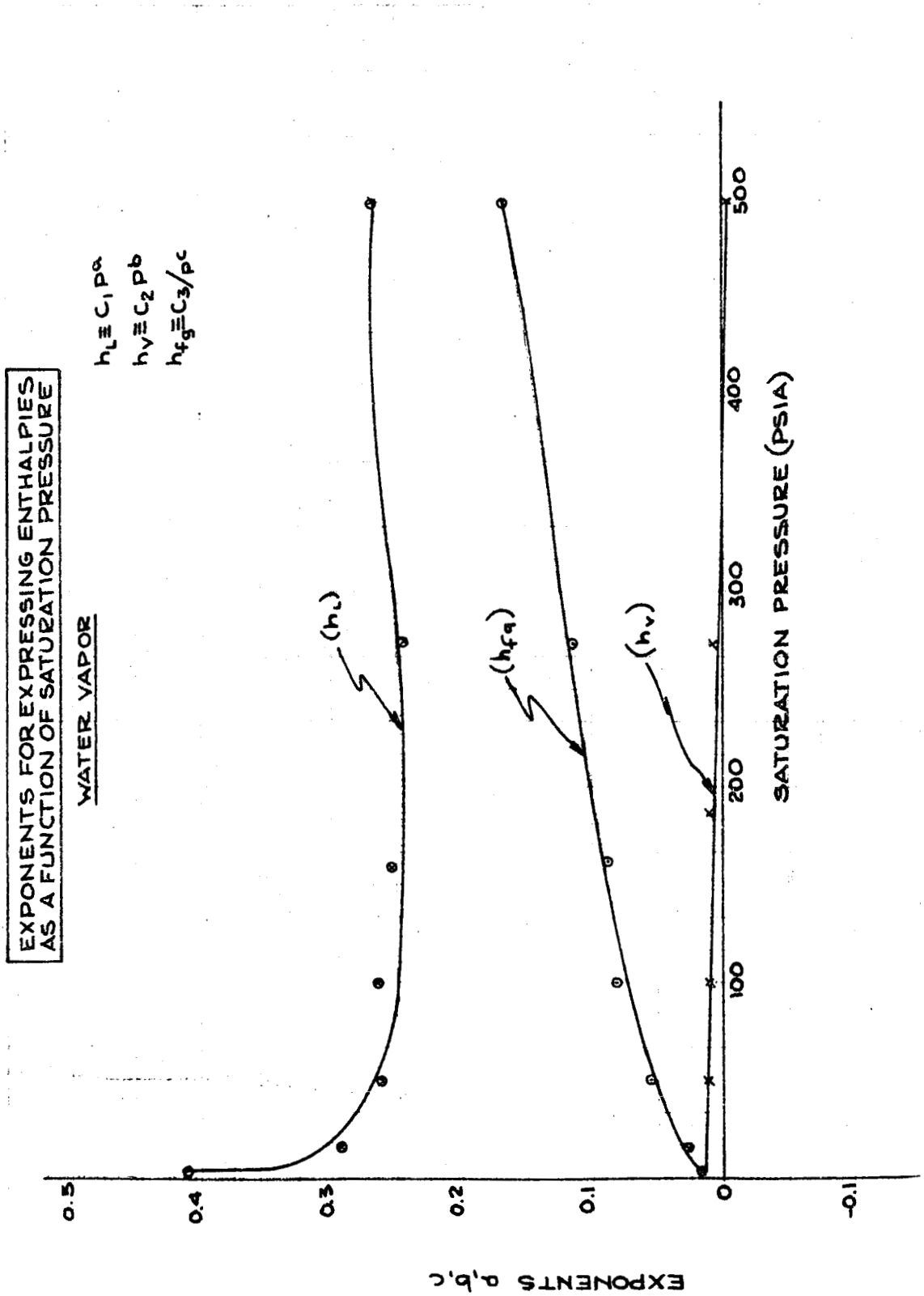
EXPONENTS FOR EXPRESSING ENTHALPIES AS A FUNCTION OF SATURATION PRESSURE
WATER VAPOR
$h_L \equiv C_1 P^a$
$h_v \equiv C_2 P^b$
$h_{fg} \equiv C_3/P^c$
(h_L)
(h_fg)
(h_v)
EXPONENTS a,b,c
SATURATION PRESSURE (PSIA)
0.5
0.4
0.3
0.2
0.1
0
-0.1
100
200
300
400
500

FIG 9

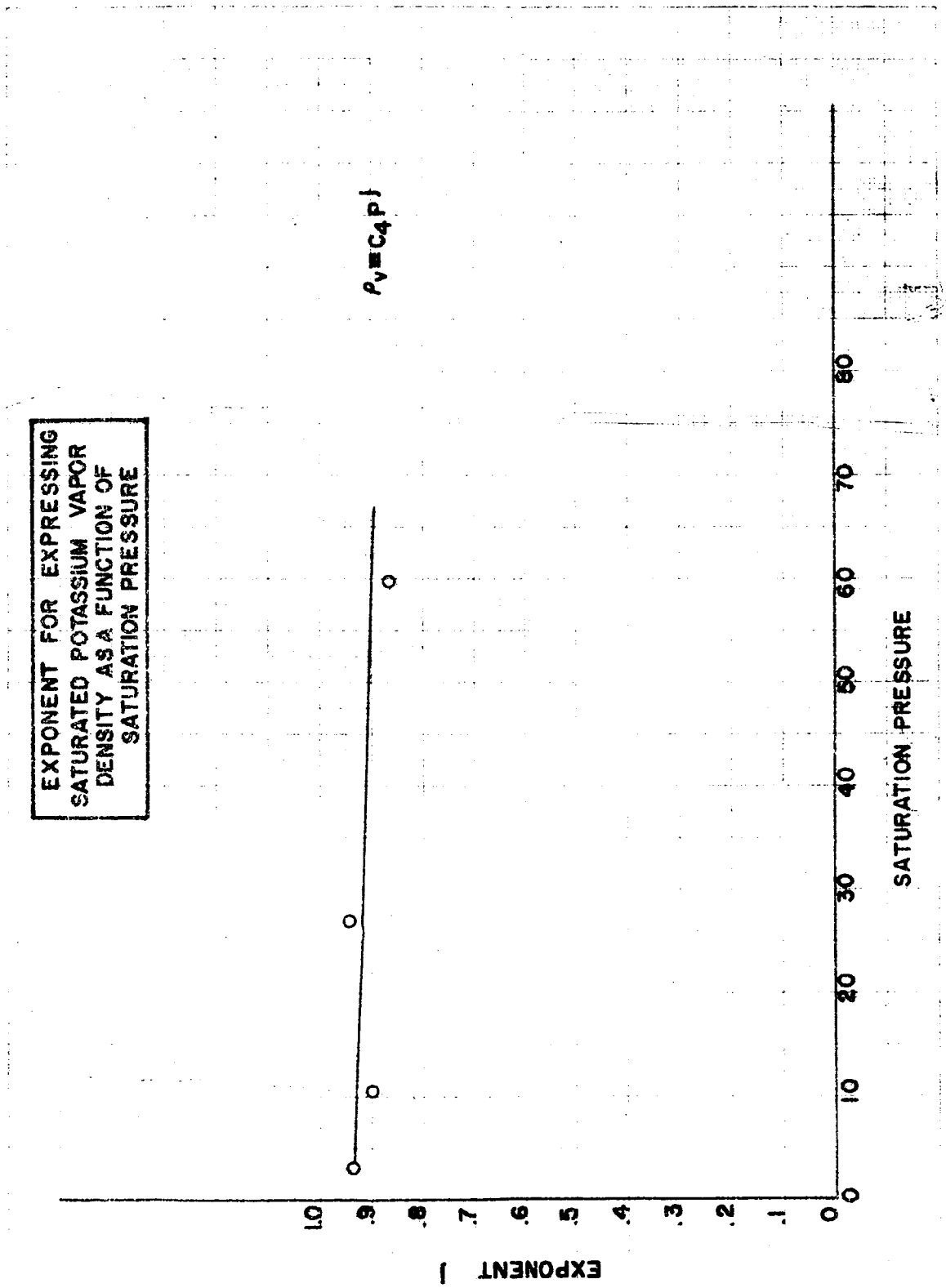
EXPONENT FOR EXPRESSING SATURATED POTASSIUM VAPOR DENSITY AS A FUNCTION OF SATURATION PRESSURE
$\rho_v = C_4 P^j$
EXPONENT j
SATURATION PRESSURE
0
.1
.2
.3
.4
.5
.6
.7
.8
.9
1.0
0
10
20
30
40
50
60
70
80

FIG 10

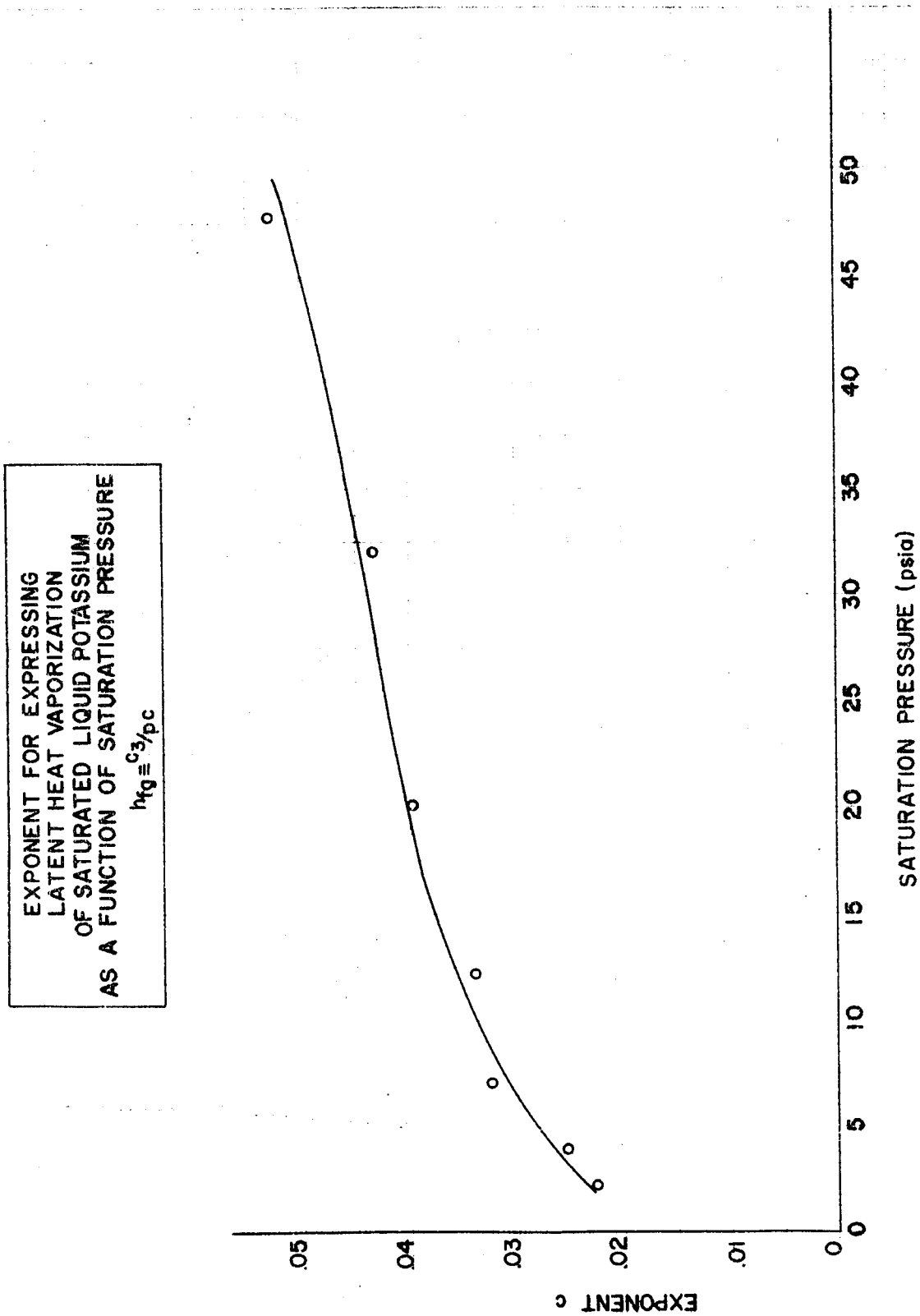
EXPONENT FOR EXPRESSING
LATENT HEAT VAPORIZATION
OF SATURATED LIQUID POTASSIUM
AS A FUNCTION OF SATURATION PRESSURE
$h_{fg} \equiv c^3/p_c$
EXPONENT c
.05
.04
.03
.02
.01
0
0
5
10
15
20
25
30
35
40
45
50
SATURATION PRESSURE (psia)

FIG II

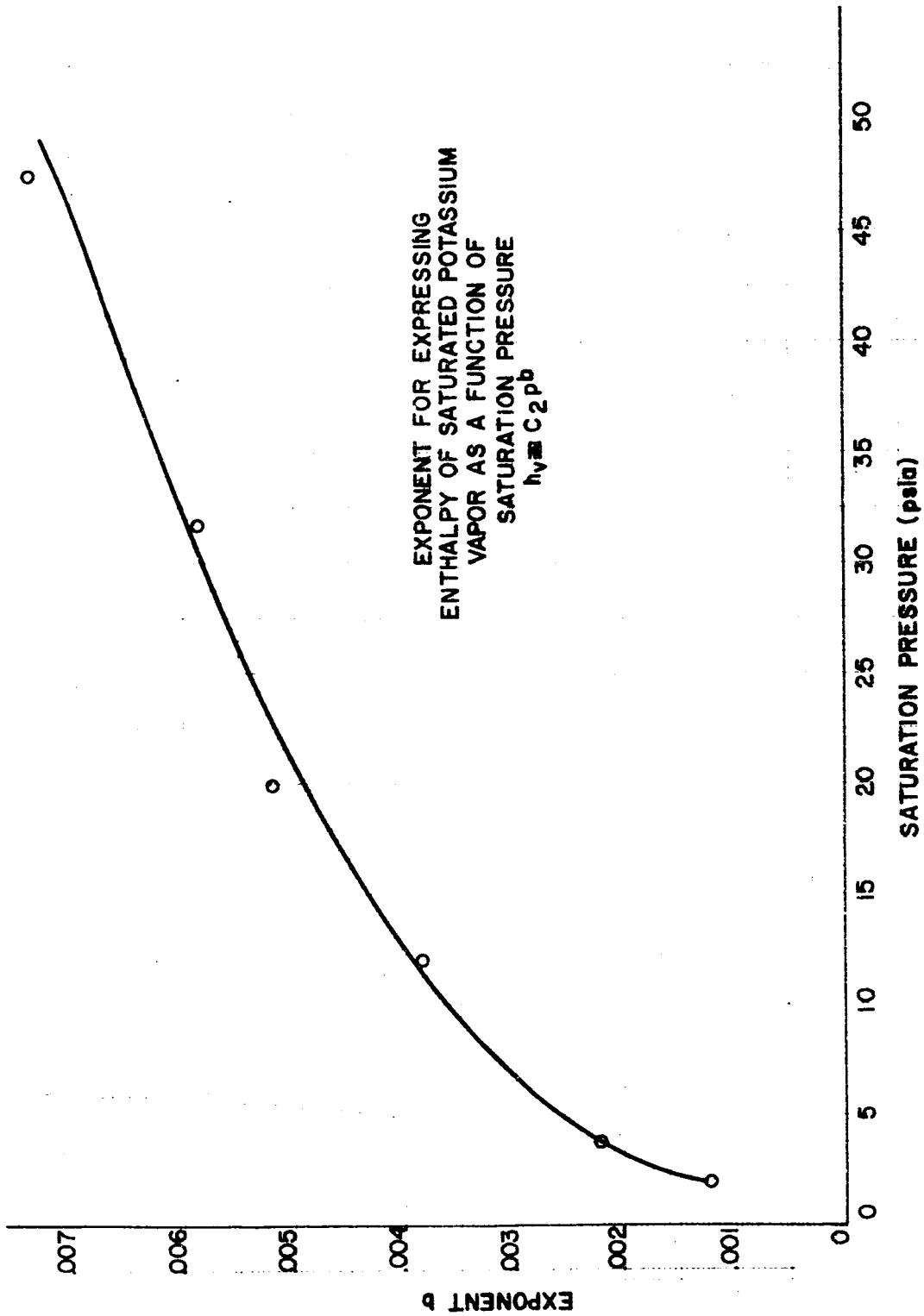
EXPONENT FOR EXPRESSING
ENTHALPY OF SATURATED POTASSIUM
VAPOR AS A FUNCTION OF
SATURATION PRESSURE
$h_v = C_2 p^b$
EXPONENT b
.007
.006
.005
.004
.003
.002
.001
0
0
5
10
15
20
25
30
35
40
45
50
SATURATION PRESSURE (psia)

FIG 12

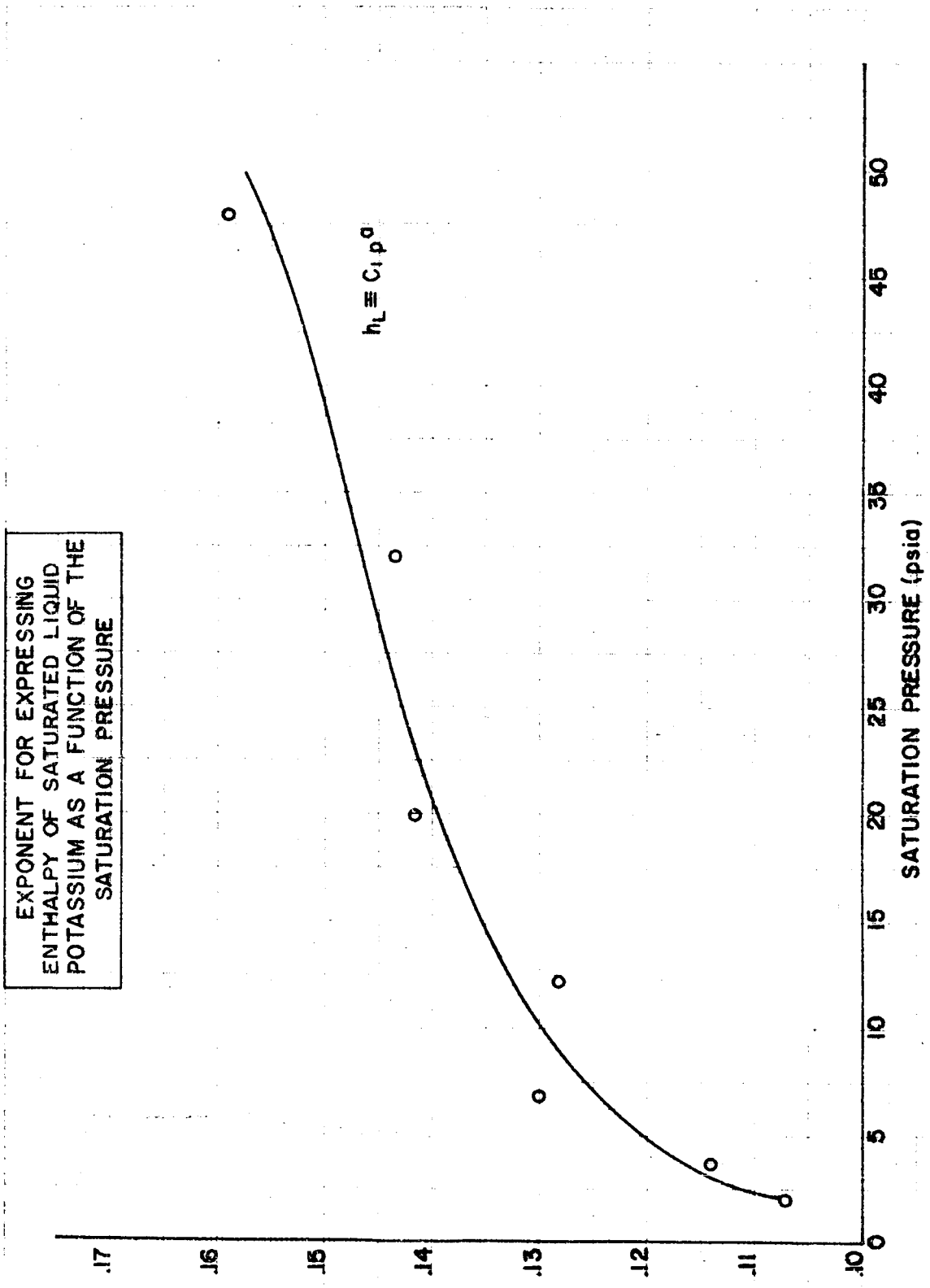
EXPONENT FOR EXPRESSING ENTHALPY OF SATURATED LIQUID POTASSIUM AS A FUNCTION OF THE SATURATION PRESSURE
$h_L \equiv C_1 p^a$
.17
.16
.15
.14
.13
.12
.11
.10
0
5
10
15
20
25
30
35
40
45
50
SATURATION PRESSURE (psia)

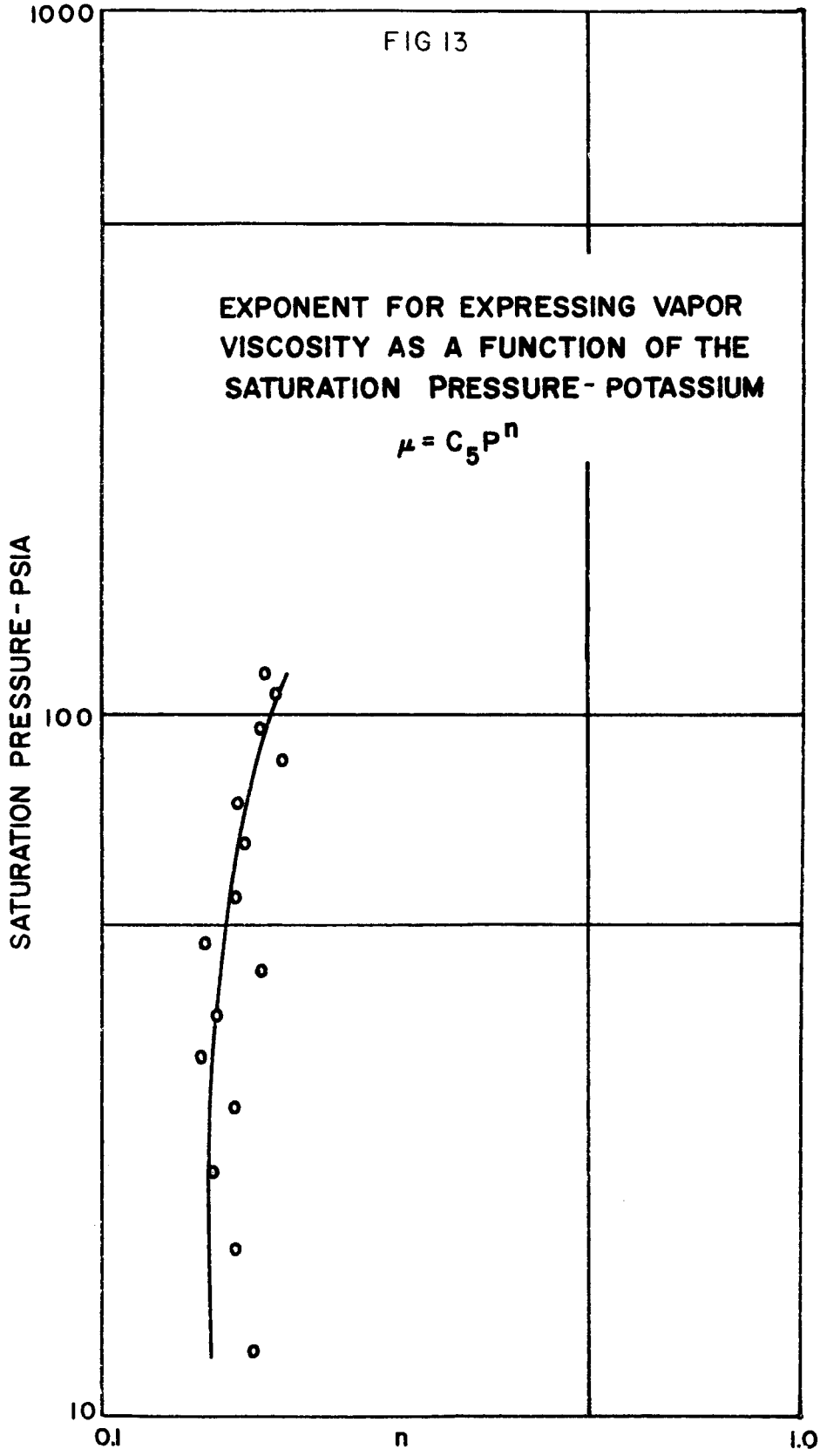
FIG 13
EXPONENT FOR EXPRESSING VAPOR VISCOSITY AS A FUNCTION OF THE SATURATION PRESSURE - POTASSIUM
$\mu = C_5 P^n$
SATURATION PRESSURE - PSIA
1000
100
10
0.1
n
1.0

FIG 14

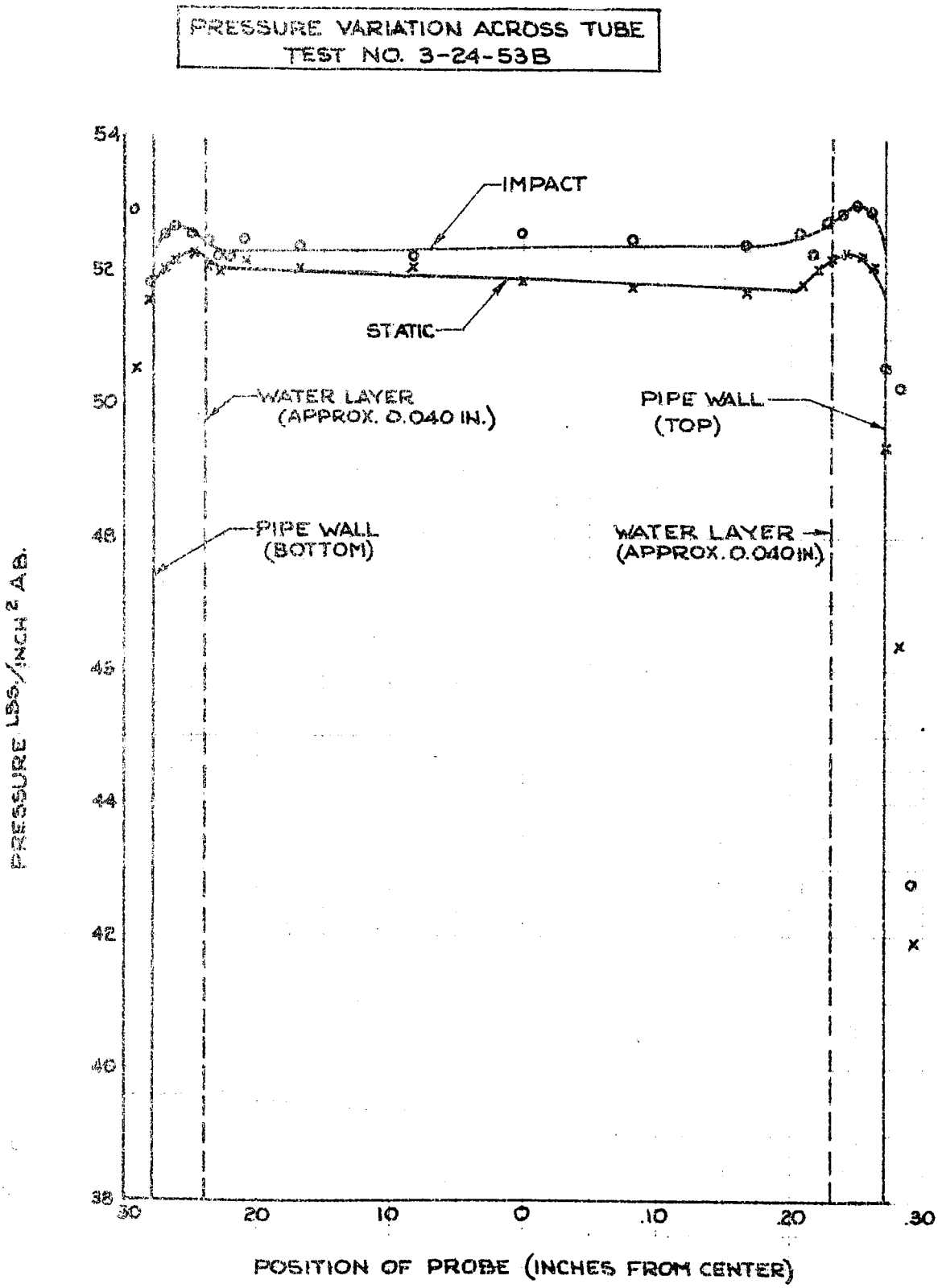
PRESSURE VARIATION ACROSS TUBE
TEST NO. 3-24-53B
IMPACT
STATIC
WATER LAYER
(APPROX. 0.040 IN.)
PIPE WALL
(TOP)
PIPE WALL
(BOTTOM)
WATER LAYER
(APPROX. 0.040 IN.)
PRESSURE LBS./INCH² A.B.
54
52
50
48
46
44
42
38
.30
.20
.10
0
.10
.20
.30
POSITION OF PROBE (INCHES FROM CENTER)

FIG 14B

DETERMINATION OF THE LIQUID LAYER THICKNESS FOR STEAM CONDENSING IN LONG, SMALL TUBES

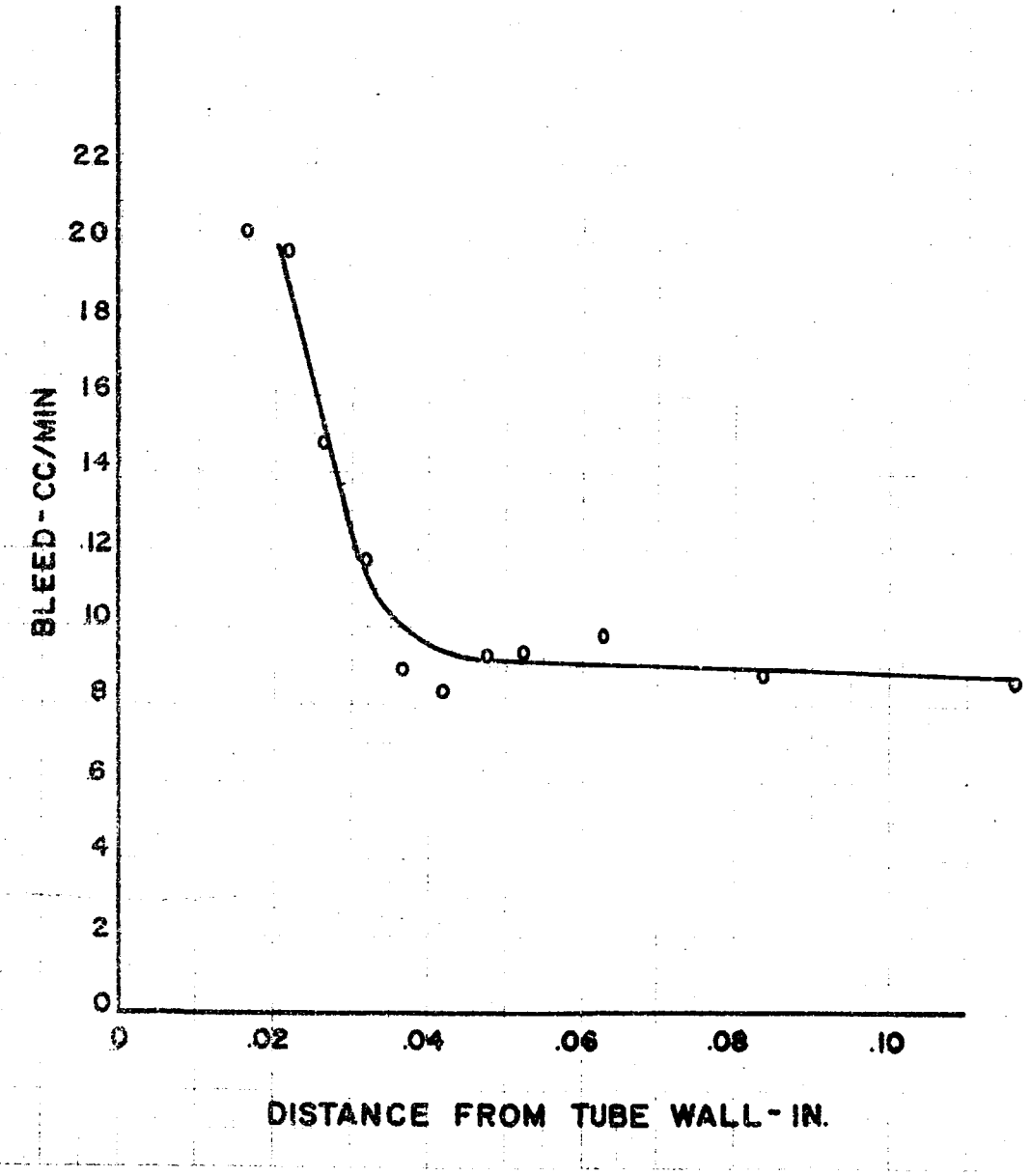

FIG 15

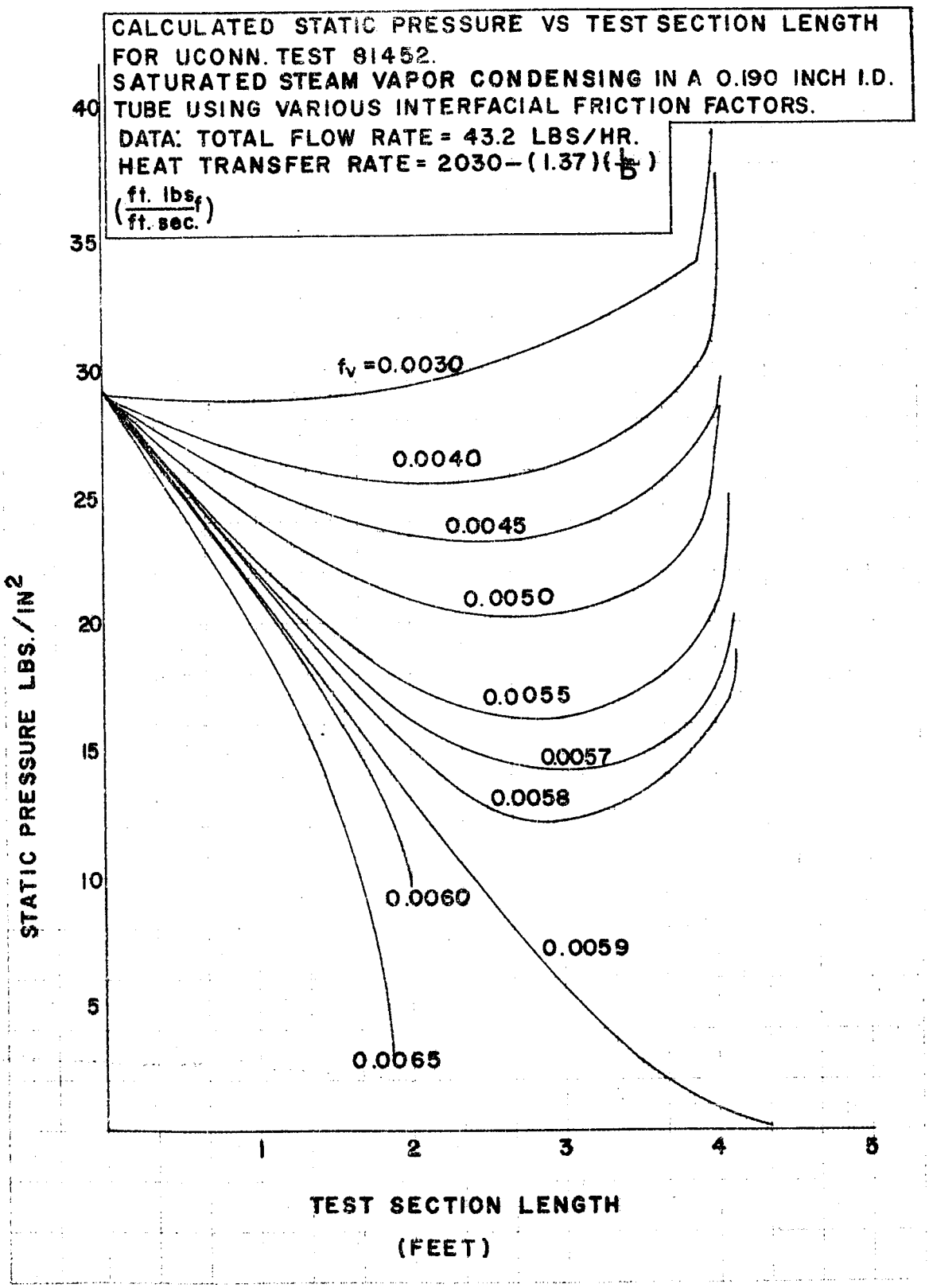
CALCULATED STATIC PRESSURE VS TEST SECTION LENGTH
FOR UCONN. TEST 81452.
SATURATED STEAM VAPOR CONDENSING IN A 0.190 INCH I.D.
TUBE USING VARIOUS INTERFACIAL FRICTION FACTORS.
DATA: TOTAL FLOW RATE = 43.2 LBS/HR.
HEAT TRANSFER RATE = 2030 − (1.37)(L/B)
(ft. lbs_f / ft. sec.)
STATIC PRESSURE LBS./IN.²
TEST SECTION LENGTH
(FEET)
f_v = 0.0030
0.0040
0.0045
0.0050
0.0055
0.0057
0.0058
0.0059
0.0060
0.0065
40
35
30
25
20
15
10
5
1
2
3
4
5

FIG 16

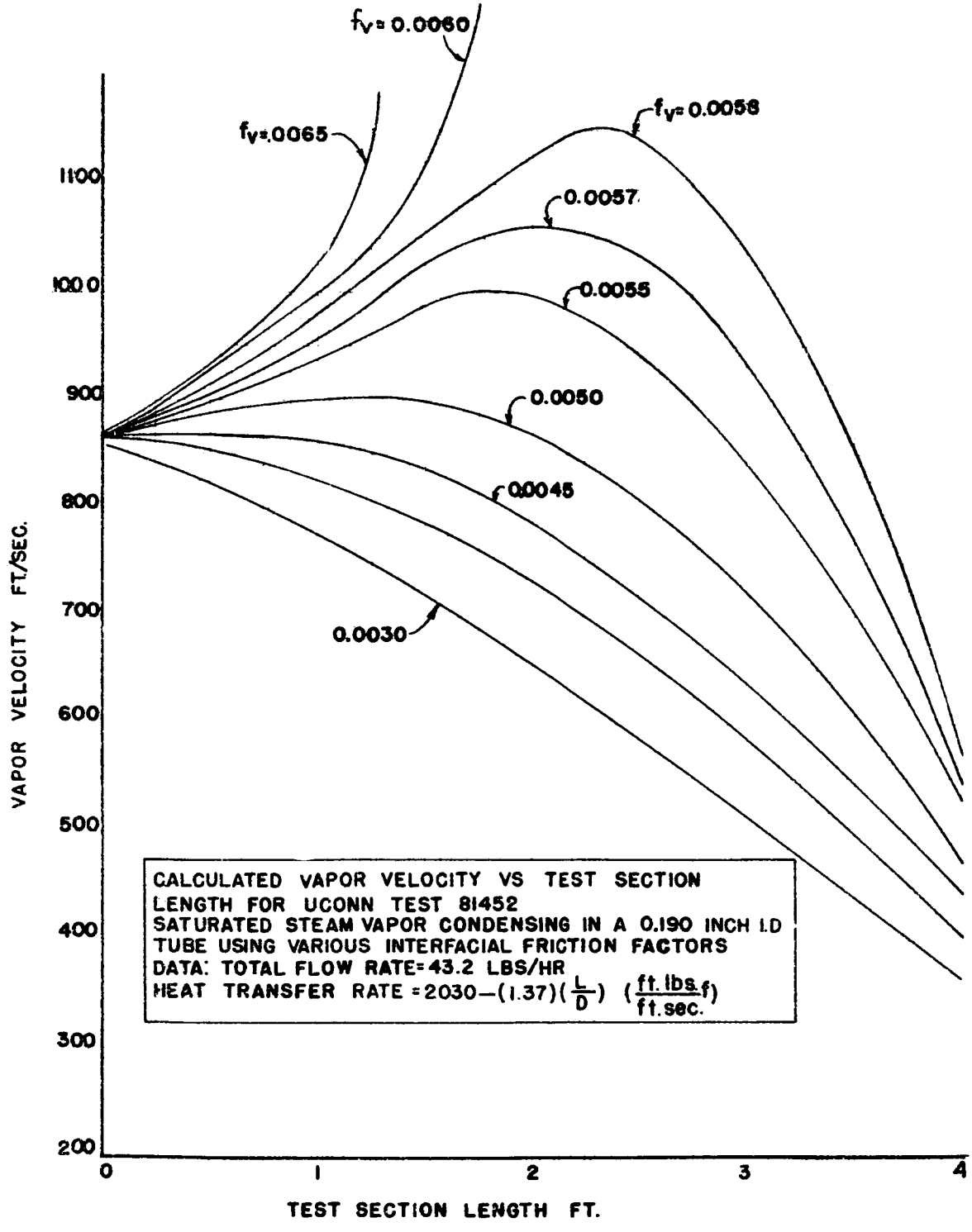
f_v= 0.0060
f_v=.0065
f_v= 0.0058
0.0057
0.0055
0.0050
0.0045
0.0030
1100
1000
900
800
700
600
500
400
300
200
VAPOR VELOCITY FT/SEC.
0
1
2
3
4
TEST SECTION LENGTH FT.
CALCULATED VAPOR VELOCITY VS TEST SECTION LENGTH FOR UCONN TEST 81452
SATURATED STEAM VAPOR CONDENSING IN A 0.190 INCH I.D TUBE USING VARIOUS INTERFACIAL FRICTION FACTORS
DATA: TOTAL FLOW RATE=43.2 LBS/HR
HEAT TRANSFER RATE = 2030—(1.37)(L/D) (ft.lbs.f / ft.sec.)

FIG 17

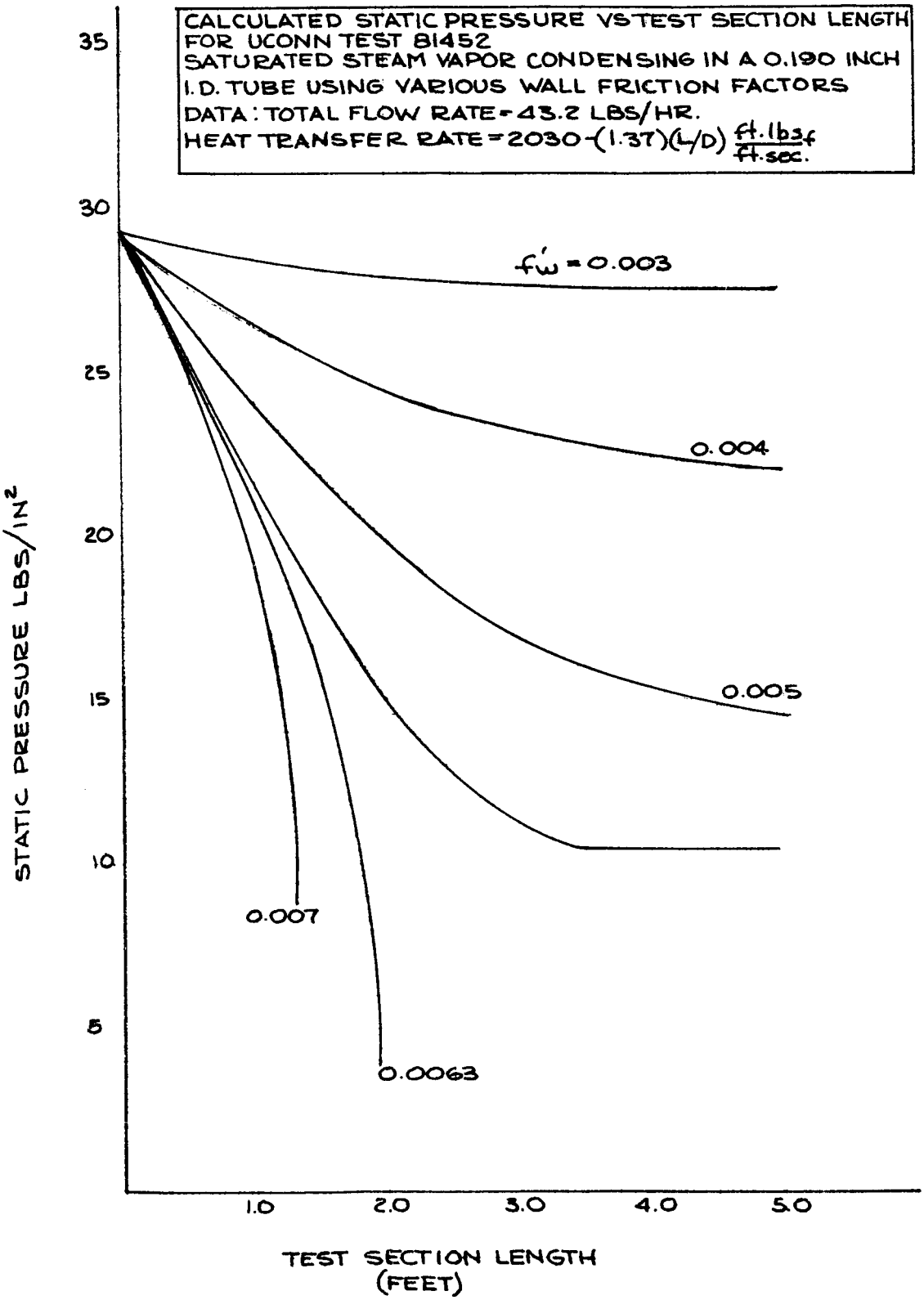
CALCULATED STATIC PRESSURE VS TEST SECTION LENGTH
FOR UCONN TEST 81452
SATURATED STEAM VAPOR CONDENSING IN A 0.190 INCH
I.D. TUBE USING VARIOUS WALL FRICTION FACTORS
DATA: TOTAL FLOW RATE = 43.2 LBS/HR.
HEAT TRANSFER RATE = 2030 - (1.37)(L/D) ft.lbf/ft.sec.
35
30
25
20
15
10
5
f'w = 0.003
0.004
0.005
0.007
0.0063
STATIC PRESSURE LBS/IN²
1.0
2.0
3.0
4.0
5.0
TEST SECTION LENGTH
(FEET)

FIG 18

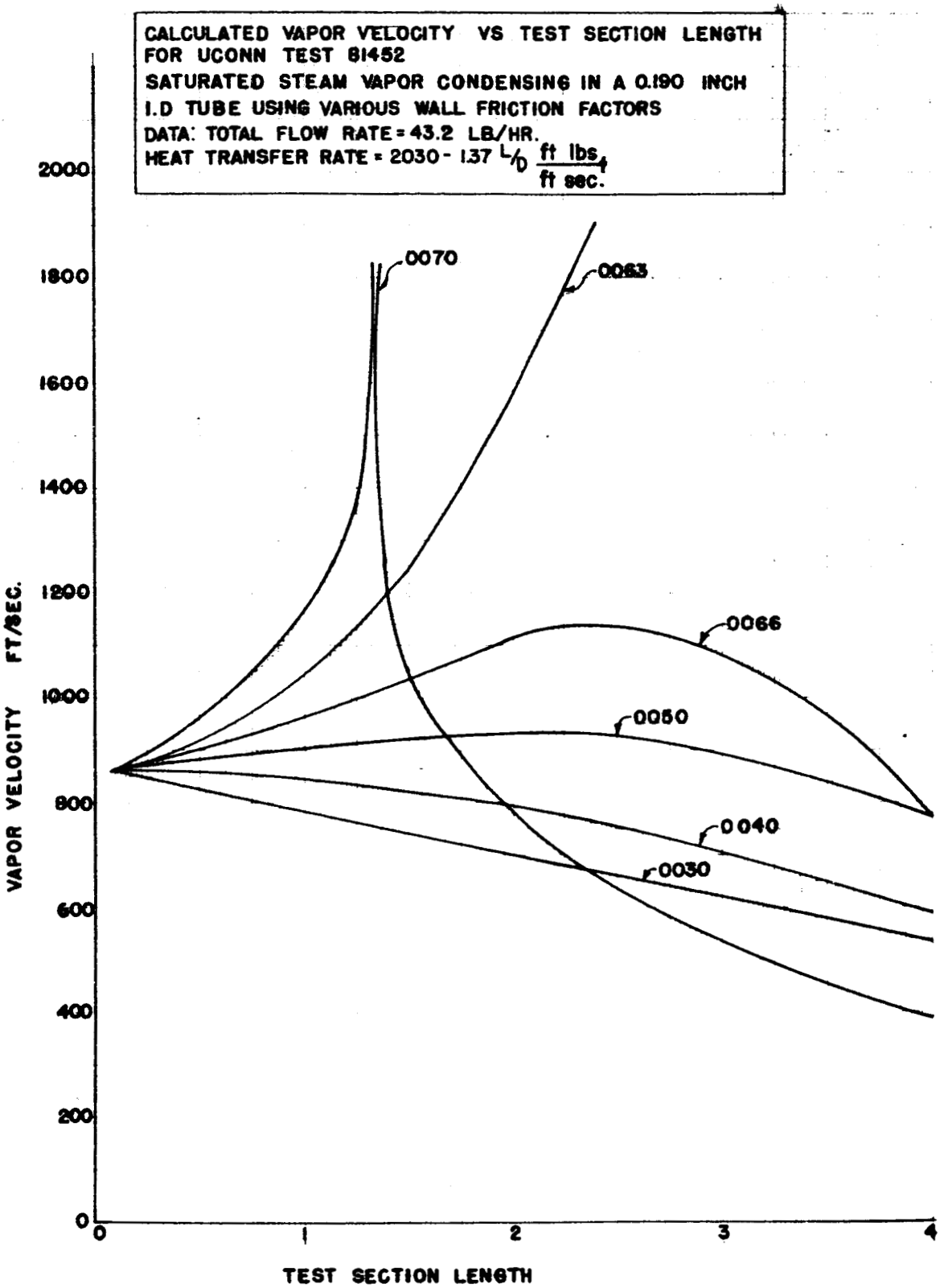
CALCULATED VAPOR VELOCITY VS TEST SECTION LENGTH
FOR UCONN TEST 81452
SATURATED STEAM VAPOR CONDENSING IN A 0.190 INCH
I.D TUBE USING VARIOUS WALL FRICTION FACTORS
DATA: TOTAL FLOW RATE = 43.2 LB/HR.
HEAT TRANSFER RATE = 2030 - 1.37 L/D ft lbs / ft sec.
VAPOR VELOCITY FT/SEC.
2000
1800
1600
1400
1200
1000
800
600
400
200
0
0
1
2
3
4
TEST SECTION LENGTH
.0070
.0063
.0066
.0050
.0040
.0030

FIG 19

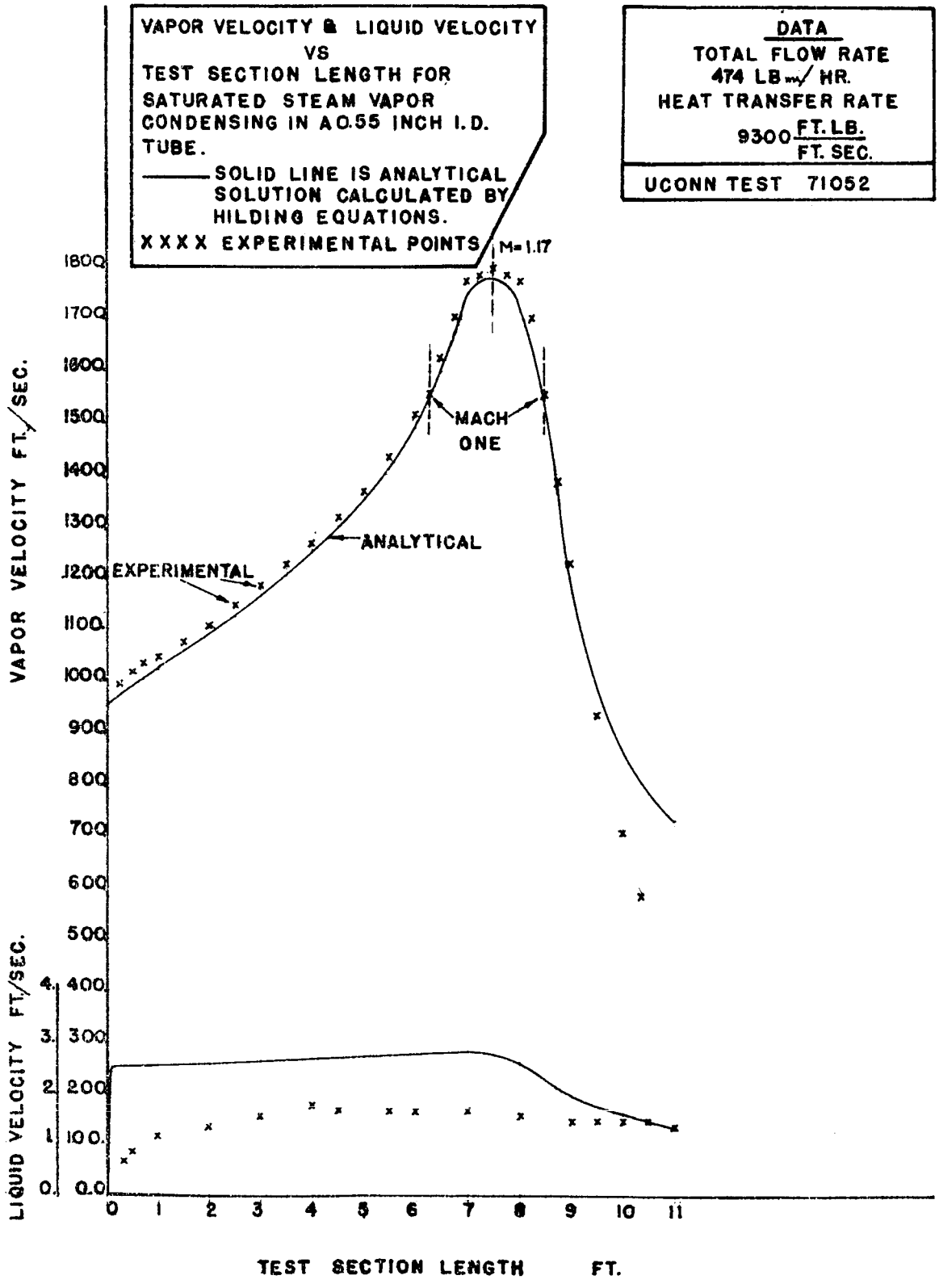
VAPOR VELOCITY & LIQUID VELOCITY
VS
TEST SECTION LENGTH FOR
SATURATED STEAM VAPOR
CONDENSING IN A 0.55 INCH I.D.
TUBE.
——— SOLID LINE IS ANALYTICAL SOLUTION CALCULATED BY HILDING EQUATIONS.
XXXX EXPERIMENTAL POINTS
DATA
TOTAL FLOW RATE
474 LB m/ HR.
HEAT TRANSFER RATE
9300 FT. LB. / FT. SEC.
UCONN TEST 71052
M=1.17
MACH ONE
ANALYTICAL
EXPERIMENTAL
VAPOR VELOCITY FT./SEC.
LIQUID VELOCITY FT./SEC.
TEST SECTION LENGTH FT.

FIG 20

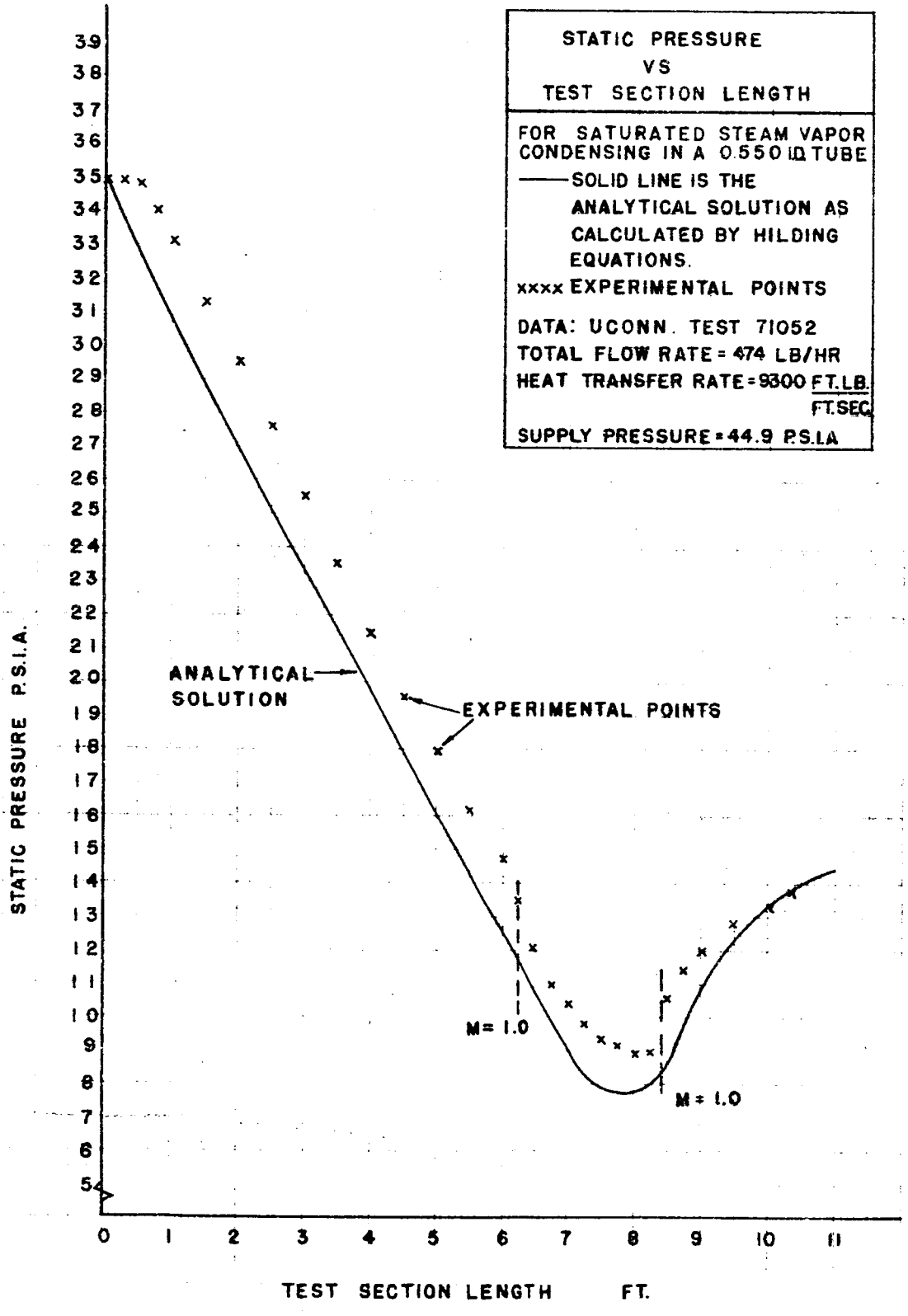
STATIC PRESSURE
VS
TEST SECTION LENGTH
FOR SATURATED STEAM VAPOR CONDENSING IN A 0.550 I.D. TUBE
——SOLID LINE IS THE ANALYTICAL SOLUTION AS CALCULATED BY HILDING EQUATIONS.
xxxx EXPERIMENTAL POINTS
DATA: UCONN. TEST 71052
TOTAL FLOW RATE = 474 LB/HR
HEAT TRANSFER RATE = 9300 FT.LB./FT.SEC.
SUPPLY PRESSURE = 44.9 P.S.I.A.
STATIC PRESSURE P.S.I.A.
ANALYTICAL SOLUTION
EXPERIMENTAL POINTS
M = 1.0
M = 1.0
TEST SECTION LENGTH FT.

FIG 21

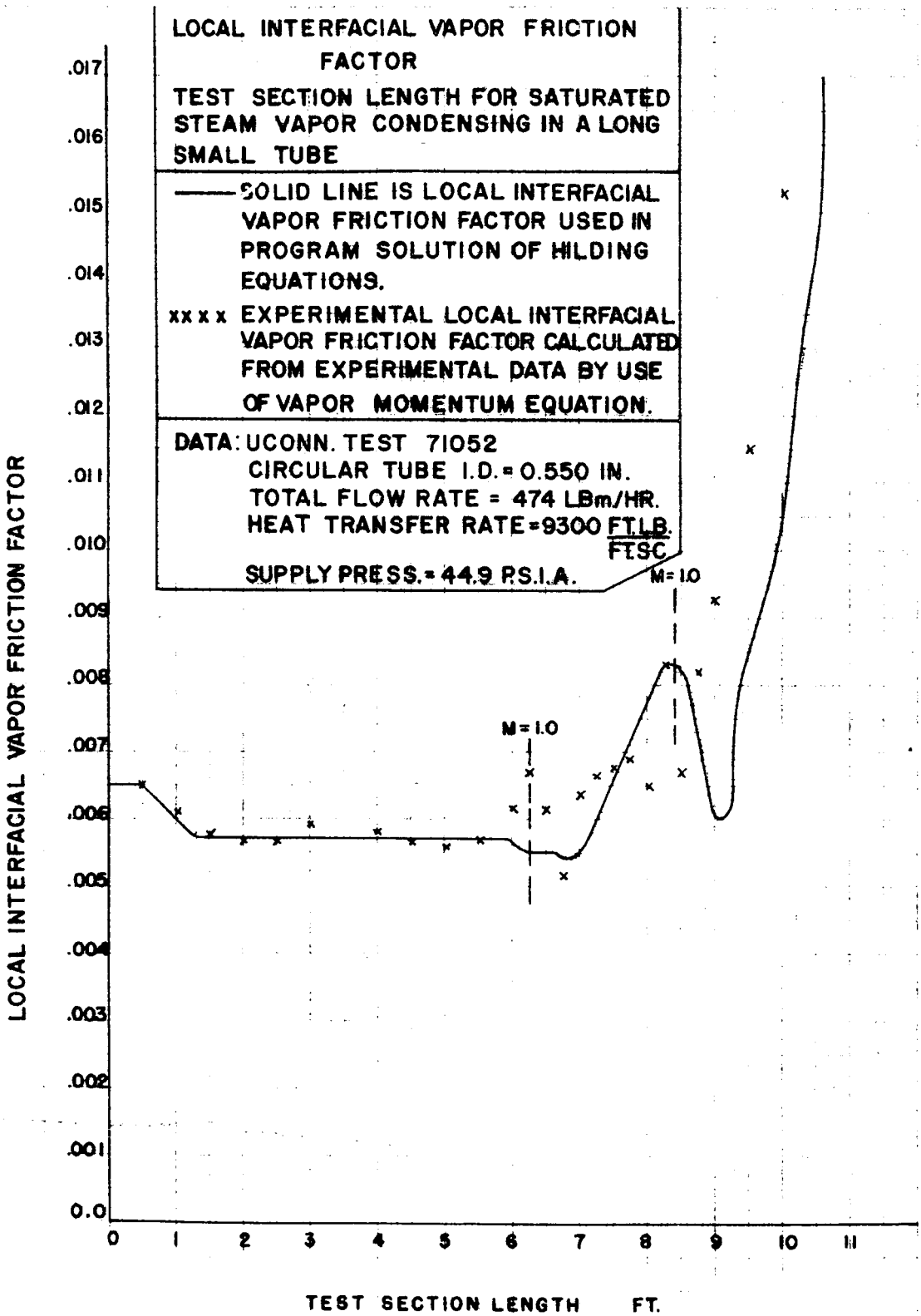
LOCAL INTERFACIAL VAPOR FRICTION FACTOR
TEST SECTION LENGTH FOR SATURATED STEAM VAPOR CONDENSING IN A LONG SMALL TUBE
——SOLID LINE IS LOCAL INTERFACIAL VAPOR FRICTION FACTOR USED IN PROGRAM SOLUTION OF HILDING EQUATIONS.
xxxx EXPERIMENTAL LOCAL INTERFACIAL VAPOR FRICTION FACTOR CALCULATED FROM EXPERIMENTAL DATA BY USE OF VAPOR MOMENTUM EQUATION.
DATA: UCONN. TEST 71052
CIRCULAR TUBE I.D. = 0.550 IN.
TOTAL FLOW RATE = 474 LBm/HR.
HEAT TRANSFER RATE = 9300 FT.LB./FT.SC
SUPPLY PRESS. = 44.9 P.S.I.A.
M = 1.0
M = 1.0
LOCAL INTERFACIAL VAPOR FRICTION FACTOR
.017
.016
.015
.014
.013
.012
.011
.010
.009
.008
.007
.006
.005
.004
.003
.002
.001
0.0
0
1
2
3
4
5
6
7
8
9
10
11
TEST SECTION LENGTH FT.

FIG 22

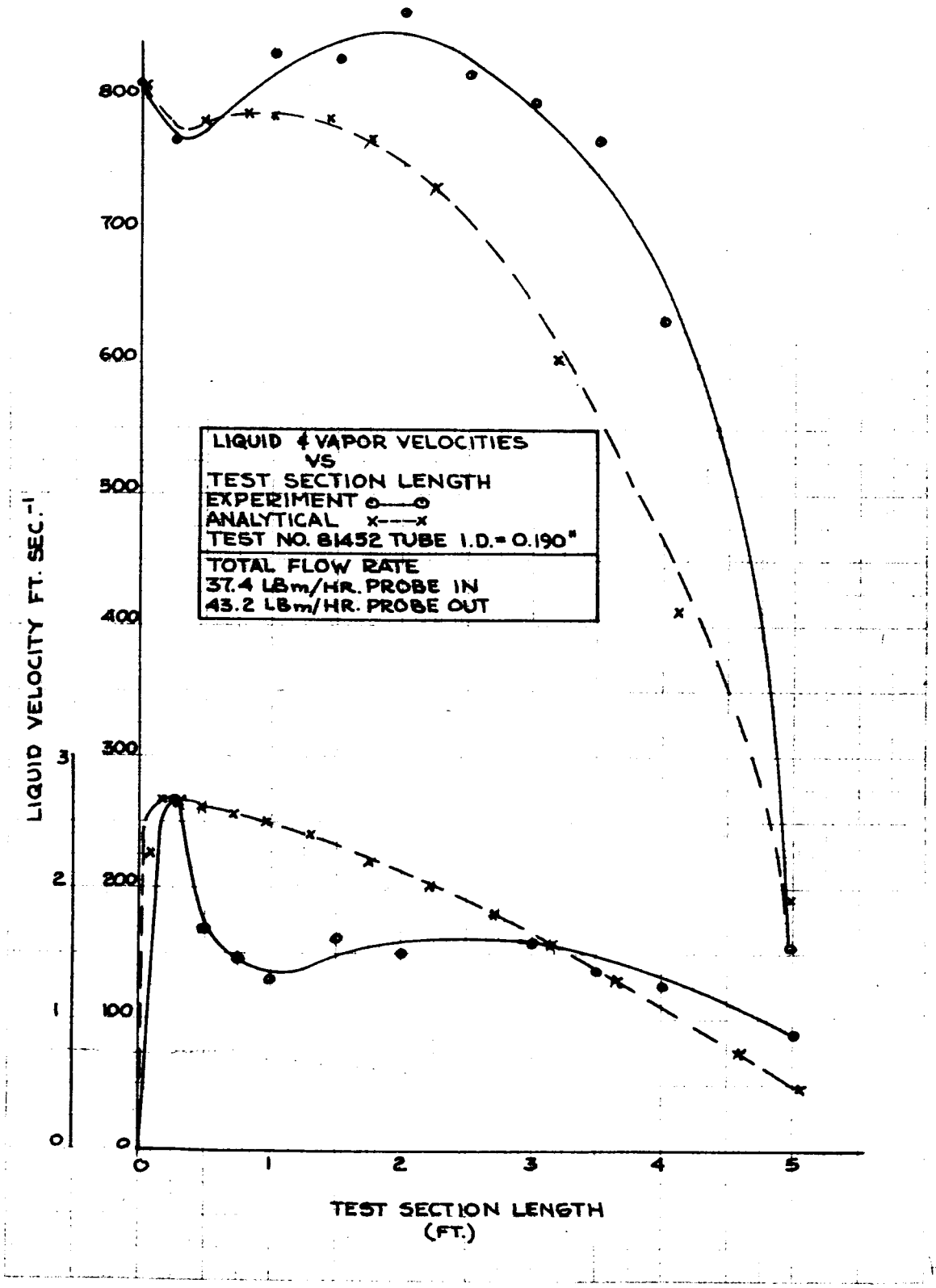
LIQUID & VAPOR VELOCITIES
VS
TEST SECTION LENGTH
EXPERIMENT o——o
ANALYTICAL x---x
TEST NO. 81452 TUBE I.D.= 0.190"
TOTAL FLOW RATE
37.4 LBm/HR. PROBE IN
43.2 LBm/HR. PROBE OUT
LIQUID VELOCITY FT. SEC.-1
TEST SECTION LENGTH
(FT.)
800
700
600
500
400
300
200
100
0
1
2
3
4
5

FIG 23

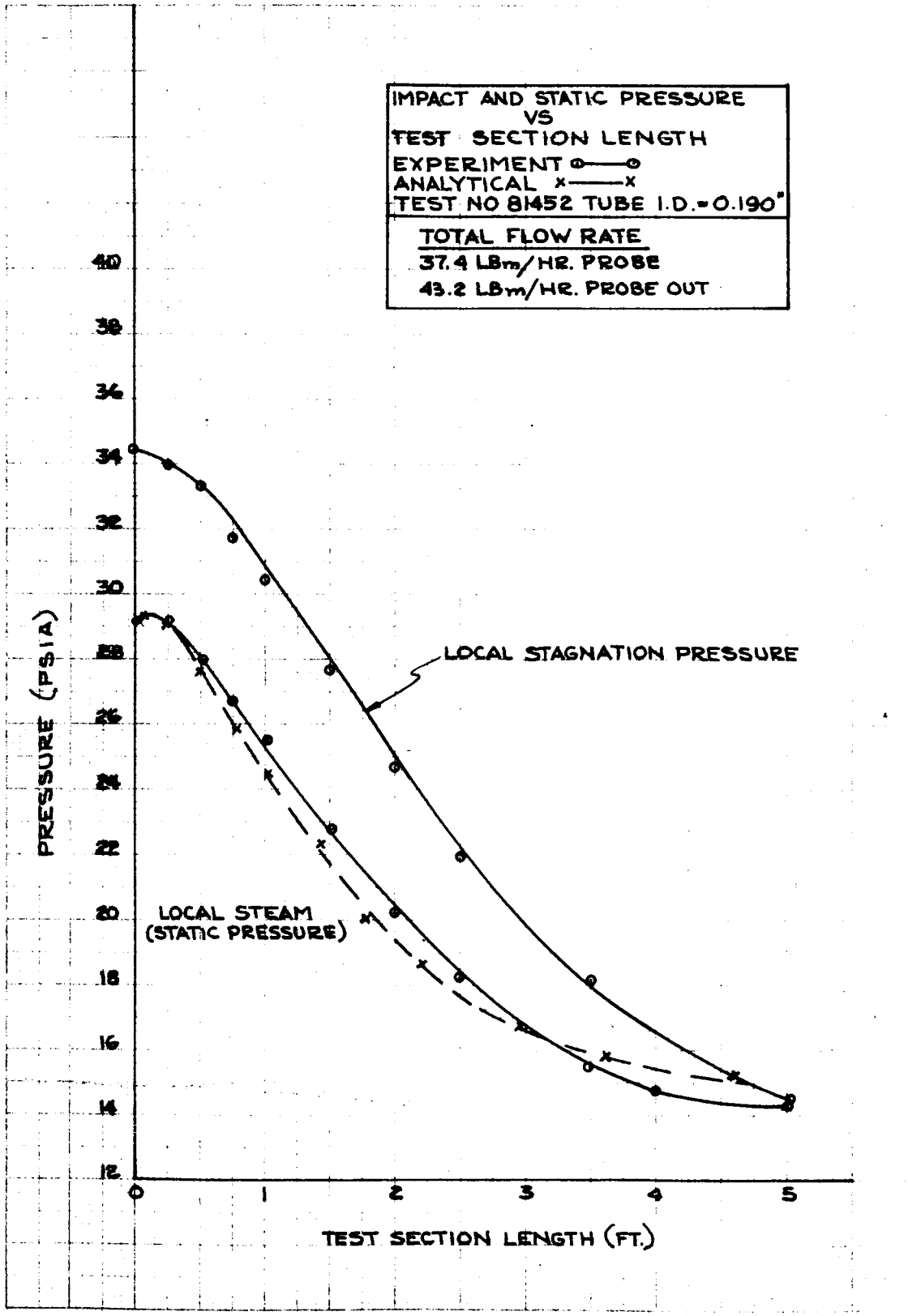
IMPACT AND STATIC PRESSURE
VS
TEST SECTION LENGTH
EXPERIMENT
ANALYTICAL
TEST NO 81452 TUBE I.D.=0.190"
TOTAL FLOW RATE
37.4 LBm/HR. PROBE
43.2 LBm/HR. PROBE OUT
LOCAL STAGNATION PRESSURE
LOCAL STEAM
(STATIC PRESSURE)
PRESSURE (PSIA)
TEST SECTION LENGTH (FT.)
40
38
36
34
32
30
28
26
24
22
20
18
16
14
12
0
1
2
3
4
5

FIG 24

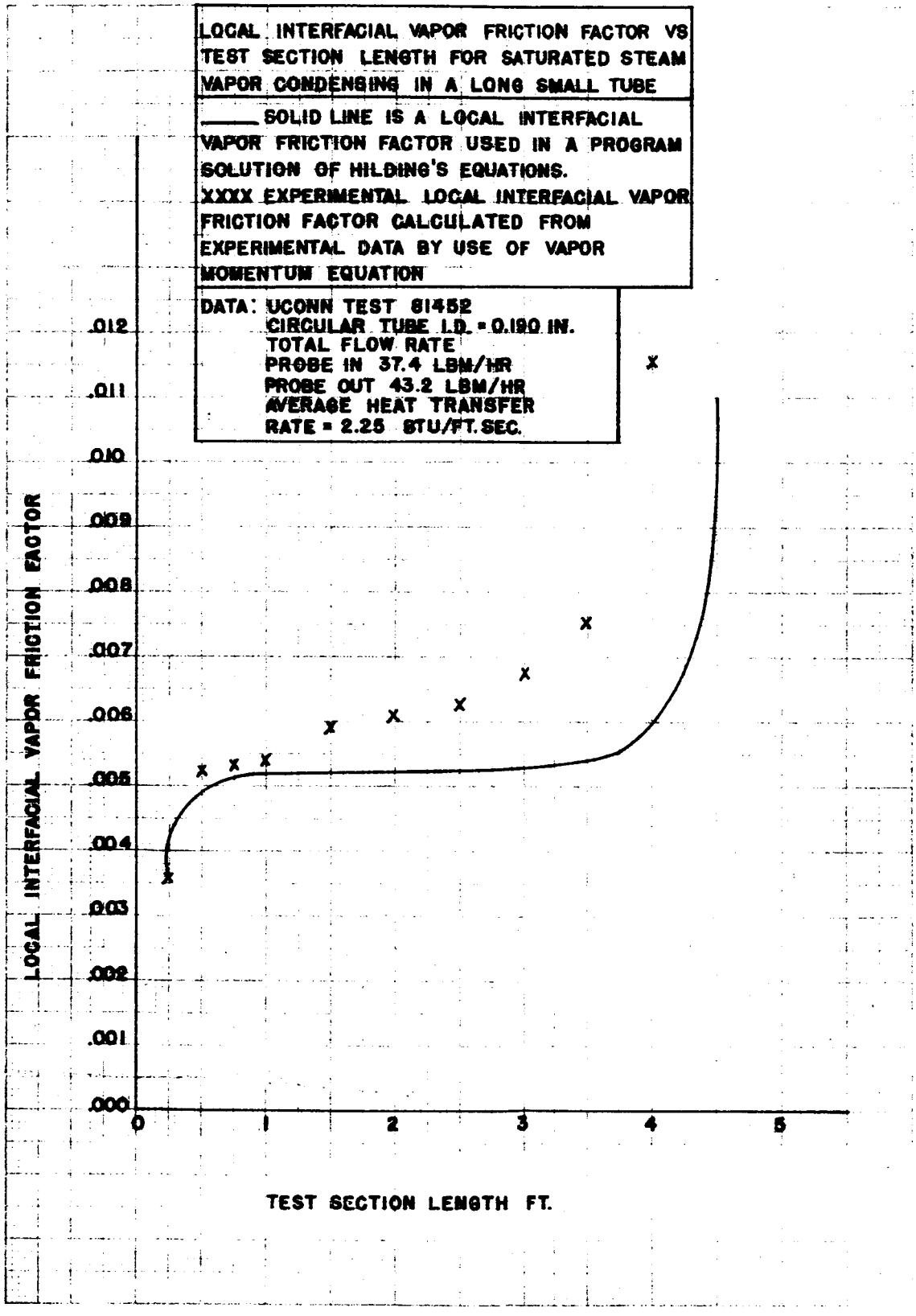
LOCAL INTERFACIAL VAPOR FRICTION FACTOR VS TEST SECTION LENGTH FOR SATURATED STEAM VAPOR CONDENSING IN A LONG SMALL TUBE
_____ SOLID LINE IS A LOCAL INTERFACIAL VAPOR FRICTION FACTOR USED IN A PROGRAM SOLUTION OF HILDING'S EQUATIONS.
XXXX EXPERIMENTAL LOCAL INTERFACIAL VAPOR FRICTION FACTOR CALCULATED FROM EXPERIMENTAL DATA BY USE OF VAPOR MOMENTUM EQUATION
DATA: UCONN TEST 81452
CIRCULAR TUBE I.D. = 0.190 IN.
TOTAL FLOW RATE
PROBE IN 37.4 LBM/HR
PROBE OUT 43.2 LBM/HR
AVERAGE HEAT TRANSFER RATE = 2.25 BTU/FT.SEC.
LOCAL INTERFACIAL VAPOR FRICTION FACTOR
.012
.011
.010
.009
.008
.007
.006
.005
.004
.003
.002
.001
.000
0
1
2
3
4
5
TEST SECTION LENGTH FT.

FIG 25

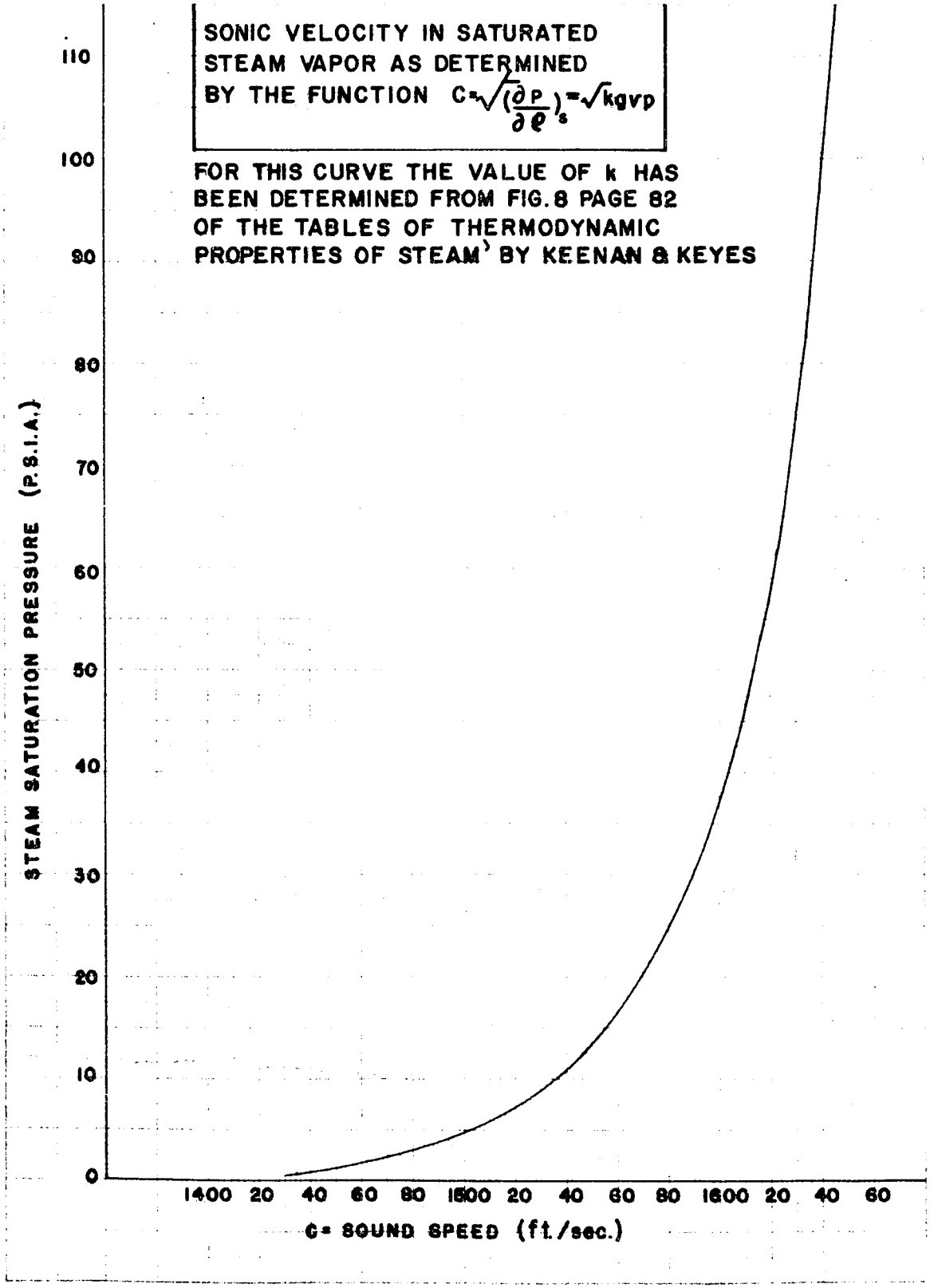
SONIC VELOCITY IN SATURATED STEAM VAPOR AS DETERMINED BY THE FUNCTION $C=\sqrt{(\frac{\partial P}{\partial \rho})_s}=\sqrt{kgvp}$
FOR THIS CURVE THE VALUE OF k HAS BEEN DETERMINED FROM FIG. 8 PAGE 82 OF THE TABLES OF THERMODYNAMIC PROPERTIES OF STEAM' BY KEENAN & KEYES
STEAM SATURATION PRESSURE (P.S.I.A.)
110
100
90
80
70
60
50
40
30
20
10
0
1400 20 40 60 80 1500 20 40 60 80 1600 20 40 60
C= SOUND SPEED (ft./sec.)

FIG 26

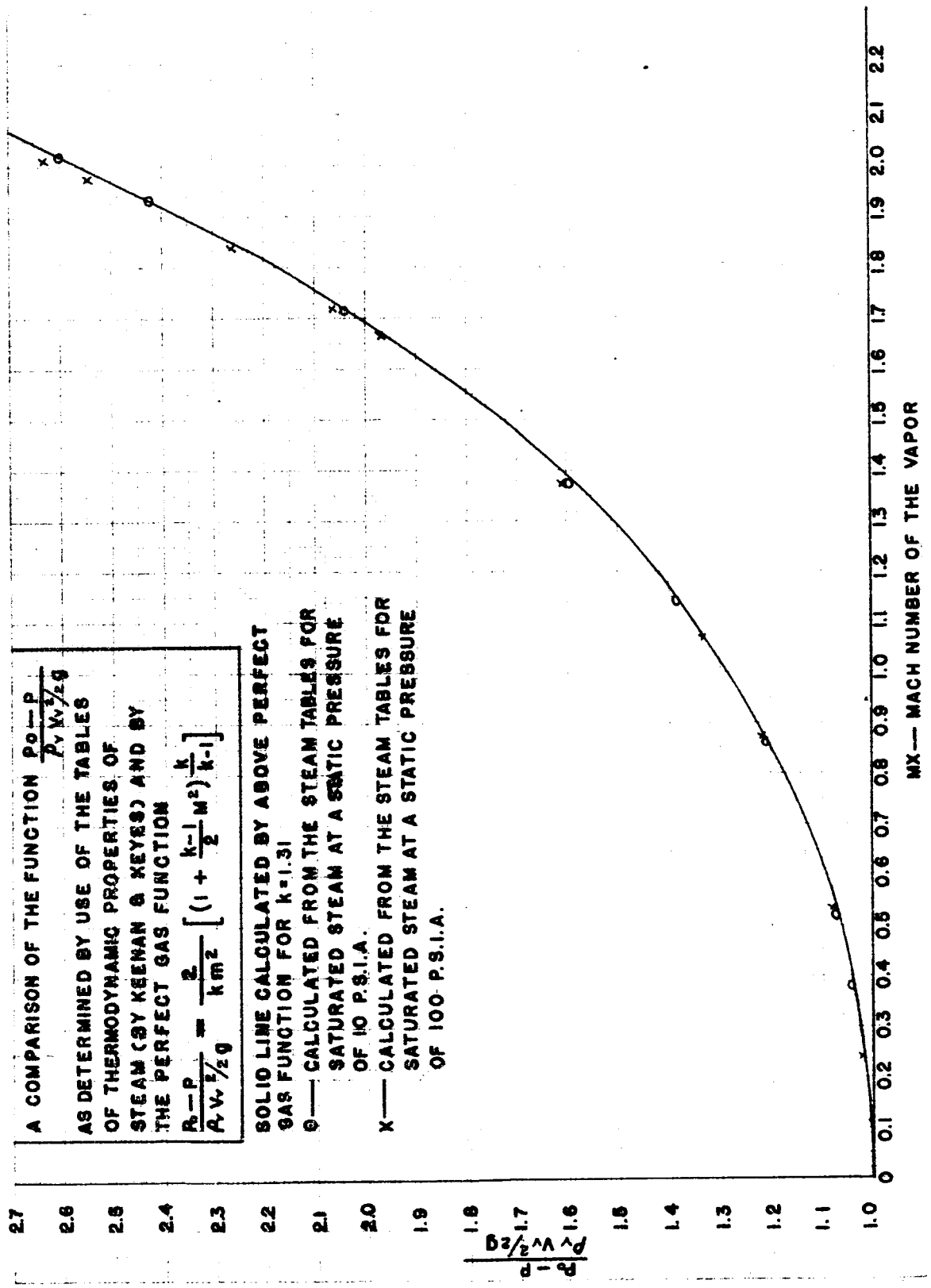
A COMPARISON OF THE FUNCTION $\frac{P_o - P}{\rho_v V_v^2/2g}$
AS DETERMINED BY USE OF THE TABLES OF THERMODYNAMIC PROPERTIES OF STEAM (BY KEENAN & KEYES) AND BY THE PERFECT GAS FUNCTION
$\frac{P_o - P}{\rho_v V_v^2/2g} = \frac{2}{km^2}\left[\left(1 + \frac{k-1}{2}M^2\right)^{\frac{k}{k-1}} - 1\right]$
SOLID LINE CALCULATED BY ABOVE PERFECT GAS FUNCTION FOR k=1.31
O—— CALCULATED FROM THE STEAM TABLES FOR SATURATED STEAM AT A STATIC PRESSURE OF 10 P.S.I.A.
X—— CALCULATED FROM THE STEAM TABLES FOR SATURATED STEAM AT A STATIC PRESSURE OF 100 P.S.I.A.
$\frac{P_o - P}{\rho_v V_v^2/2g}$
MX— MACH NUMBER OF THE VAPOR

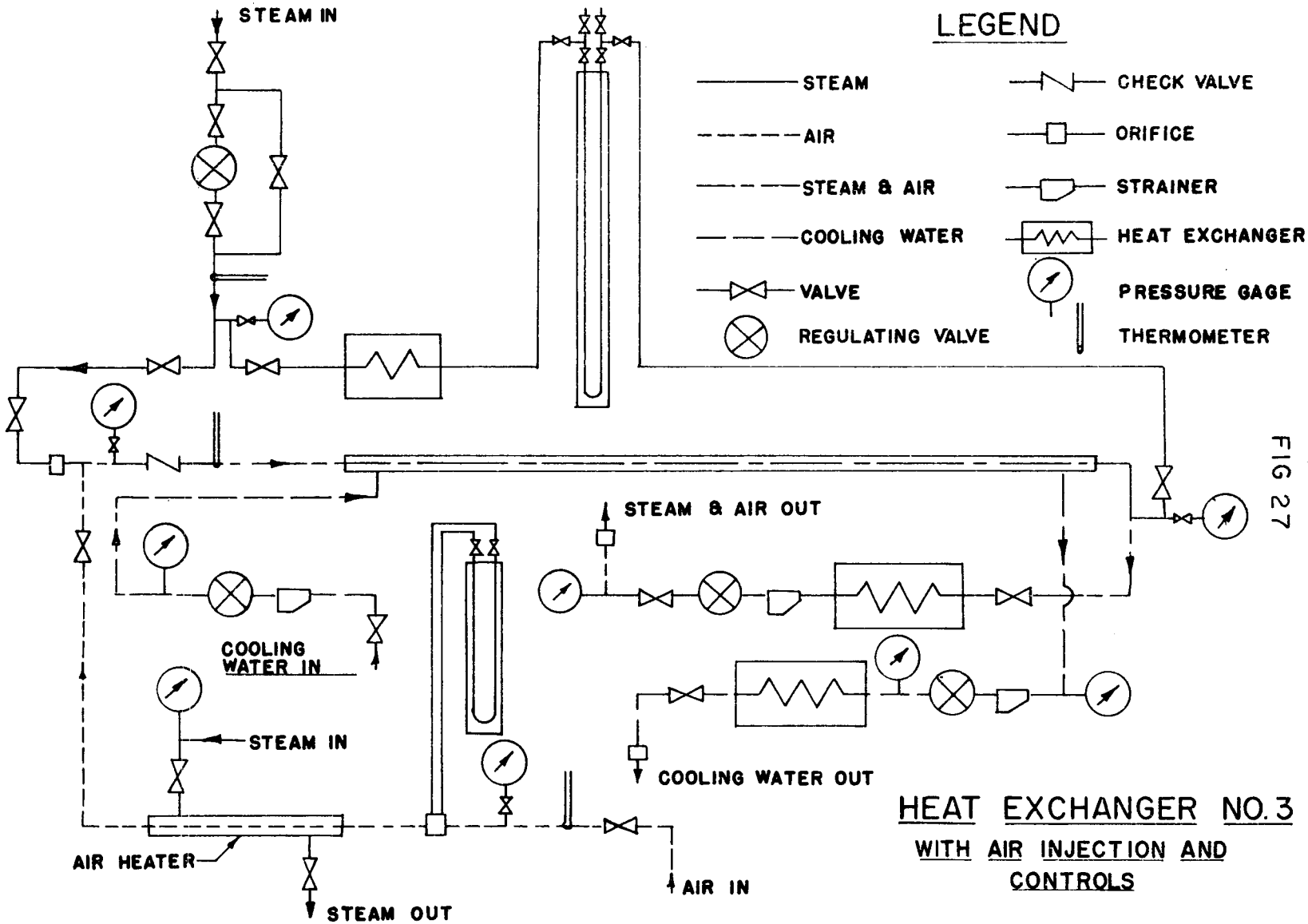

FIG 27

HEAT EXCHANGER NO. 3
WITH AIR INJECTION AND CONTROLS

DETAIL DIAGRAM OF
HEAT EXCHANGER NO. 2

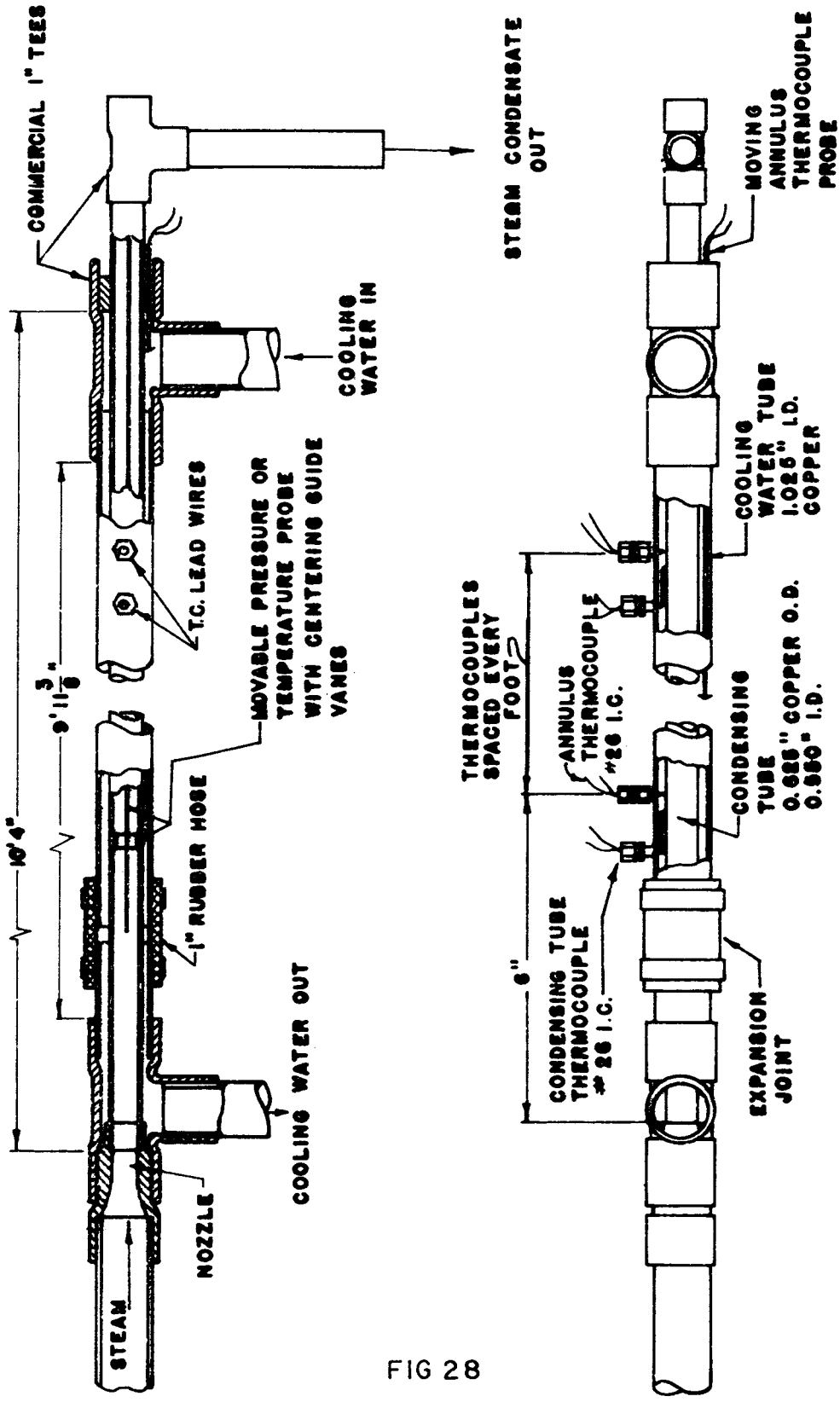

FIG 28

FIG 29 EXCHANGER NO. 3

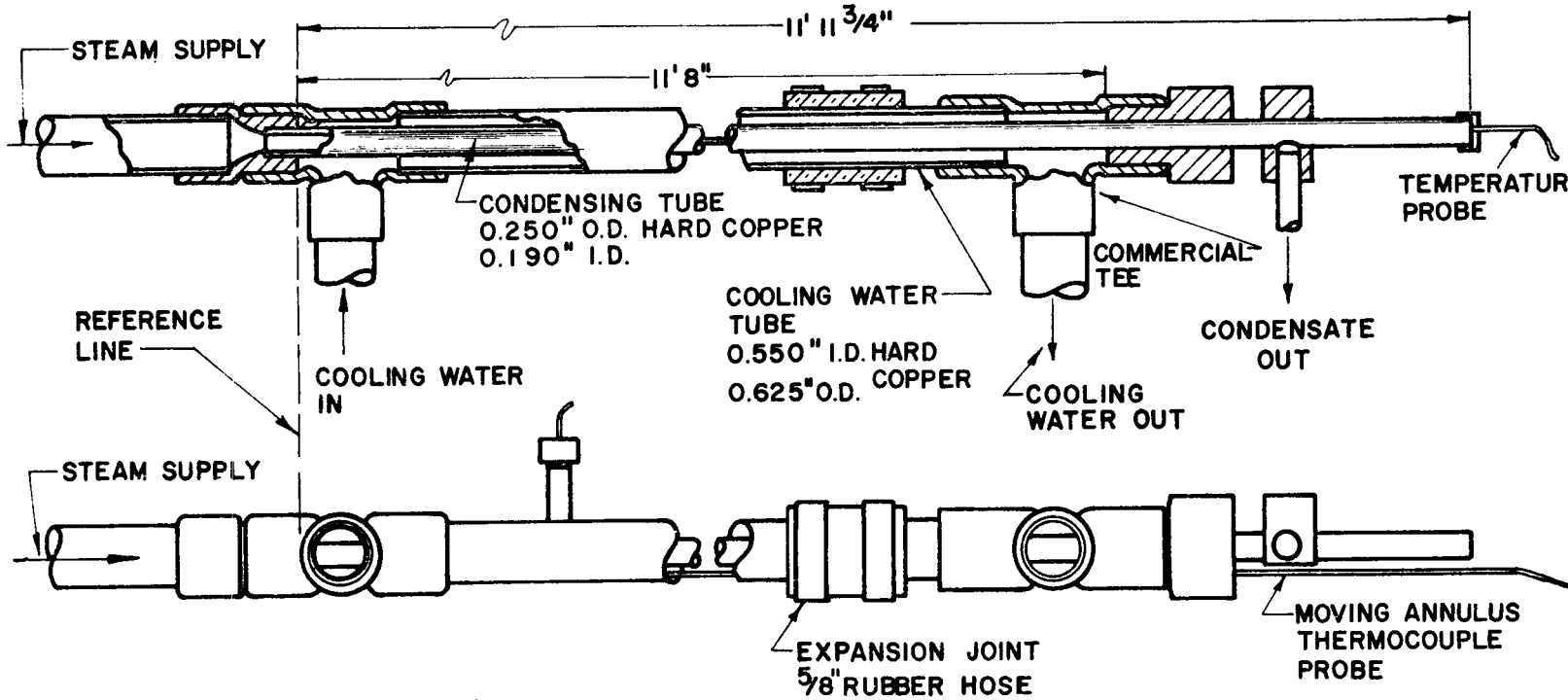

THERMOCOUPLE	SPACING
2, 3	2" (2 is 2" from ref. line)
4 to 10 inc.	3"
11 to 16 inc.	6"
17 to 21 inc.	12"
22	17"

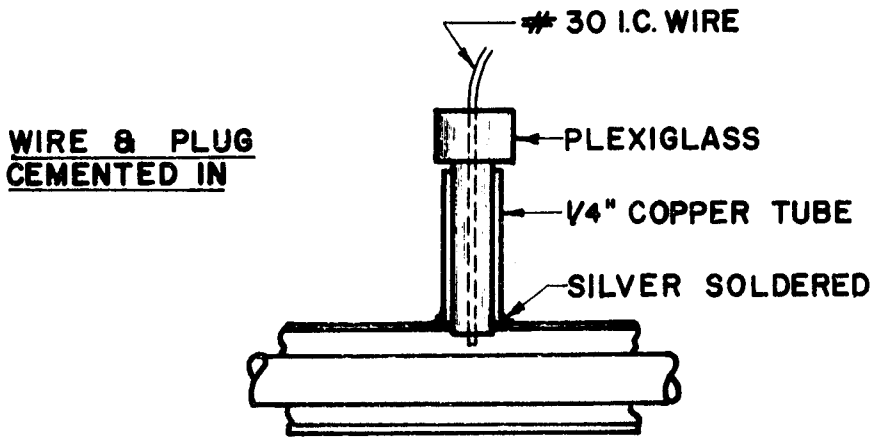

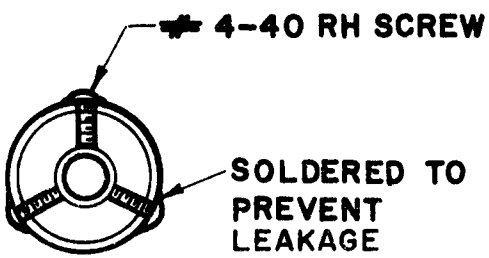

DETAIL OF CONDENSING TUBE SUPPORT

FIG 30 DETAIL OF THERMOCOUPLE INSTALLATION IN ANNULUS

FIG 31 PROBES FOR HEAT EXCHANGER NO. 3

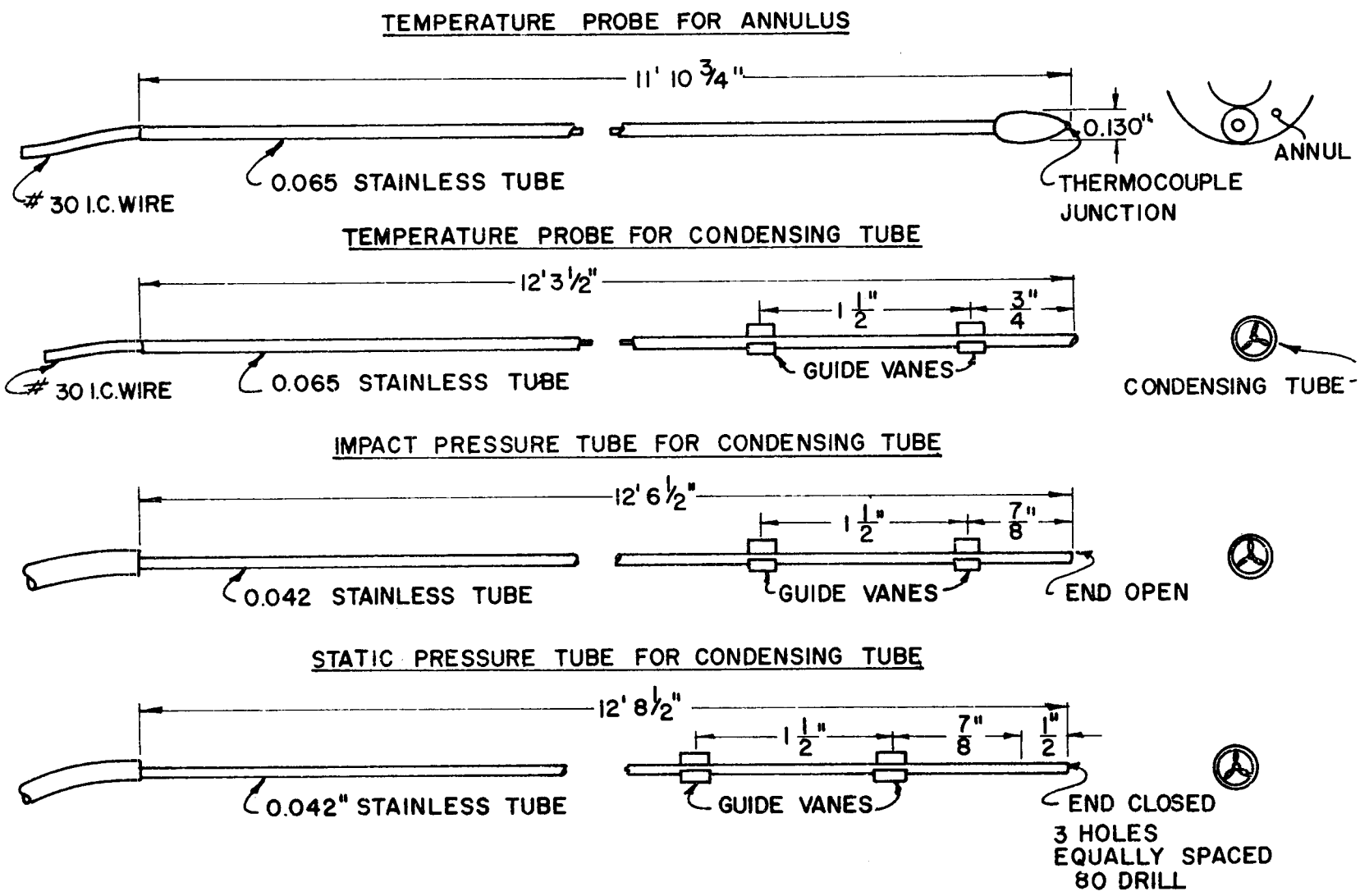

FIG 32

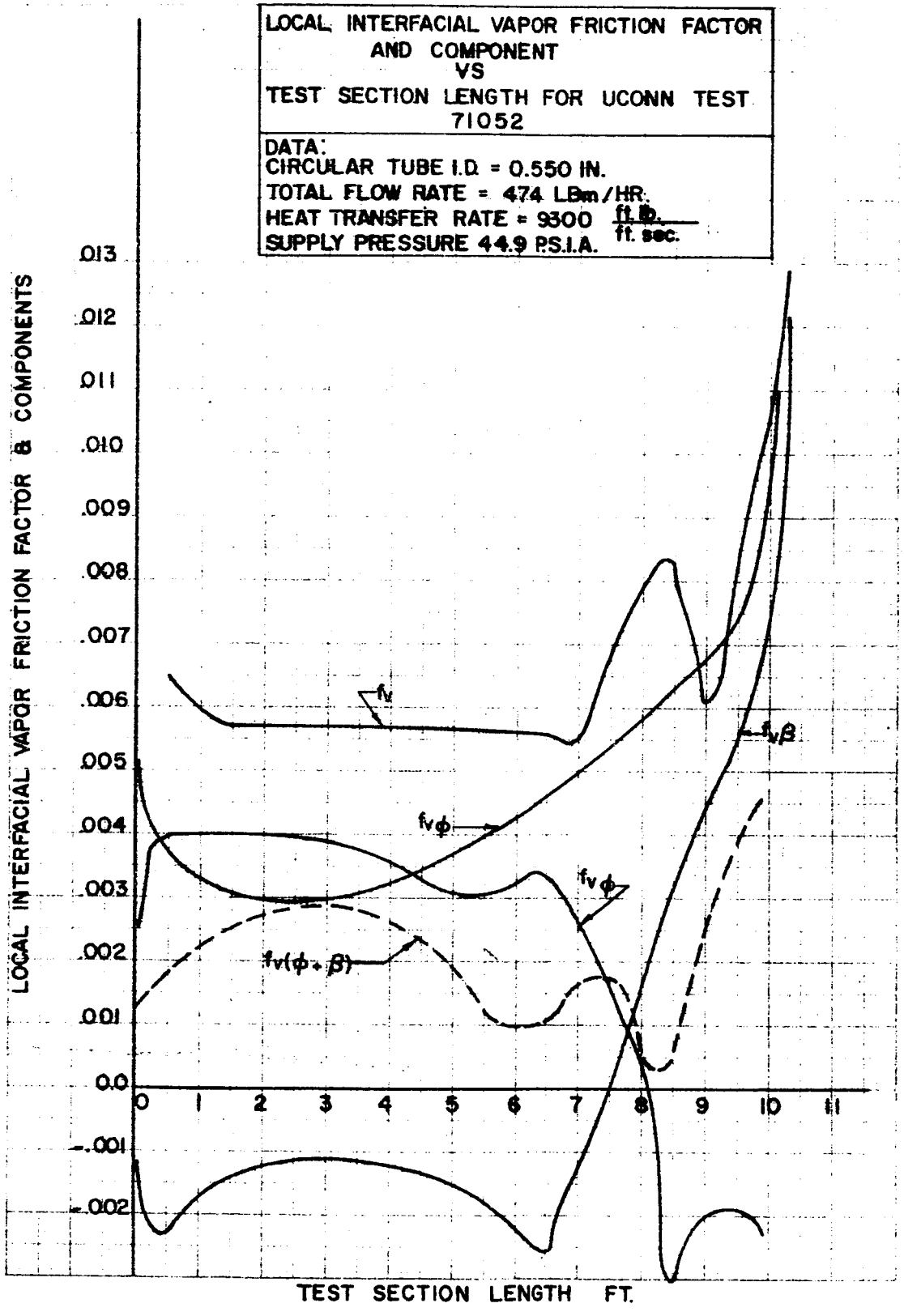
LOCAL INTERFACIAL VAPOR FRICTION FACTOR AND COMPONENT VS TEST SECTION LENGTH FOR UCONN TEST 71052
DATA:
CIRCULAR TUBE I.D. = 0.550 IN.
TOTAL FLOW RATE = 474 LBm/HR.
HEAT TRANSFER RATE = 9300 ft. lb./ft. sec.
SUPPLY PRESSURE 44.9 P.S.I.A.
LOCAL INTERFACIAL VAPOR FRICTION FACTOR & COMPONENTS
.013
.012
.011
.010
.009
.008
.007
.006
.005
.004
.003
.002
.001
0.0
-.001
-.002
0
1
2
3
4
5
6
7
8
9
10
11
f_v
$f_v\beta$
$f_v\phi$
$f_v\phi$
$f_v(\phi+\beta)$
TEST SECTION LENGTH FT.

FIG 33

LOCAL INTERFACIAL VAPOR FRICTION FACTOR AND COMPONENTS VS TEST SECTION LENGTH FOR UCONN TEST NO. 81452 SATURATED STEAM VAPOR CONDENSING IN A 0.190 INCH I.D. TUBE

DATA: TOTAL FLOW RATE = 37.4 LBS/HR (PROBE IN)
= 43.2 LBS/HR (PROBE OUT)
HEAT TRANSFER RATE = $2030 - 1.37\ L/D\ \left(\frac{ft\ lb_f}{ft\ sec}\right)$
PARALLEL FLOW

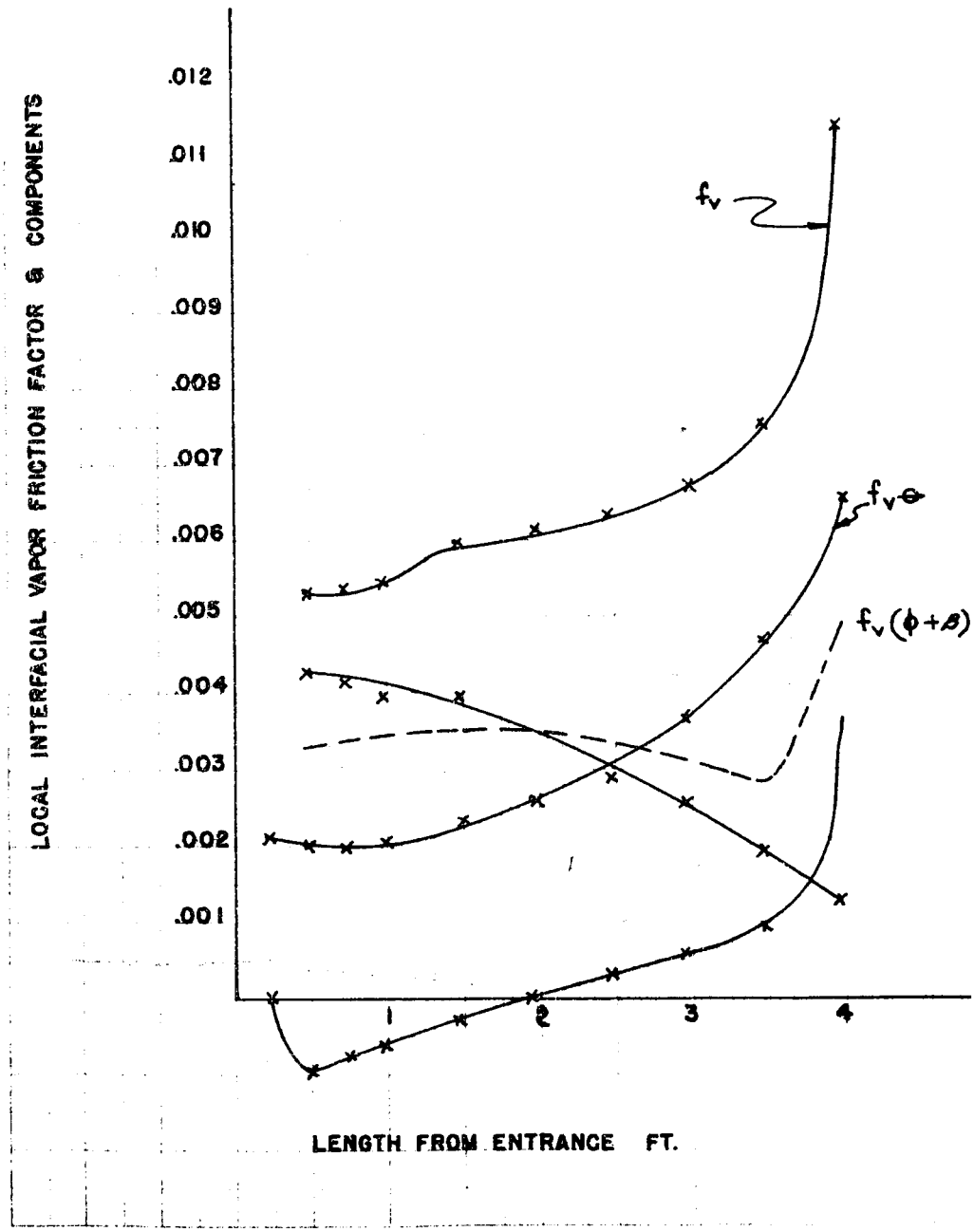

FIG 34

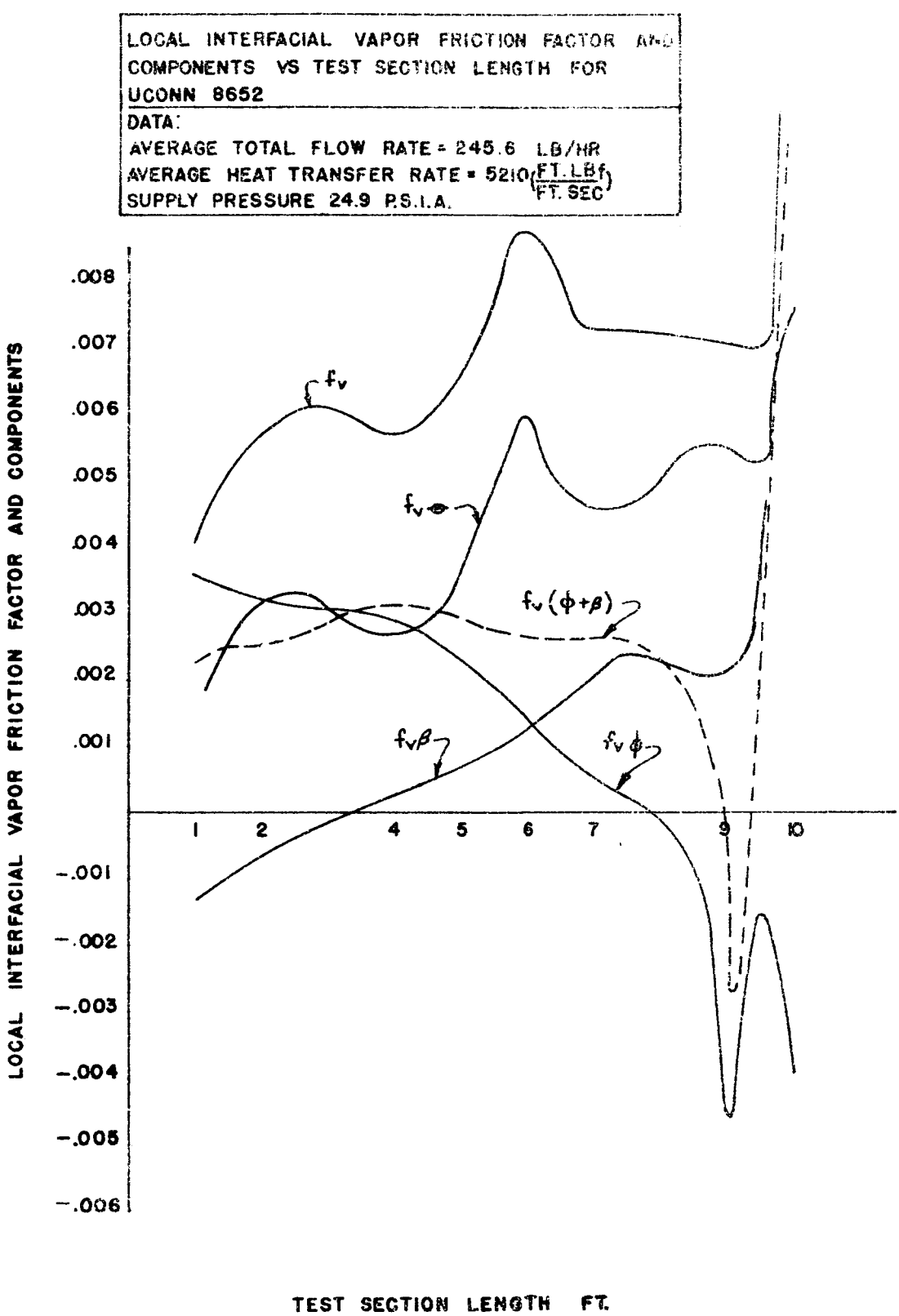
LOCAL INTERFACIAL VAPOR FRICTION FACTOR AND COMPONENTS VS TEST SECTION LENGTH FOR UCONN 8652
DATA:
AVERAGE TOTAL FLOW RATE = 245.6 LB/HR
AVERAGE HEAT TRANSFER RATE = 5210 (FT. LBf / FT. SEC)
SUPPLY PRESSURE 24.9 P.S.I.A.
LOCAL INTERFACIAL VAPOR FRICTION FACTOR AND COMPONENTS
.008
.007
.006
.005
.004
.003
.002
.001
-.001
-.002
-.003
-.004
-.005
-.006
f_v
f_v
$f_v(\phi+\beta)$
$f_v\beta$
$f_v\phi$
1
2
4
5
6
7
9
10
TEST SECTION LENGTH FT.

FIG 35

SUPERFICIAL WALL FRICTION FACTOR & COMPONENTS
VS
TEST SECTION LENGTH FOR UCONN TEST NO. 71052
SATURATED STEAM VAPOR CONDENSING IN A 0.550
ID. TUBE

DATA:
TOTAL FLOW RATE = 474 LBm/HR
HEAT TRANFER RATE = 9300 ($\frac{ft.\,lbf.}{ft.sec.}$)
SUPPLY PRESSURE = 44.9 p.s.i.a.

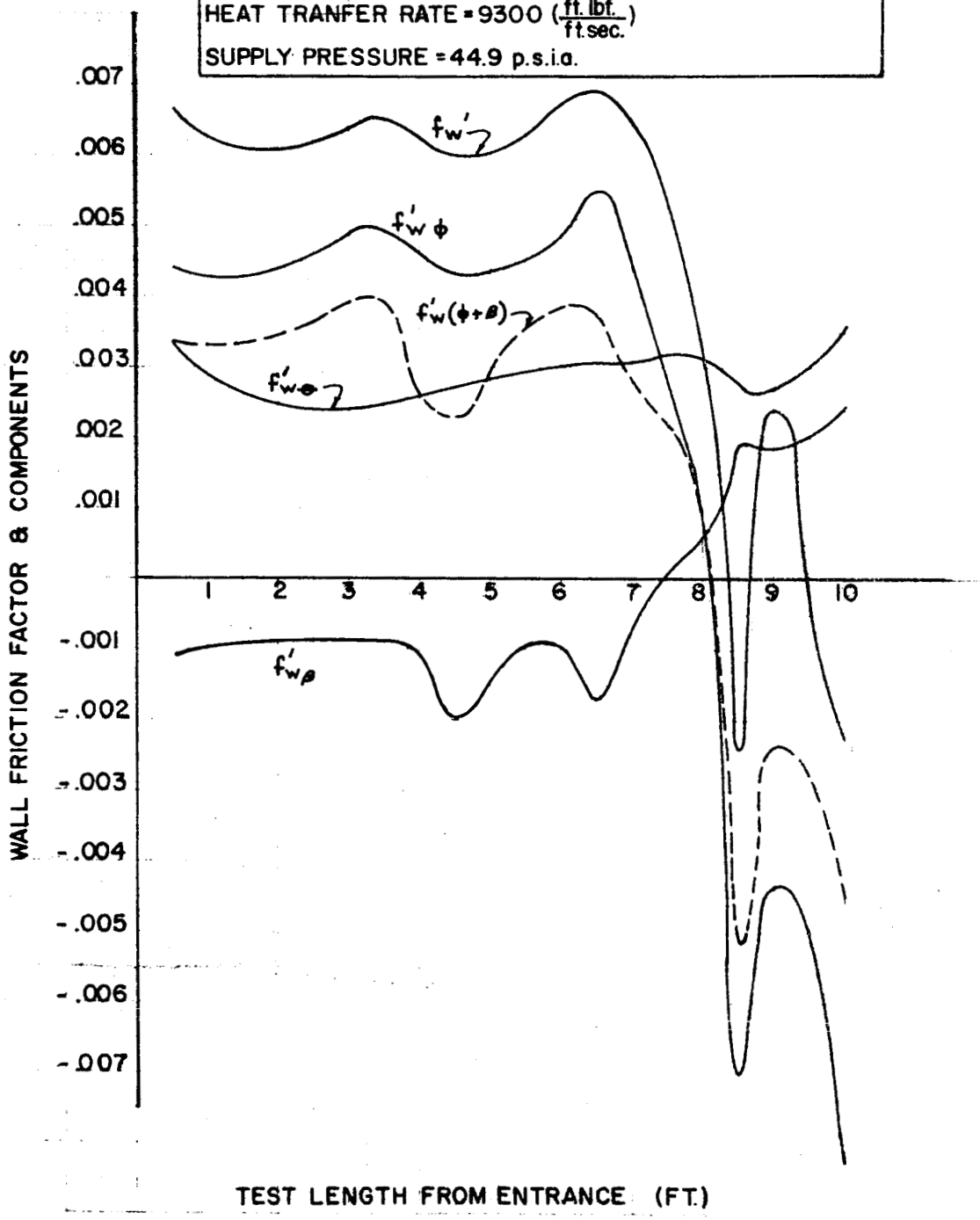

FIG 36

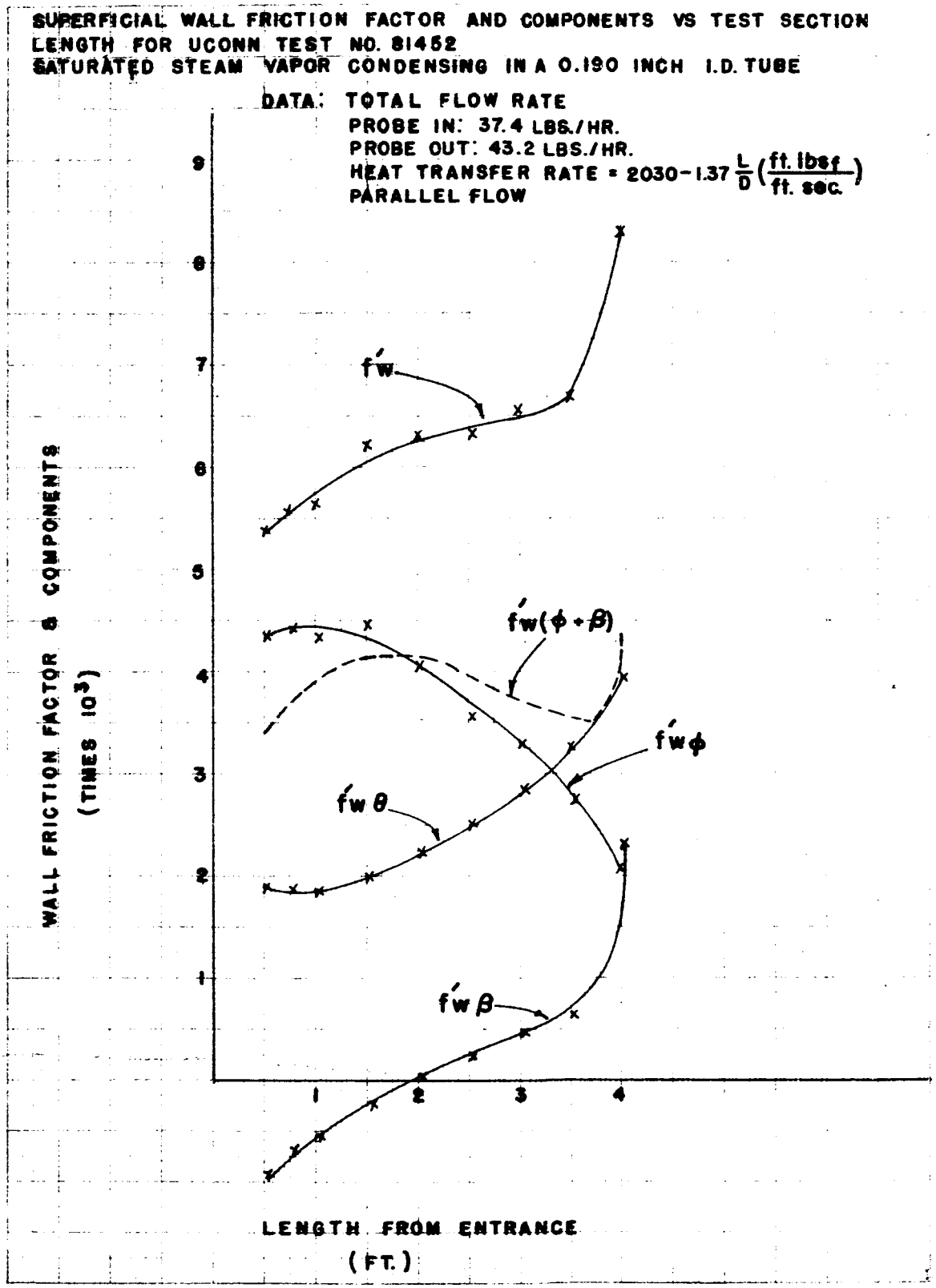
SUPERFICIAL WALL FRICTION FACTOR AND COMPONENTS VS TEST SECTION LENGTH FOR UCONN TEST NO. 81452
SATURATED STEAM VAPOR CONDENSING IN A 0.190 INCH I.D. TUBE
DATA: TOTAL FLOW RATE
PROBE IN: 37.4 LBS./HR.
PROBE OUT: 43.2 LBS./HR.
HEAT TRANSFER RATE = 2030 - 1.37 L/D (ft. lbsf / ft. sec.)
PARALLEL FLOW
WALL FRICTION FACTOR & COMPONENTS (TIMES 10³)
f'w
f'w(ϕ + β)
f'wϕ
f'w θ
f'w β
LENGTH FROM ENTRANCE (FT.)

FIG 37

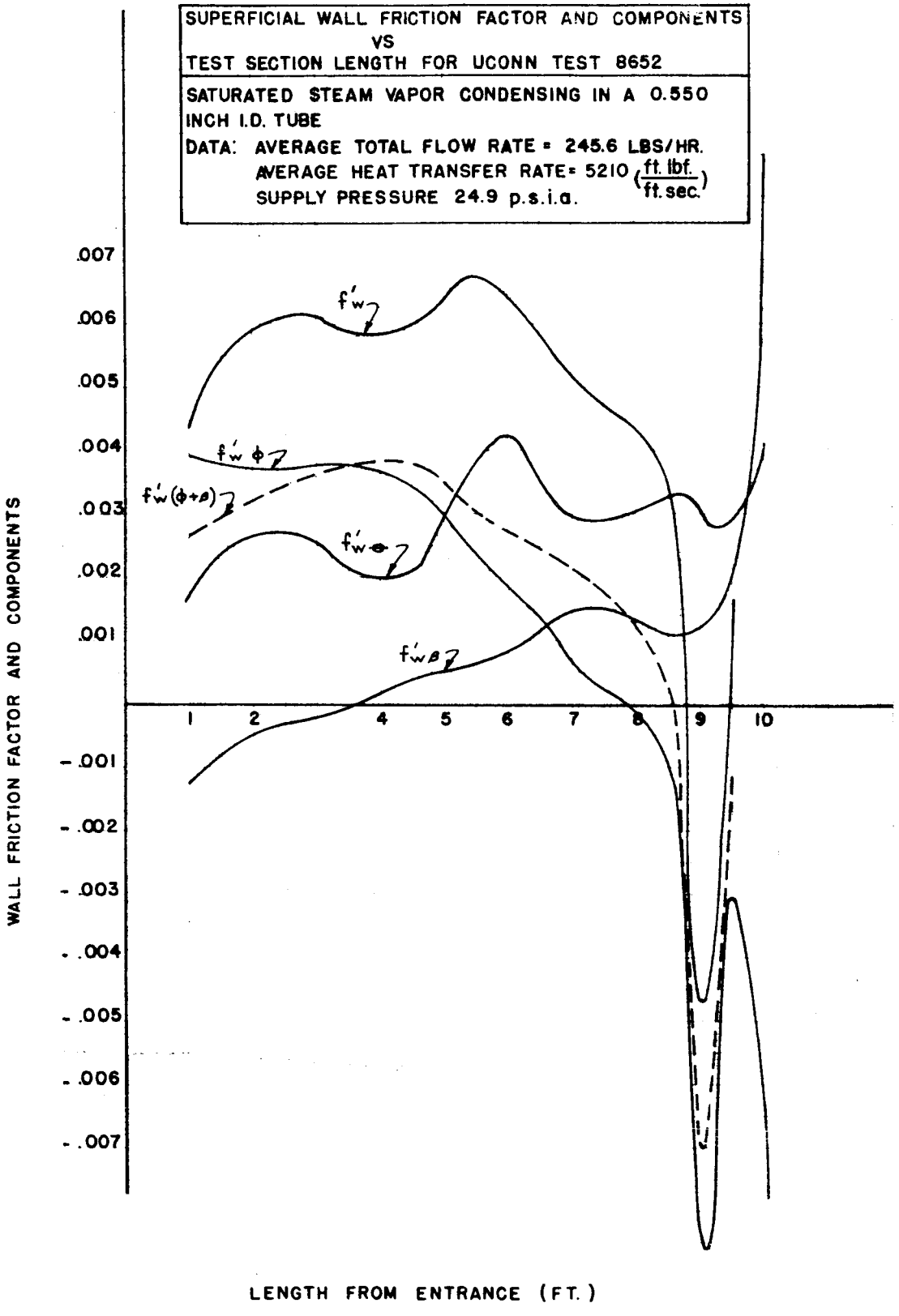
SUPERFICIAL WALL FRICTION FACTOR AND COMPONENTS
VS
TEST SECTION LENGTH FOR UCONN TEST 8652
SATURATED STEAM VAPOR CONDENSING IN A 0.550 INCH I.D. TUBE
DATA: AVERAGE TOTAL FLOW RATE = 245.6 LBS/HR.
AVERAGE HEAT TRANSFER RATE= 5210 (ft. lbf. / ft. sec.)
SUPPLY PRESSURE 24.9 p.s.i.a.
.007
.006
.005
.004
.003
.002
.001
- .001
- .002
- .003
- .004
- .005
- .006
- .007
f'w
f'w ϕ
f'w (ϕ+β)
f'w σ
f'w β
1
2
4
5
6
7
8
9
10
WALL FRICTION FACTOR AND COMPONENTS
LENGTH FROM ENTRANCE (FT.)

FIG 38

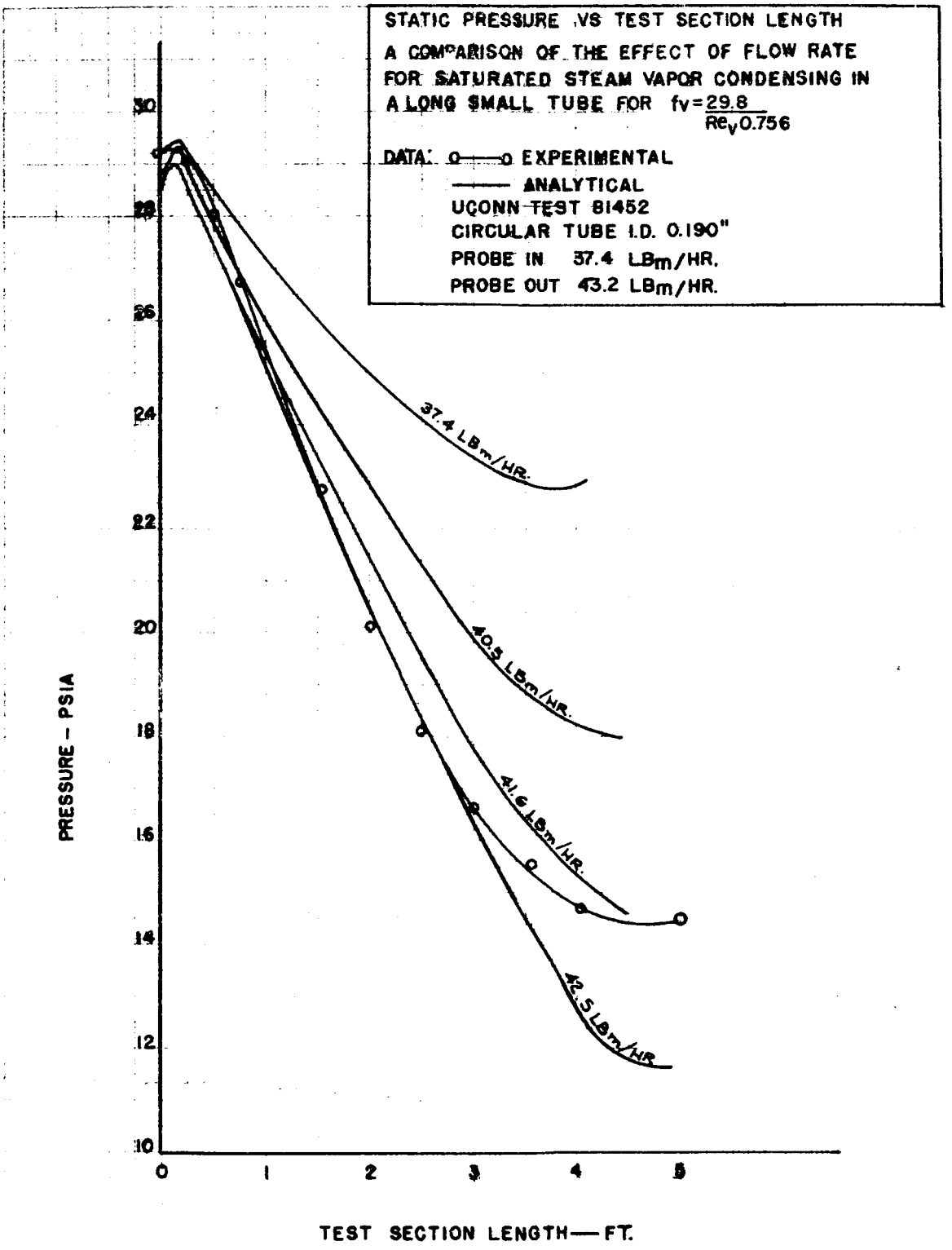
STATIC PRESSURE VS TEST SECTION LENGTH
A COMPARISON OF THE EFFECT OF FLOW RATE FOR SATURATED STEAM VAPOR CONDENSING IN A LONG SMALL TUBE FOR fv=29.8/Re_v 0.756
DATA: o——o EXPERIMENTAL
——— ANALYTICAL
UCONN TEST 81452
CIRCULAR TUBE I.D. 0.190"
PROBE IN 37.4 LBm/HR.
PROBE OUT 43.2 LBm/HR.
37.4 LBm/HR.
40.5 LBm/HR.
41.6 LBm/HR.
42.5 LBm/HR
PRESSURE - PSIA
30
28
26
24
22
20
18
16
14
12
10
0
1
2
3
4
5
TEST SECTION LENGTH — FT.

FIG 39

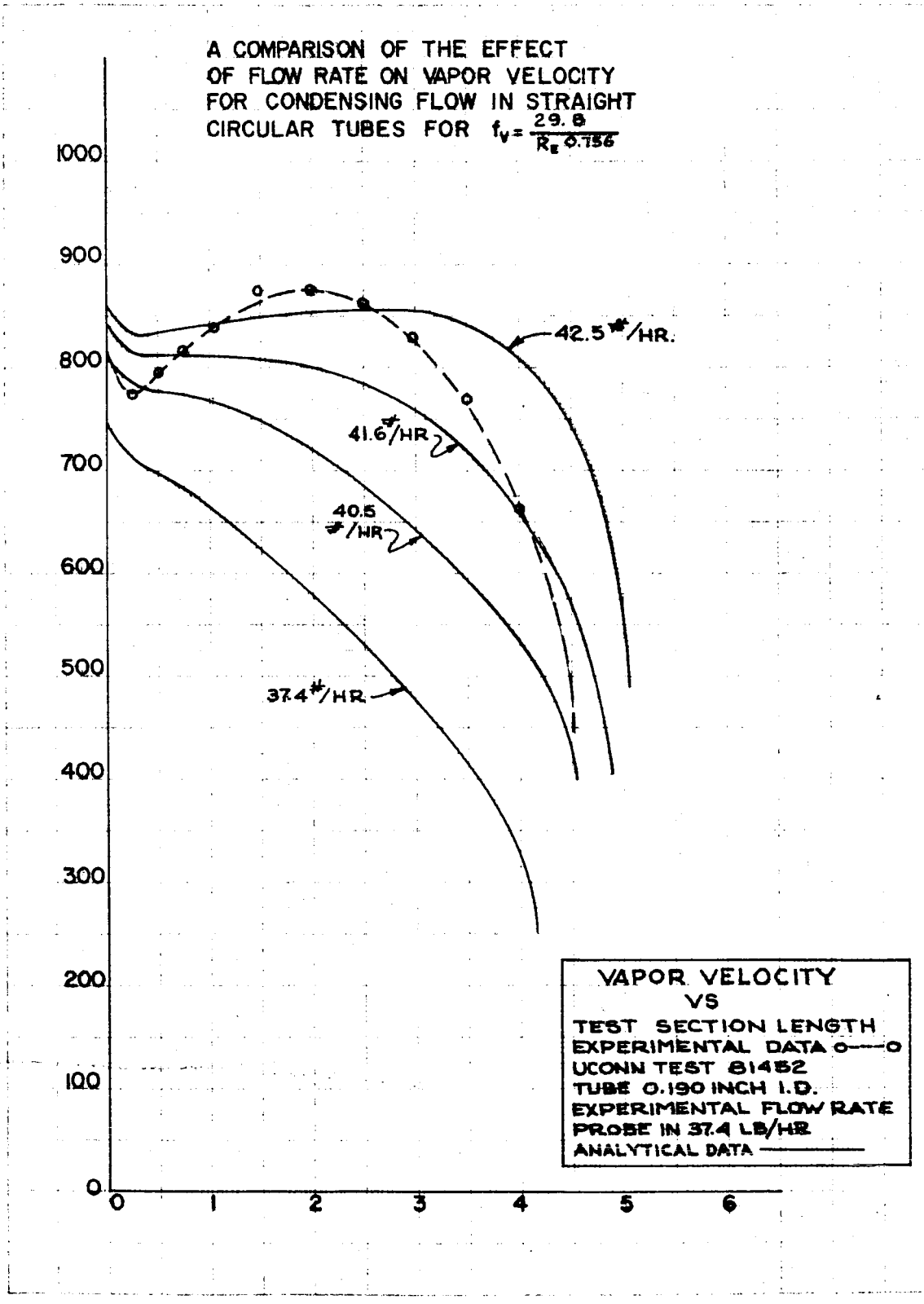
A COMPARISON OF THE EFFECT
OF FLOW RATE ON VAPOR VELOCITY
FOR CONDENSING FLOW IN STRAIGHT
CIRCULAR TUBES FOR $f_v = \frac{29.8}{R_E^{0.156}}$
1000
900
800
700
600
500
400
300
200
100
0
0
1
2
3
4
5
6
42.5 #/HR.
41.6 #/HR
40.5 #/HR
37.4 #/HR
VAPOR VELOCITY
VS
TEST SECTION LENGTH
EXPERIMENTAL DATA o—o
UCONN TEST 81452
TUBE 0.190 INCH I.D.
EXPERIMENTAL FLOW RATE
PROBE IN 37.4 LB/HR
ANALYTICAL DATA ————

FIG 40

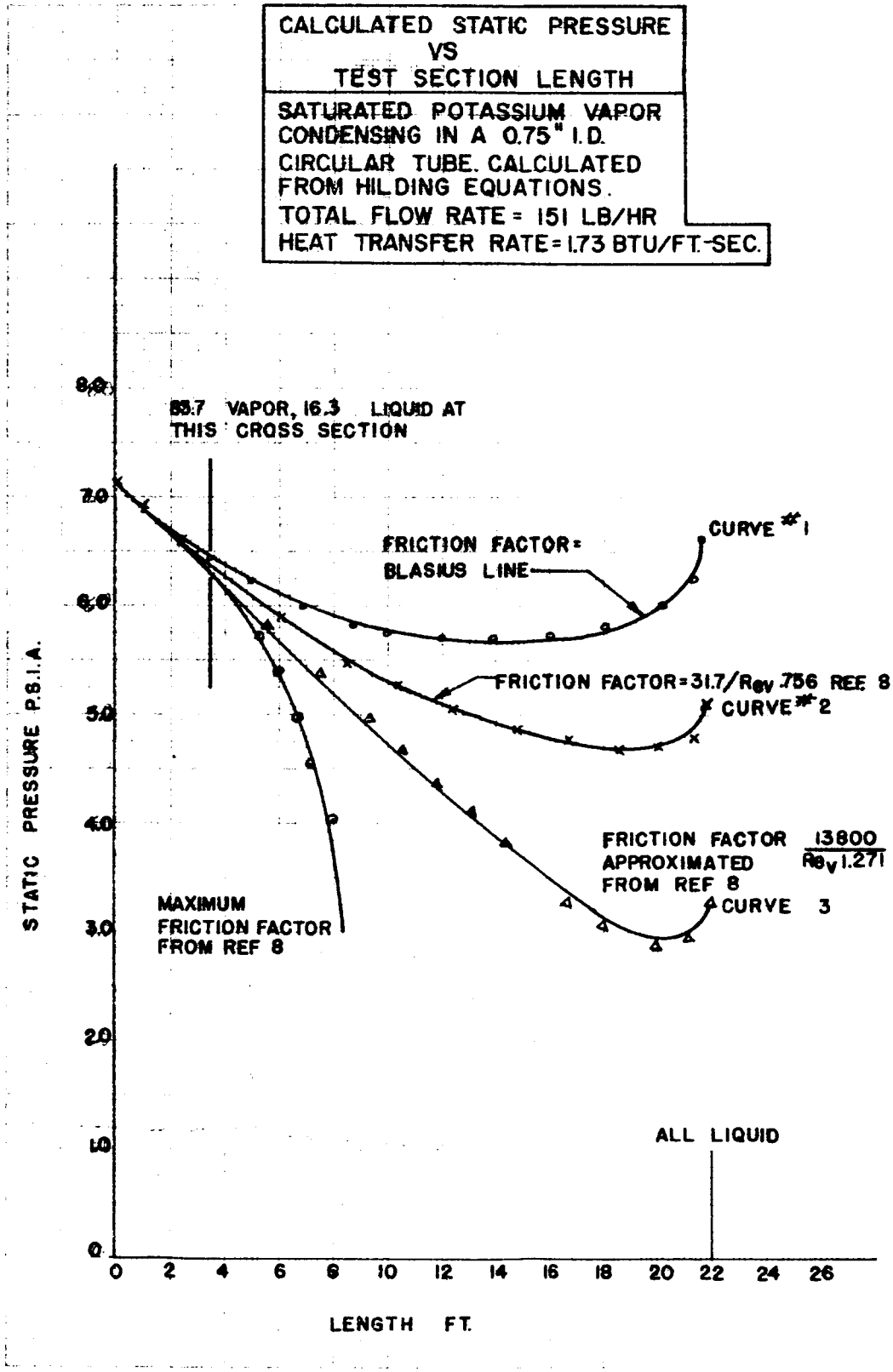
CALCULATED STATIC PRESSURE VS TEST SECTION LENGTH
SATURATED POTASSIUM VAPOR CONDENSING IN A 0.75" I.D. CIRCULAR TUBE. CALCULATED FROM HILDING EQUATIONS.
TOTAL FLOW RATE = 151 LB/HR
HEAT TRANSFER RATE = 1.73 BTU/FT.-SEC.
83.7 VAPOR, 16.3 LIQUID AT THIS CROSS SECTION
FRICTION FACTOR = BLASIUS LINE
CURVE # 1
FRICTION FACTOR = 31.7/Rev .756 REF 8
CURVE # 2
FRICTION FACTOR 13800/Rev 1.271 APPROXIMATED FROM REF 8
CURVE 3
MAXIMUM FRICTION FACTOR FROM REF 8
ALL LIQUID
STATIC PRESSURE P.S.I.A.
LENGTH FT.
8.0
7.0
6.0
5.0
4.0
3.0
2.0
1.0
0
0 2 4 6 8 10 12 14 16 18 20 22 24 26

FIG 41

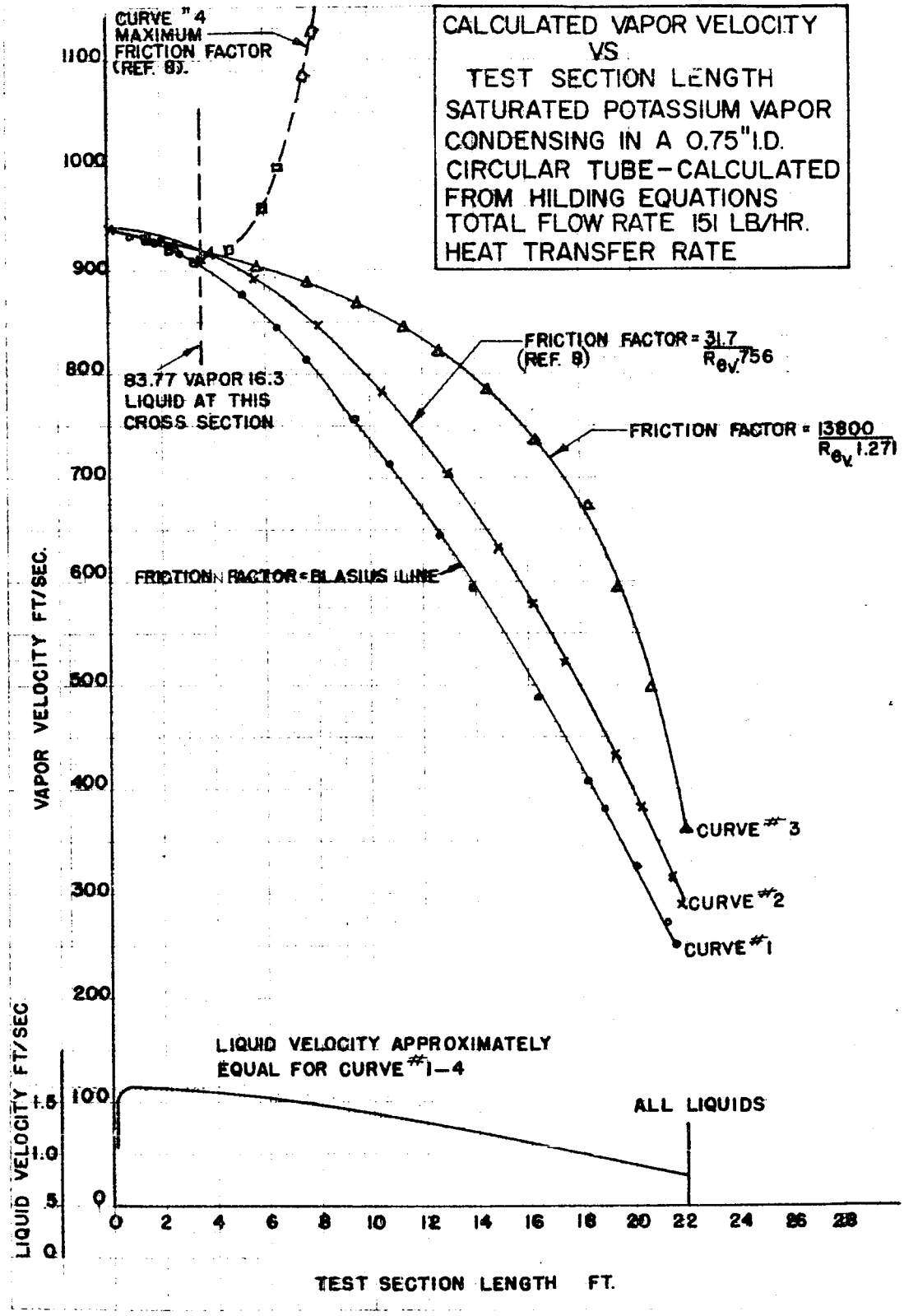
CALCULATED VAPOR VELOCITY
VS
TEST SECTION LENGTH
SATURATED POTASSIUM VAPOR
CONDENSING IN A 0.75" I.D.
CIRCULAR TUBE - CALCULATED
FROM HILDING EQUATIONS
TOTAL FLOW RATE 151 LB/HR.
HEAT TRANSFER RATE
CURVE #4
MAXIMUM
FRICTION FACTOR
(REF. 8).
83.77 VAPOR 16.3
LIQUID AT THIS
CROSS SECTION
FRICTION FACTOR = 31.7 / Re_v^.756
(REF. 8)
FRICTION FACTOR = 13800 / Re_v^1.271
FRICTION FACTOR = BLASIUS LINE
CURVE #3
CURVE #2
CURVE #1
VAPOR VELOCITY FT/SEC.
1100
1000
900
800
700
600
500
400
300
200
100
0
LIQUID VELOCITY FT/SEC
1.5
1.0
.5
0
LIQUID VELOCITY APPROXIMATELY
EQUAL FOR CURVE #1-4
ALL LIQUIDS
0 2 4 6 8 10 12 14 16 18 20 22 24 26 28
TEST SECTION LENGTH FT.

FIG 42 AN EMPIRICAL CORRELATION OF THE LOCAL SURFACE COEFFICIENT OF HEAT TRANSFER IN HIGH SPEED, TWO-PHASE FLOW OF A CONDENSING PURE VAPOR-STEAM

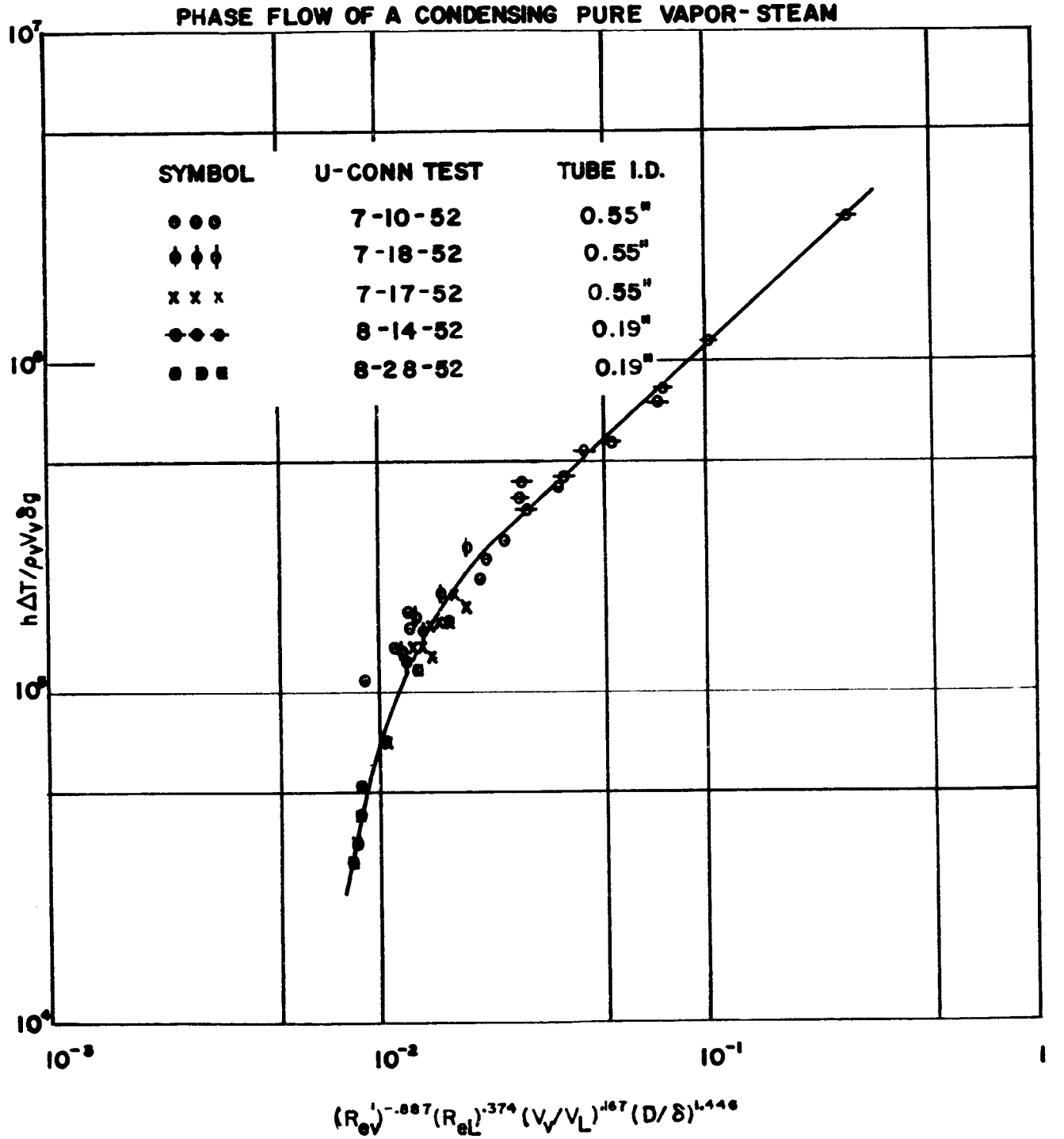

FIG 43

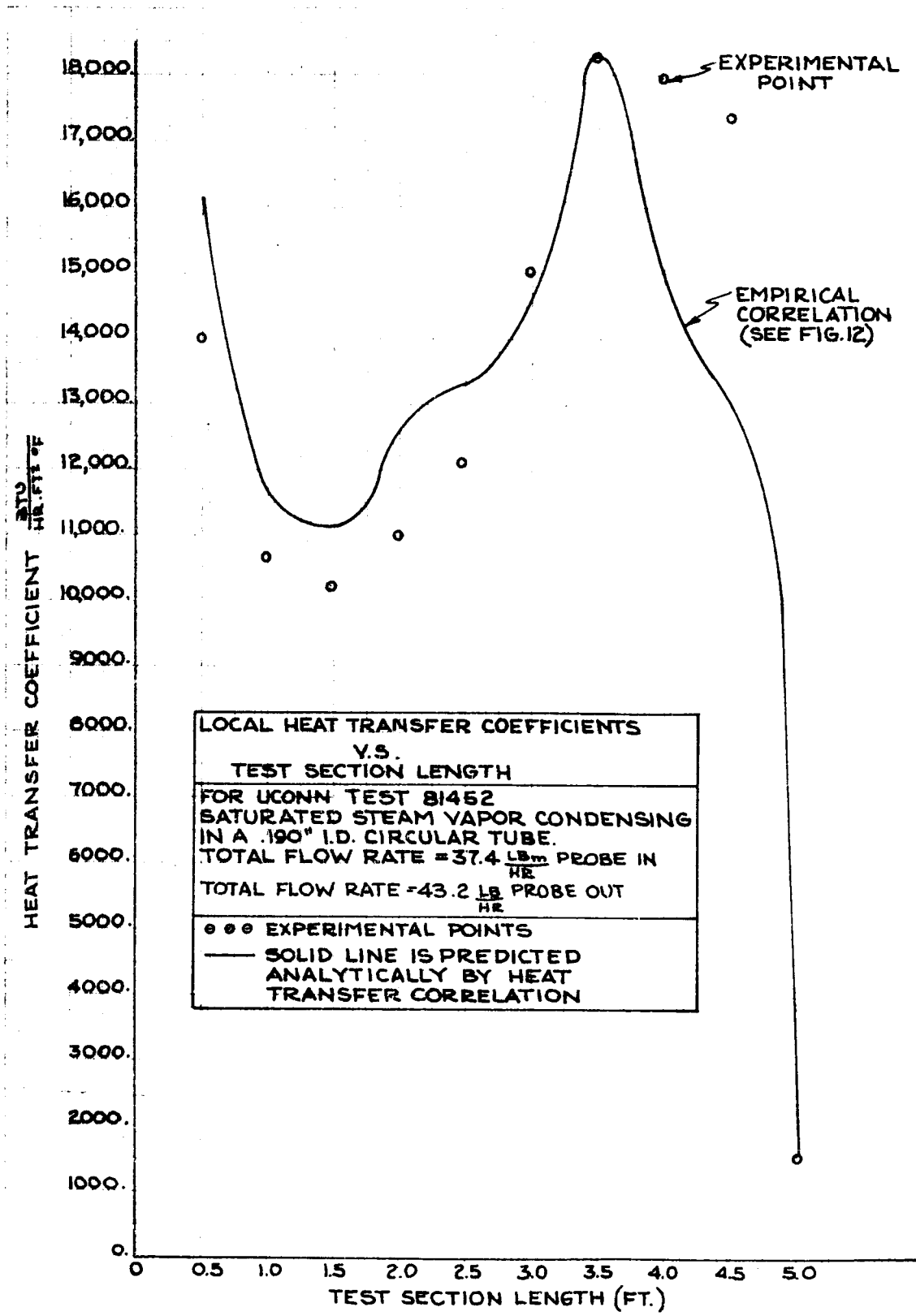
EXPERIMENTAL POINT
EMPIRICAL CORRELATION (SEE FIG. 12)
HEAT TRANSFER COEFFICIENT BTU/HR.FT²°F
18,000.
17,000.
16,000.
15,000.
14,000.
13,000.
12,000.
11,000.
10,000.
9000.
8000.
7000.
6000.
5000.
4000.
3000.
2000.
1000.
0.
0
0.5
1.0
1.5
2.0
2.5
3.0
3.5
4.0
4.5
5.0
TEST SECTION LENGTH (FT.)
LOCAL HEAT TRANSFER COEFFICIENTS V.S. TEST SECTION LENGTH
FOR UCONN TEST 81452
SATURATED STEAM VAPOR CONDENSING IN A .190" I.D. CIRCULAR TUBE.
TOTAL FLOW RATE = 37.4 LBm/HR PROBE IN
TOTAL FLOW RATE = 43.2 LB/HR PROBE OUT
EXPERIMENTAL POINTS
SOLID LINE IS PREDICTED ANALYTICALLY BY HEAT TRANSFER CORRELATION

FIG 44

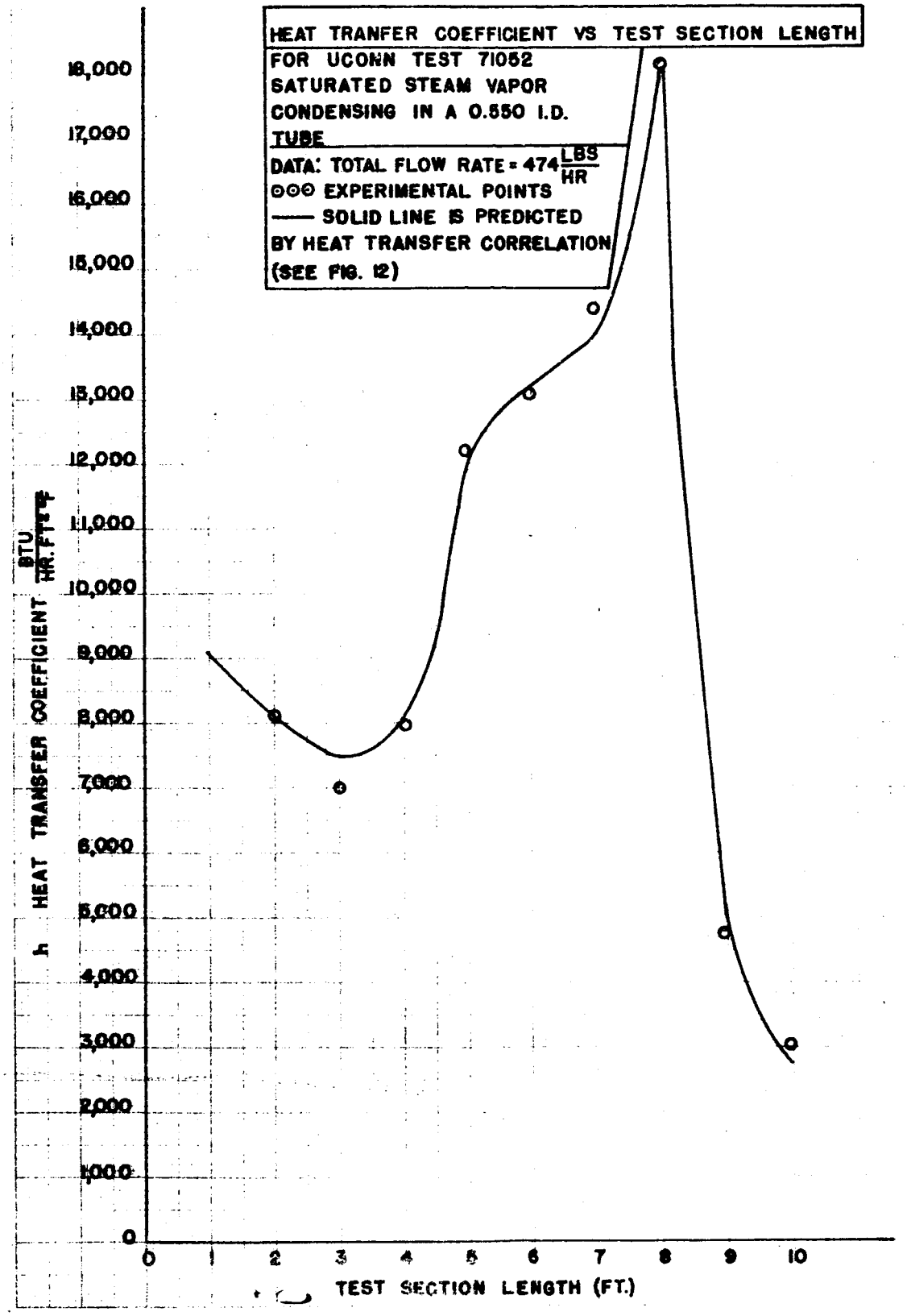
HEAT TRANFER COEFFICIENT VS TEST SECTION LENGTH
FOR UCONN TEST 71052
SATURATED STEAM VAPOR
CONDENSING IN A 0.550 I.D.
TUBE
DATA: TOTAL FLOW RATE = 474 LBS/HR
⊙⊙⊙ EXPERIMENTAL POINTS
—— SOLID LINE IS PREDICTED
BY HEAT TRANSFER CORRELATION
(SEE FIG. 12)
h HEAT TRANSFER COEFFICIENT BTU/HR.FT²°F
18,000
17,000
16,000
15,000
14,000
13,000
12,000
11,000
10,000
9,000
8,000
7,000
6,000
5,000
4,000
3,000
2,000
1,000
0
0
1
2
3
4
5
6
7
8
9
10
TEST SECTION LENGTH (FT.)